DOKUZ EYLÜL UNIVERSITY

GRADUATE SCHOOL OF NATURAL AND APLIED SCIENCES

REPAIR OF DAMAGED COMPOSITE LAMINATES

by

Mustafa İlhan UYSAL

August, 2009

İZMİR

REPAIR OF DAMAGED COMPOSITE LAMINATES

A Thesis Submitted to the
Graduate School of Natural and Applied Sciences of Dokuz Eylül University
In Partial Fulfillment of the Requirements for the Degree of Master of Science
in Mechanical Engineering, Mechanics Program

by

Mustafa İlhan UYSAL

August, 2009
İZMİR

M. Sc THESIS EXAMINATION RESULT FORM

We have read the thesis entitled **"REPAIR OF DAMAGED COMPOSITE LAMINATES"** completed by **MUSTAFA İLHAN UYSAL** under supervision of **ASSOC. PROF. DR. CESİM ATAŞ** and we certify that in our opinion it is fully adequate, in scope and in quality, as a thesis for the degree of Master of Science.

Assoc. Prof. Dr. Cesim ATAŞ

Supervisor

(Jury Member)

(Jury Member)

Prof. Dr. Cahit HELVACI

Director

Graduate School of Natural and Applied Sciences

ACKNOWLEDGEMENTS

I would like to offer my thanks and my gratitude to my supervisor, Assoc. Prof. Dr. Cesim ATAŞ, for his excellent guidance, tolerant approach and continuous encouragement throughout the preparation of this study.

I also would like to thank Dr. Bülent Murat İÇTEN for his great help during my study.

I wish to express my thanks to the research assistants at the Department of Mechanical Engineering for their help and moral support.

This study is done in scope of a TÜBİTAK project with number 107M406. So, I would like to express my thanks to TÜBİTAK for financial support.

Finally, I am deeply indebted to my family members for their patience, support and their tenderness.

Mustafa İlhan UYSAL

REPAIR OF DAMAGED COMPOSITE LAMINATES

ABSTRACT

The aim of this study was to examine the mechanical performance of the repaired glass-epoxy composite laminates experimentally and numerically and comparing the results with each other. The specimens used in experiments were manufactured by vacuum assisted resin infusion molding method in Composite Research Laboratory at Dokuz Eylul University. Woven glass fabrics were used in fabrication of the specimens. Shimadzu AUTOGRAPH AG-IS Series universal tensile test machine was used in the experiments. In the numerical analysis, LUSAS 14.1 software was utilized.

Three different types of tensile specimens, i.e. unpatched, two stepped patched and three stepped patched specimens, were examined experimentally and numerically. Besides this, different types of tensile specimens, according to the tensile test standards, are modelled and analyzed with LUSAS. Interface elements were used to simulate uncontinuous regions in the patched specimens. Analysis results are evaluated and discussed. Eventually, different types of bending specimens, according to the three point bending test standards, are also analyzed with LUSAS followed by the discussions.

The conclusions drawn from the study are summarized in conclusions section.

Keywords: repair, composite laminates, vacuum assisted resin infusion molding method

HASARLI KOMPOZİT PLAKLARIN ONARIMI

ÖZ

Bu çalışmanın amacı, onarılmış cam-epoksi kompozit plakların mekanik performanslarının deneysel ve sayısal yolla incelenmesidir. Deney esnasında kullanılan numuneler, vakum destekli reçine infüzyon sistemi kullanılarak Dokuz Eylül Üniversitesi Kompozit Araştırma Laboratuarı'nda üretilmiştir. Numunelerin üretiminde, örgülü cam-fiber kumaşlar kullanılmıştır. Deneylerde Shimadzu AUTOGRAPH AG-IS Serisi üniversal çekme testi makinası kullanılmıştır. Sayısal analizlerde LUSAS 14.1 yazılımından yararlanılmıştır.

Yamasız, iki basamaklı yamalı ve üç basamaklı yamalı olmak üzere üç farklı çekme numunesi deneysel ve sayısal olarak incelenmiştir. Bunun dışında çekme testi standartlarına uygun farklı tiplerde çekme numuneleri LUSAS'la modellenip analiz edilmiştir. Süreksiz bölgeleri simüle etmek için arayüzey elemanları kullanılmıştır. Analiz sonuçları değerlendirilip tartışılmıştır. Son olarak eğilme testi standartlarına uygun, farklı tiplerde eğilme numuneleri de LUSAS ile analiz edilmiştir.

Çalışmadan elde edilen sonuçlar, sonuçlar kısmında özetlenmiştir.

Anahtar Kelimeler: onarım, kompozit plaklar, vakum destekli reçine infüzyon kalıplama yöntemi

CONTENTS

Page

CHAPTER ONE
INTRODUCTION

Repair can be defined as turning the material which has been damaged because of various reasons into a form that is available to reuse. The aim of an ideal repair is approaching the damaged material's mechanical properties to the closest values of the undamaged material.

By the increase of the usage of composite materials, the subject of repairing damaged composites has gained great importance in recent years. As a result of the analytical and experimental studies in this subject, different repair methods have been developed in reply to the different damage types and many advantages-disadvantages of these methods have been determined.

There are many ongoing and completed works about repair of composite materials. Some of them are summarized herein.

Koh et al. (1999) studied on damage assessment in a bonded composite structure by means of surface mounted PZT sensor/actuator elements. Bleay et al. (2001) performed a technique for 'smart' repair of delaminations in polymer composites involving hollow fibres with resin, which is released into the damaged area when the fibres are fractured. Kessler and White (2001) investigated the self healing of delamination damage in woven E-glass/epoxy composites. Pang and Bond (2005) studied on the development and demonstration of a self repairing 'bleeding' fibre reinforced composites which provide enhanced damage visibility for the concealed damages and recovery of the mechanical strength.

Wilmarth (1985) developed an analysis tool, BREPAIR, for bolted repair based on the boundary collocation method. However, the program was limited to the analysis of doubly symmetric configurations subjected to uniform biaxial or shear loadcases.

By using the BREPAIR analysis tool, Bohlmann et al. (1981) studied the bolted repair field for wing skin laminates and verified BREPAIR predictions by experimental data. Her and Shie (1998) analyzed the bolted repair of composites by employing a conventional finite element approach. Widagdo and Aliabadi (2001) studied on a two dimensional boundary element method for analysis of mechanically fastened composite repair patches and developed a boundary element formulation for modeling cracked panels repaired by mechanically fastened composite patches. They showed that the stiffness ratio E_2 / E_1 influences the SIF (stiffness intensity factor) value of the repaired panel. Zhang (2001) formulated a boundary element method to assess the structural integrity of bolted composite joints and repairs. He showed that the formulated boundary element method gives very good predictions on the force distributions and maximum failure loads.

Leiborich et al.(1990) investigated the effect of composite patches on the fatigue crack growth behavior of repaired parts. Naboulsi and Mall (1998) investigated the effects of nonlinear analysis of the adhesively bonded composite patch on the damage tolerance of cracked aluminum panels. Schubbe and Mall (1999) carried out a numerical and experimental study on the capability of a two-dimensional finite element method in order to characterize the fatigue crack growth behavior of thick metallic panels repaired asymmetrically with adhesively bonded composite patch. Chester et al. (1999) studied on the development of an adhesively bonded composite repair for a 48 mm long crack in the lower wing skin of an F-111 aircraft. They investigated both shear strain range and strain energy release rate as parameters to describe the fatigue behavior by developing a test specimen to generate design data for the fatigue endurance of the adhesives used in bonded repairs. Baker (1999) studied on two approaches: The first one was based on a demonstrated ability to predict the patch system's fatigue behavior and to assure its environmental durability. The second approach was based on the "smart patch" concept in which the patch system monitors its own health. Rao et al. (1999) investigated the residual strength and fatigue crack-growth life of an edge-cracked aluminum specimen repaired using glass epoxy composite patch. Duong et al. (2002) carried out an analytical and experimental study on load attraction and fatigue crack growth in

two-sided bonded repairs. Bouiadjra et al. (2002) showed that for a single patch repair a 50% increase in patch thickness reduces the stress intensity factors at the same order and they confirmed that for a better distribution of the stresses, it is preferable to use a multiple layers of bonded composite patch. Bouiadjra et al. (2008) also analyzed the behavior of a cracked aluminum plate repaired with a circular bonded composite patch in mode I and mixed mode with and without the presence of disbond. Seo and Lee (2002) investigated the fatigue crack growth behavior of thick aluminum panel repaired with bonded composite patch experimentally and numerically using the stress intensity factor range (ΔK) and fatigue crack growth rate (da/dN). Tsai and Shen (2004) performed the stress analysis for four different aluminum plates, including no crack, with crack, with crack and single-side patched composites, as well as crack and double-side patched composites experimentally and numerically. Jones et al. (2006) examined the cracks repaired with a composite patch and showed that in the low to mid ΔK region there is a near linear relationship between the "log" of the crack length and number of cycles. Harman and Wang (2006) developed an analytic technique to facilitate the optimized design of isotropic adherend scarf joints between dissimilar adherend materials. The technique specified a linearly varying scarf angle that generates a characteristic scarf profile for a given adherend modulus ratio. Fujimoto and Sekine (2007) studied on a method to identify the locations and shapes of crack and disbond fronts in aircraft structural panels repaired with bonded FRP composite patches. Megueni and Lousdad (2008) evaluated and compared the performance of a double sided patch and stepped patch by using two dimensional finite element method of a centre cracked metallic panel repaired using an externally bonded composite patch. They showed that a stepped patch gives better results. Madani et al. (2008) investigated the numerical behavior of centrally cracked aluminum panels repaired with single and double sided composite graphite/epoxy patches and subjected to uni-axial loading to obtain stress intensity factors and crack opening displacements. Fekirini et al. (2008) analyzed the performance of bonded composite repair having two adhesive bands with different properties by the FE method.

Ratwani (n.d.) observed experimentally that a large difference exists in crack growth rates between thin and thick repaired panels. Chen and Cheng (1983) determined the stresses in a single lap joint by using fourth-order ordinary differential equations. Kairuz and Matthews (1993) calculated stress distributions in single lap joints with initial cracks using finite element method. A closed-form analytical solution by the complex potential method for bonded scarf patches under pure in-plane and bending load has been addressed by Katzenschwanz (1996). Oztelcan and Ochoa (1997) applied a finite element model using a user routine based on the ultimate stress, allowing detecting damage initiation and progression in the adhesive of overlap and scarf repaired joints. Charalambides et al. (1998), (1998) performed a finite element analysis to predict the experimentally observed failure paths and strength of adhesively-bonded carbon/epoxy scarf repairs. Zhang et al. (1998) investigated the performance of repaired thin-skinned, blade-stiffened composite panels under compression in the post-buckling range. Soutis et al. (1999) used a three-dimensional model to estimate the stress field of a compression loaded laminate repaired with an external patch and compare with experimental results. Hu and Soutis (2000) studied compression loaded repaired laminates and performed a three-dimensional finite element analysis using a FE-77 finite element package to identify critical stressed areas and predict the failure load of repair. Chotard et al. (2001) investigated the residual mechanical behaviour of scarf patch-repaired composite pultruded structures initially submitted to low-velocity impact loading. Chan and Vedhagiri (2001) compared numerical and experimental results for bonded, bolted and bonded/bolted joints. For the three dimensional models they used non-linear contact elements as gap elements to model the hole/pin interface and the interface between the parent and repair laminates. Barut et al. (2002) studied on an analysis method for determining transverse shear and normal stresses in the adhesive and in-plane stresses in the repair patch. They also studied on displacement fields in a patch-repaired skin with a circular cutout under in-plane loading. Engels and Becker (2002) investigated the problem of a laminate plate with an elliptical hole repaired by elliptical patches under in-plane and/or bending load. Li et al. (2003) experimentally investigated the effectiveness of using UV curing resin to fast repair laminated beams damaged by low velocity impact. Hosur et al. (2003) carried out a

study to repair strategies for thick section woven S2-glass/vinyl ester composites subjected to ballistic impact loading. Mahdi and Kinloch (2003) used two dimensional and quasi-three-dimensional finite element models to predict the performance of undamaged repaired beams. The 2-D model was found to describe the repair geometries quite accurately and was considered suitable to qualitatively design the repair patches. Duong (2004) studied on an engineering approach which combines existing methods for two-dimensional and one-dimensional geometrically nonlinear analysis of a composite repair under either purely thermal loads or purely mechanical loads. Belhouari et al. (2004) studied on analyzing the advantage of the use of the bonded symmetric composite patch for repairing crack, numerically by the finite element method. They showed that the use of the double patch reduces appreciably the stress intensity factor compared to single patch and the stress intensity factor decreases asymptotically according to the thickness of the patch. Yang and Huang (2004) developed an analytical model based on the Laminated Anisotropic Plate Theory to obtain the stress distribution in a single-lap joint. Yunpeng et al. (2005) did compressive experiments and FEM simulation on the repaired composite laminates to predict the damage initiation and progression. Campilho et al. (2005) studied on the single and double-lap repairs in tensile loaded composite structures reinforced with carbon fibres by using ABAQUS FEA software to obtain stress distributions and to evaluate the residual strength of the repaired plates, as well as to assess the effect of geometric changes in the plates and patches on the residual strength. Vaziri and Hashemi (2006) investigated the dynamic response of repaired composite beams with an adhesively bonded patch under a harmonic peeling load theoretically and experimentally. Caliskan (2006) checked the efficiencies of the patch under mechanical forces using an analytical method for bonded and bolted repairing methods using composite single lap joint. The results showed that for low-rate loads, repair was obtained as homogenous load distribution, but bolted repair as heterogeneous. Liu and Wang (2007) investigated, by conducting experimental tests and developing a 3-D progressive damage model, different repair parameters' effects on the ultimate strength and failure mechanism of adhesively bonded repaired structures. Mollenhauer et al. (2008) used Moiré interferometry, a full-optical displacement measuring method capable of high spatial resolution and

high displacement sensitivity, to gather detailed information about the distribution of interlaminate strain on the edge of laminated composite bonded repair coupons. Wang and Gunnion (2008) investigated the strength of scarf joints in composite structures and developed an improved design methodology. They showed that the stacking sequence of composite adherents influences the scarf joint strength. Yala and Megueni (2008) used an experimental design method to investigate the effect of different parameters such as the size and the intrinsic properties of the adhesive, the patch and the plate that affect the stress intensity factor K at the crack tip to achieve an optimization of the repair operation. Fredrickson et al. (2008) applied a computer program to model and predict strain fields in two composite repairs, the scarf joint and the stepped-lap joint, subjected to static tensile loading. They used Moiré interferometry to determine experimental strain data and showed that Moiré experimental results were in good agreement with the predictions for the free-edge normal strains $\varepsilon_X, \varepsilon_Z$ and the free-edge shear strain γ_{XZ}.

Sherwin (1999) used the double vacuum/staging process for curing laminates that typically can not be cured under a conventional vacuum bag. Tzetzis and Hogg (2006), (2008) studied on the bondline fracture characteristics of vacuum infused repairs under mode I loading regime and investigated the performance of the vacuum-assisted resin infused repair technique as an alternative processing method for repairing relatively thick glass/vinyl ester composite laminates using the flush scarf configuration.

This study is concerned with the repair of damaged fiberglass composite laminates by using stepped lap method. The specimens which were repaired with this method is subjected to tensile tests and the result of these tests are compared with each other. In a similar way, finite element analysis of the specimens are done by the use of LUSAS software.

CHAPTER TWO
INTRODUCTION TO COMPOSITE MATERIALS

2.1 History of Composite Materials

The material that can be formed by joining two or more materials macroscopically in certain conditions and ratios is called composite material.

Composite is not a new idea. Papyrus is a paper type in which fiber reinforcements can be seen clearly. About B.C. 2000, by using papyrus reeds coated with pitch, waterproof baskets were being produced by Egyptians. Since the times of old, it is known that, bricks' strengths increase when they are filled with chopped straw (Armstrong & Barrett, 1998). The Mayan and Inca tribes had used plant fibers to strengthen their bricks and pots (Staab, 1999). The "mud" huts in Africa are reinforced by weeds and thin sticks. Butser Hill Farm Project showed that, in B.C.1500, woven sticks which were bonded with the mixture of cow dung and mud, were being used in the construction of house walls in England (Armstrong & Barrett, 1998). Similarly, Eskimos use moss to improve the strength of ice while they are building their igloos. In the Middle Ages, plating process was performed on swords and armors to increase their strength. For example, Samurai sword was produced by repeated folding and reshaping to form a multilayered composite (it is estimated that several million layers could have been used) (Staab, 1999). Other than these, there are natural composites like fog, mist, clouds, rain, feather, bone, cobweb and wood. Bone is a porous composite. Cobweb is formed by a gel, coated with a solid composition that consists of aligned molecules. The structure of the tree consists of long, strong cellulose fibers bonded together by a protein-like substance called lignin. The fibers that draw up the trunk and the branches, are aligned in optimum form to resist the stresses caused by gravity and wind forces (Armstrong & Barrett, 1998).

Although the concept is too old, the materials have changed in a form that includes special combination of properties (e.g. catalytic magnetic, magnetic-

transparent, conductive-transparent, etc.) to meet the requirements. Carbon, aramid, glass fibers and epoxy resins which are being used widespread nowadays, are too expensive in comparison with straw, cow dung and mud. But their performance is much higher for a given weight. The usage of these modern composites is started about the years of 1930. Fiberglass had been made, almost by accident in 1930, when an engineer became intrigued by a fiber that was formed during the process of applying lettering to a glass milk bottle. It had started to spread all around the world by Nitto Boseki in Japan and The Owens Corning Fiberglass Company that was founded in U.S.A. in 1935 (Strong, n.d.). At the present time, modern composites are being used widespread in many areas like town planning, household equipments, industry of electric and electronic, aeronautics, caterpillar and automotive, construction and agriculture sector.

2.2 Advantages and Disadvantages of Composite Materials

In comparison with metals, composite materials have both advantages and disadvantages. Some of the advantages are given below:

- Composite materials have vibration damping, shock and noise gulping properties because of their ductility.

- Besides their high tensile, bending and fatigue strength, composites have excellent strength-to-weight and stiffness-to-weight ratios because of their lightness. Thus, light and strong products can be produced while saving the material.

- Composites are fairly resistant to corrosion, chemicals (there are some exceptions like paint stripper) and outdoor weathering (e.g. heat) (Armstrong & Barrett, 1998).

- Large and complex parts can be obtain by the feature of being able to easily fabricated.

- By joining the appropriate materials, composites can be used as good conductors or insulators in electric field.

- Using different orientation angles in laminated composites provides desired higher mechanical properties.

- Composite structures provide in-service monitoring or online process monitoring with the help of embedded sensors. This feature is used to monitor fatigue damage in aircraft structures… [M]aterials with embedded sensors are known as “smart materials” (Mazumdar, 2002).

Some of the disadvantages are given below:

- In comparison with metals such as steel and aluminum, the costs of composite materials are too high.

- The manufacturing processes require precision and experience.

- Composites are more brittle than forged metals. Therefore, they can easily get damaged (Armstrong & Barrett, 1998).

- All resin matrixes and some of the fibers absorb moisture, to some extent affecting properties and dimensional stability of the composites. Therefore, drying process should be applied before the repair treatment.

- In repair treatment, usually, hot curing and special equipments are required. Long time is needed for curing process cycle (Armstrong & Barrett, 1998).

2.3 Classification of Composite Materials

Composite materials can be classified structurally in four main groups:

- Fiber reinforced composites
- Particulate composites
- Hybrid composites
- Laminated composites

2.3.1 Fiber Reinforced Composites

They are obtained by joining fibers and matrixes. Fibers ensure the strength of the material, while matrixes keep fibers all together and distribute the load applied homogeneously between them. Glass fibres, carbon fibres, aramid fibres, boron fibres and graphite fibres are some examples for this group of composite materials (Figure 2.1).

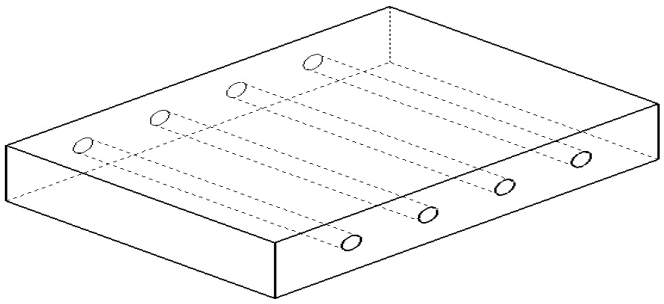

Figure 2.1 A unidirectional fiber reinforced composite.

2.3.2 Particulate Composites

They are obtained by joining one or more materials' particles with another matrix material. For example concrete is a particulate composite which is formed by joining particles of sand and aggregate with water and cement (Figure 2.2).

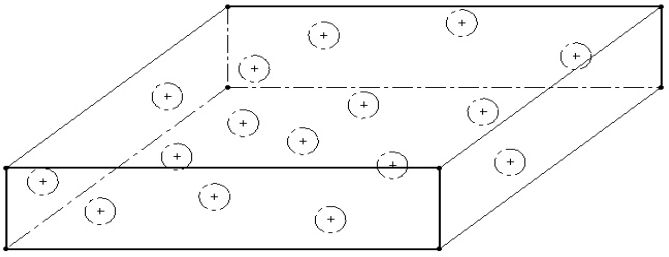

Figure 2.2 Particulate composite.

2.3.3 Hybrid Composites

These composites consist of two or more high performance fibers and resin materials. Most common hybrid composites are carbon-aramid reinforced epoxy and glass-carbon reinforced epoxy (Figure 2.3).

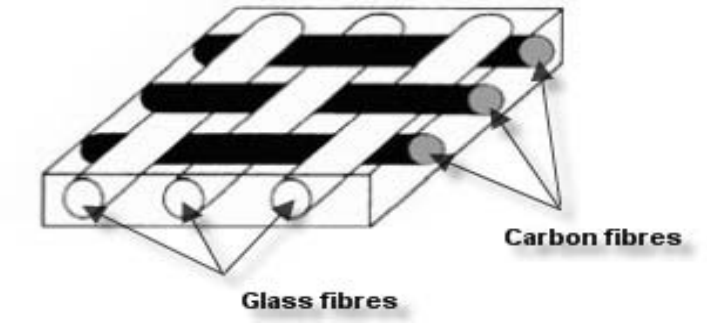

Figure 2.3 A glass – carbon reinforced epoxy hybrid composite.

2.3.4 Laminated Composites

They are obtained by laying at least two fiber reinforced layers; one on the top of the other at same or different directions. By means of layering process, strength, corrosion resistance, thermal insulation and stiffness of composite materials maybe increased. This is the most commonly used type of composites, and is used in the present work.

An x, y, z orthogonal coordinate system is used in analyzing laminates with the z coordinate being perpendicular to the mid plane of the laminate. The orientations of continuous, unidirectional plies are specified by the angle θ (in degree) with respect to the x axis. The angle θ is positive in the counter clockwise direction. The number of plies within a stacking sequence is specified by a numerical subscript. For example $[90_2/0/0/90_2]$ contains four ply groups. The first one contains two plies in 90° direction, the second and third contain one ply in 0° direction and the fourth ply contains two plies making 90° with x-axis (Figure 2.4).

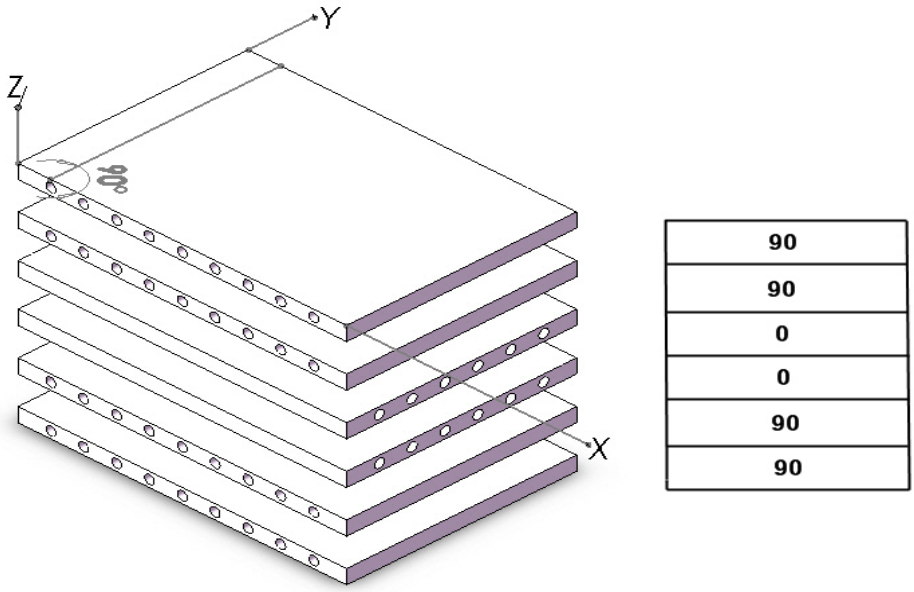

Figure 2.4 The *x*, *y*, *z* laminate coordinate system and the description of the layup in a laminate consisting of unidirectional plies $[90_2/0/0/90_2]$.

There are five types of laminates:

2.3.4.1 Balanced Laminate: In balanced laminates, for every ply in the $+\theta$ direction there is an identical ply in the $-\theta$ direction (Figure 2.5).

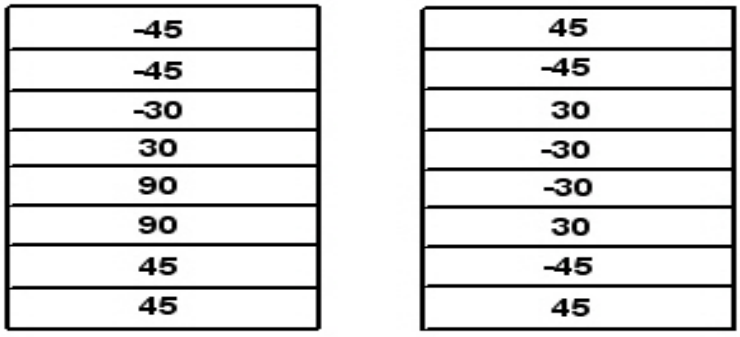

Figure 2.5 Examples of balanced laminates.
$[-45_2/90/30/-30/45]$-left side, $[45/-45/30/-30]_S$-right side.

2.3.4.2 Symmetrical Laminate: When the laminate is symmetrical with respect to the midplane it is referred to as a symmetrical laminate. An example of this type, $[90_2/0/0/90_2]$, is shown in Figure 2.4.

$[90_2/0/0/90_2] = [90_2/0]_S$. In here, "s" indicates symmetry about the midplane.

2.3.4.3 Π / 4 Laminate: Π/4 laminates consist of plies in which the fibers are in the *0°, 45°, 90°* and *-45°* directions. The number of plies in each direction is the same (balanced laminate) In addition, the layup is also symmetrical.

2.3.4.4 Angle-Ply Laminate: Angle-ply laminates consist of plies in the $+\theta$ and $-\theta$ directions. Angle-ply laminates may be symmetrical or unsymmetrical, balanced or unbalanced (Figure 2.6).

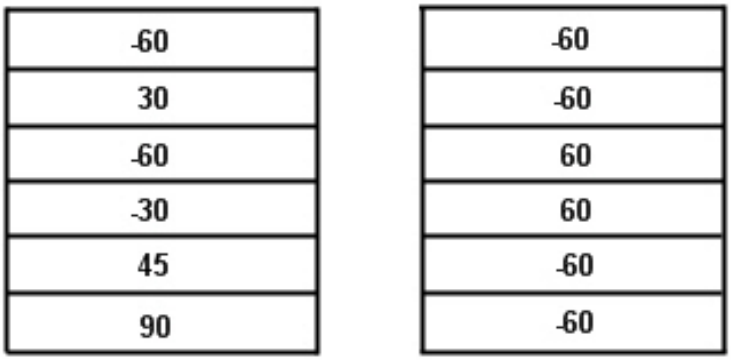

Figure 2.6 Angle-ply laminates [-60/30/-60/-30/45/90] (on the left) and $[-60_2 / 60]_S$ (on the right).

2.3.4.5 Cross-Ply Laminates: In cross-ply laminates fibers are only in the *0°* and *90°* directions. They may be symmetrical or unsymmetrical. Since there is no distinction between the *+0°* and *-0°* and *+90°* and *-90°* directions, cross-ply laminates are also balanced (Figure 2.7) (Kollár & Springer, 2003).

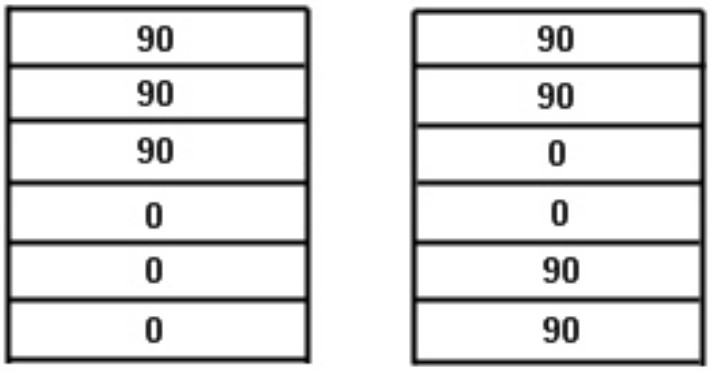

Figure 2.7 Cross–ply laminates $[90_3 / 0_3]$ (on the left) and $[90_2 / 0]_S$ (on the right).

CHAPTER THREE
REPAIR OF COMPOSITE MATERIALS

3.1 Types of Damages in Composite Materials

Most damage to fiber reinforced composites is a result of low velocity and sometimes high velocity impacts. Some types of damages are given below, Figure 3.1 - 3.5.

3.1.1 Dent Damage

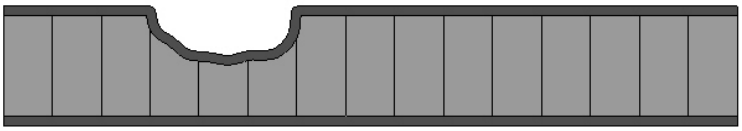

Figure 3.1 Dent that damaged only one skin of a sandwich structure

In dent damage, only one skin of the sandwich structure may be harmed.

3.1.2 Puncture Damage

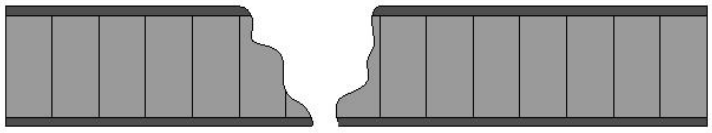

Figure 3.2 Puncture damage in a sandwich structure

In puncture damage, both skins may be harmed.

3.1.3 Delamination

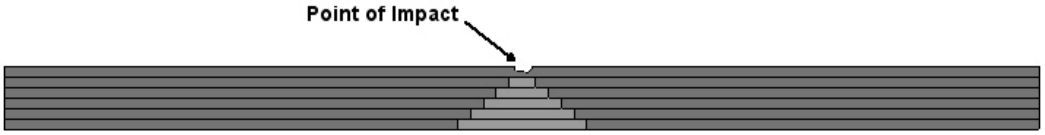

Figure 3.3 Delamination that follows the impact on a laminated composite

Delamination damages may occur between adjacent layer of laminated plates as they subjected to especially impact loadings.

The causes of delamination are below:

- Wrong cure cycle (temperature or pressure)
- Using expired material
- Impacts by foreign objects
- Entrance of humidity
- Dirt while laying the laminates

3.1.4 Laminate Splitting

Figure 3.4 Laminate splitting in a laminated composite

In this type of composite failure, damage does not extend through the full length of the part. The effects on the mechanical performance depend on the length of split relative to the composite thickness.

3.1.5 Heat Damage

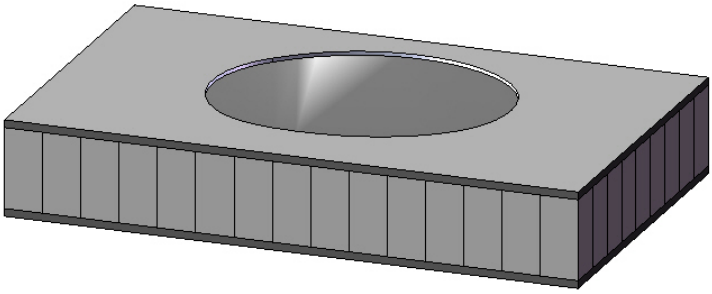

Figure 3.5 Heat damage in a sandwich structure

A local fracture with separation of surface plies. Its effect on the mechanical performance depends on the thickness of the part (Hexcel Composites, 1999).

The causes of heat damage are below:

- Exceeding the cure cycle temperature
- Fall of lightning on some parts of planes
- Sudden increase of voltage seen on the whole surface during the supersonic flights of planes

3.2 Repair Methods

Because of these damages encountered often in application, it has become important to develop repair methods for the damaged composite structures. Although there are many different repair methods, they all have some common principles that are given below:

-All repairs are secondary bonds, so they rely upon the adhesive quality of the resin for their strength.

-Increasing the surface area will increase the strength and the durability of the repair.

-Strive to duplicate the thickness, density and ply orientation of the original laminate to maintain the functionality of the part.

The repair method to be used effectively, depends on the type of damage in spite of these common principles.

3.2.1 Speedtape

Speedtape is a thin aluminium foil that can be supplied in a range of thicknesses, usually from approximately 0.025 to 0.075 mm. After removing the backing sheet and revealing a layer of pressure-sensitive adhesive, the foil can be applied to the surface to prevent water ingress or to prevent loose fibers from lifting according to the need. This is a temporary repair so it provides no strength but prevents minor damage from worsening and thus minimizes the size of the eventual permanent repair. Because of its electrical conductivity, speedtape must not be used on the areas which include electricity (Figure 3.6) (Armstrong & Barrett, 1998).

Figure 3.6 Speedtapes (http://www.packdaily.com, 2009)

3.2.2 Resin Sealing

Resin sealing is a temporary repair in which a repair resin is painted over the damage to retain loose fibers and to prevent the damage from increasing in size (Figure 3.7) (Armstrong & Barrett, 1998).

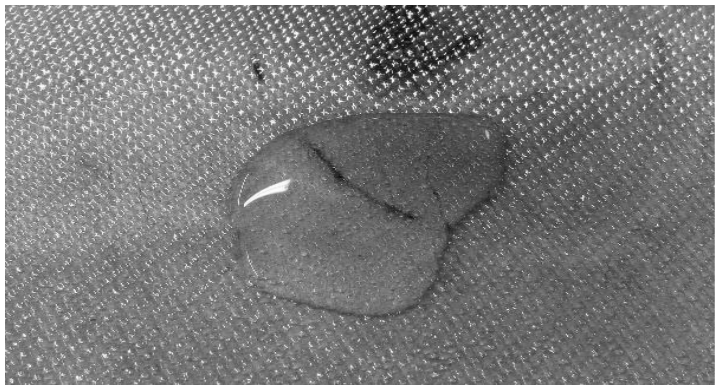

Figure 3.7 Epoxy resin sealer (http://cgi.ebay.es, 2009)

3.2.3 Potted Repairs

Potted repairs are another type of temporary repair which can be applied on small holes found in honeycomb panels. The holes can be filled with suitable potting compounds of the room-temperature curing variety (Figure 3.8) (Armstrong & Barrett, 1998).

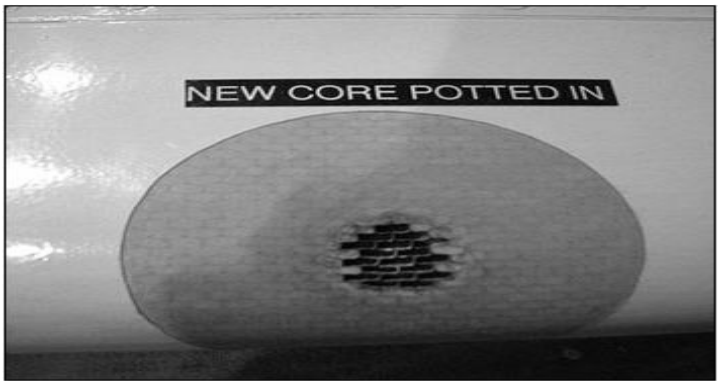

Figure 3.8 Example of a composite sandwich potted repair (www.sandwichpanels.org, 2009)

3.2.4 Room Temperature Wet Lay-Up

Because of its many advantages, this method is one of the most recommended repair methods. It requires no heating except to speed the cure and it always reaches full cure after the required period of time. Vacuum pressure is sufficient for a good bond and additional fabric layers can be used to compensate for any loss of performance. One of the two disadvantages of this method is having a high-temperature performance worse than the original. The other one is the obligation of resin's weighing and mixing accuracy (Armstrong & Barrett, 1998).

3.2.5 Elevated-Temperature Wet Lay-Up

It has all the advantages of room-temperature wet lay-up with the additional advantage of the capability of larger repairs. This method's disadvantage is its heat requirement. Thermocouples must be located correctly to ensure that the minimum temperature for cure is maintained over the entire repair area for the full time of cure (Armstrong & Barrett, 1998).

3.2.6 Pre-Preg Repairs

There are three main form of pre-preg repairs:

- Low temperature pre-pregs curing at approximately 95°C as for the hot-curing wet lay-up repairs.

- 120°C curing pre-pregs may be used to repair parts made at either 120°C or 180°C.
- 180°C pre-pregs may be used to repair parts made at 180°C and must not be used to repair parts made at 120°C.

Pre-preg repairs allow larger repairs and do not require resin mixing. It is clean and easy to work with these repairs. If a repair is made at the original curing temperature, problems occur with honeycomb structures. When the repair area is heated to cure the pre-pregs, the air pressure in the honeycomb cells surrounding the repair rises to a higher pressure than atmospheric and the temperature of cure is 180°C. The external pressure is usually only vacuum, approximately 0.7 bar, and the result is that the skin is blown from the honeycomb around the repair. This means that a larger repair then must be made at 120°C, or tooling must be provided to apply additional pressure above vacuum. One of its disadvantages is the requirement of hot curing. It is difficult to achieve a uniform temperature over the whole repair if there are any heavy members such as ribs, spars, or hinge fittings acting as heat sinks (Armstrong & Barrett, 1998).

3.2.7 Composite Repairs to Metals

3.2.7.1 Boron Repair to Aluminum : This method has been used in the United States and Australia for several years. Examples are repairs to cracks in wing skin stringers on the Lockheed Hercules and repairs to cracks in the magnesium alloy landing wheels of the Macchi trainer. As a result of much successful military and civil experience and research, it is expected that they may eventually become a standard repair technique (Armstrong & Barrett, 1998).

3.2.7.2 Glass Repair to Aluminum : This has been an accepted method of repair for thin aluminum skins in Boeing Structural Repair Manuals (SRMs) for many years (Figure 3.9) (Armstrong & Barrett, 1998).

Figure 3.9 Repair of fatigue-damaged aluminum joints using glass fibre sheets (www.civil.queensu.ca, 2009).

3.2.7.3 Carbon Repair to Aluminum : This method was tried on the wing leading edge panels of the Concorde when cracks developed many years ago. These repairs were successful, with some lasting seven years of longer. Eventually, cracks developed around the patches, and larger metal repairs had to be made. However, none of the repaired cracks suffered any extension (Figure 3.10).

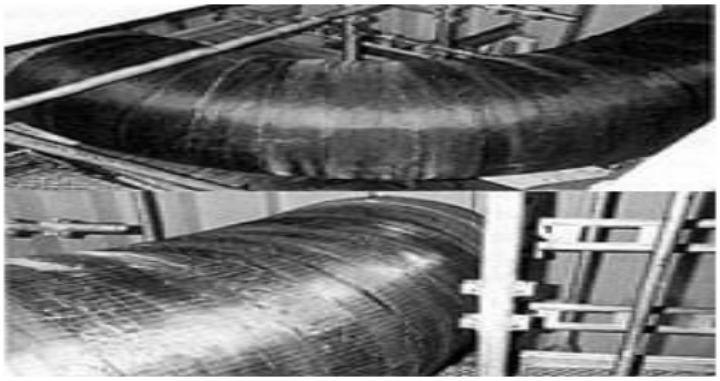

Figure 3.10 Carbon-fibre based pipe repair (www.azom.com, 2009).

It is cheaper than boron and can even use offcuts of dry fabric or pre-preg material. A layer of glass fiber is used as an insulator between the carbon and the aluminum to prevent corrosion, and a tough adhesive is used together with a good metal surface preparation (Armstrong & Barrett, 1998).

3.2.8 Bolted Repair

Bolted repair method is based on the transmission of loadings through the external patches by means of the bolts. A bolted patch repair can be applied to composite panels of various thicknesses and it enables the patch to be removed for maintenance and future inspection. It is generally used when a fast repair is required or in the field repair where less equipments are available.

The major disadvantage of the bolted composite repair is that holes and cutouts cause serious difficulties of stress concentrations due to the geometry discontinuity. Because of this, load transfer paths through mechanical fasteners are not efficient and can cause local overloads and damage in brittle composites. Fig 3.11 shows the possible failure modes of bolted composite joints as a function of the joint geometry and the fiber patterns.

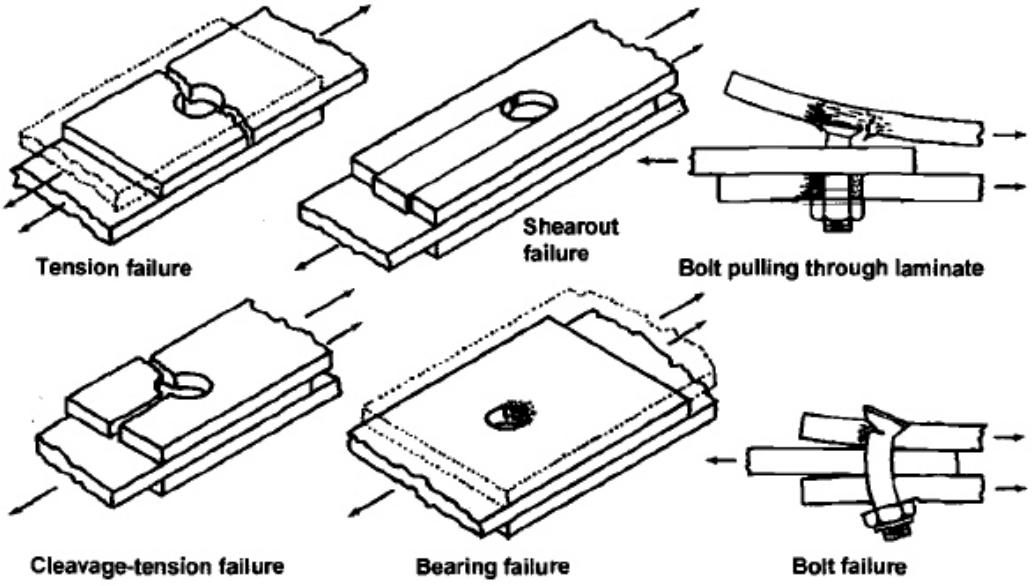

Figure 3.11 Failure modes of bolted composite joints (Hart-Smith, 2004).

3.2.9 Bonded Repair

Bonded repair is one of most common repair techniques carried out in composite structures, either in the condition of temporary repair or permanent repair. The stress

concentrations in this repair type are homogeneous because it provides more uniform and efficient load transfer into the repair patch than mechanical fastening. Also there is no distortion of material properties as is often the case in a welded joint. One of the disadvantages of this repair type is its inability to be disassembled, in case of inspection or maintenance.

Bonded repairs are not generally recommended when:

- Stringent cleaning and processing steps can not be adhered to, within a controlled environment.
- The structure to be repaired can not withstand the high cure temperatures required for bonded patch repairs.
- The structure to be repaired is subjected to very high loads for which mechanical joints may be more efficient.
- The repair will be exposed to high humidity that can prevent achievement and maintenance of a good quality bond (Duong & Wang, 2007).

As a temporary repair, the repair procedure for this method is as follows: the damaged area is removed by cutting a circular hole in the plate, then the hole is cleaned and a circular patch applied. This type of repair is also called as external bonded repair.

As a permanent repair, the repair procedure is more complex and expensive. Installation process controls are very stringent; advanced materials and processes are required. This type of repair is also called as flush patch repairs. Scarf repair and stepped-lap repair are commonly used flush patch repairs.

3.2.9.1 Scarf Repair: A scarf joint is a flush patch repair, where the bondline is at a set angle between the two laminates. The scarf repair patch is adhesively bonded to the parent material and can be used to recover a large percentage of the original parent laminate's stiffness and strength, while maintaining the parent material's original contour.

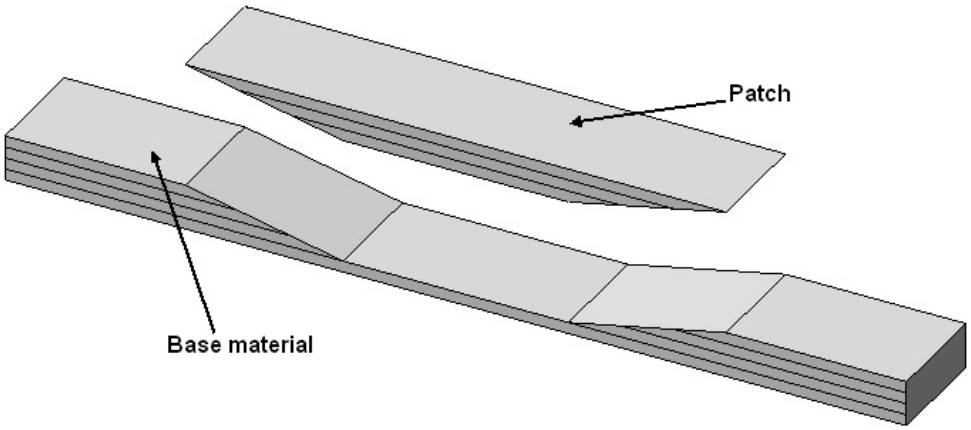

Figure 3.12 Schematic illustration of a scarf repair.

The scarf ratio can vary from 10:1 to 50:1 but the slope angle of 20:1 is often preferred. In these ratios, the small number refers to the thickness of the patch and the big number refers to the horizontal edge.

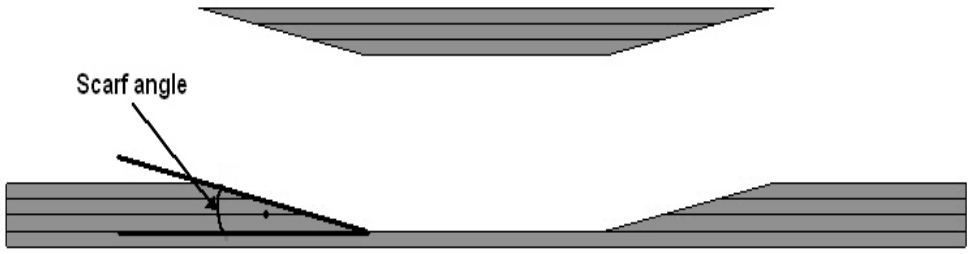

Figure 3.13 Scarf angle on the base material

There are two different types of scarf repair in practice. Boeing practice is to lay the smallest patch first, whereas Airbus practice is to lay the largest patch first. Both methods have been tested and found that both produce good joints (Figure 3.14).

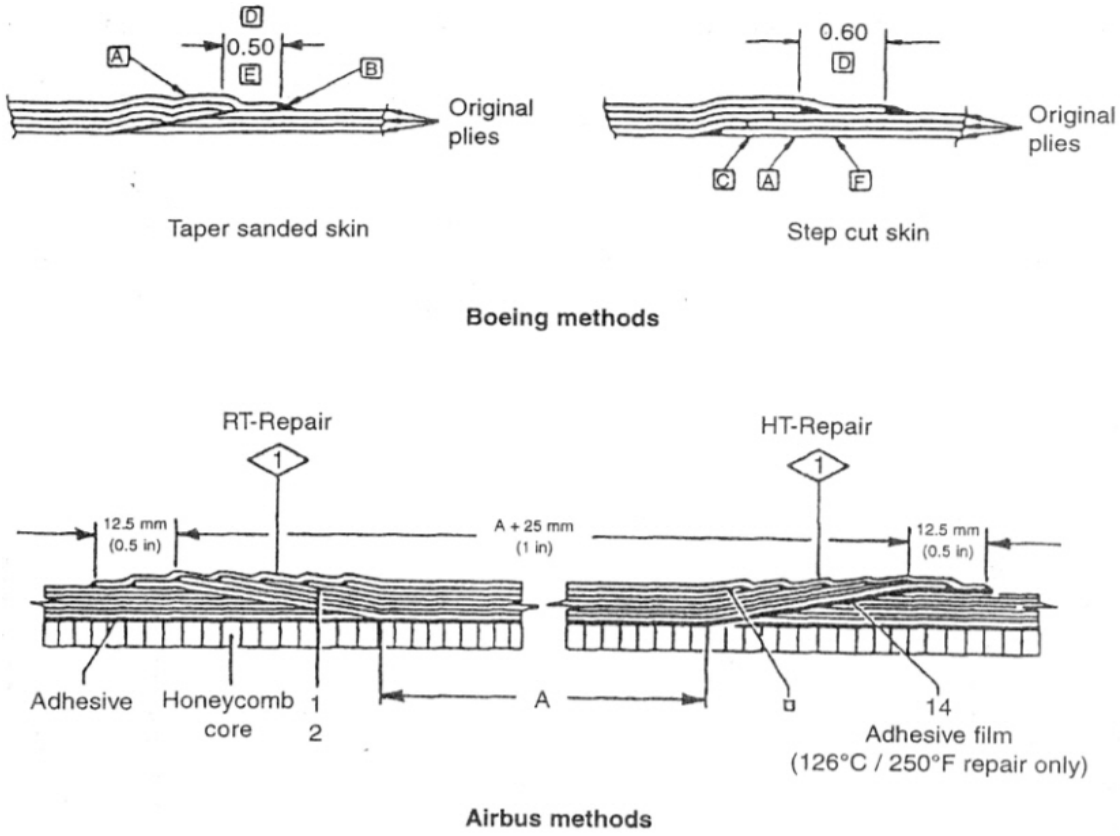

Figure 3.14 Boeing versus Airbus scarf joint lay-up methods for repair of damaged panels (Armstrong & Barrett, 1998)

The advantages of the scarf repair include a relatively uniform shear stress distribution in the adhesive and a low peel stress. Additional plies can be laid over the ends of the laps to minimize peel effects. Scarf joints tend to fail at the ends after long periods of time at high loads in fatigue tests. This is another advantage of scarf repair because the beginnings of failure can be seen in adequate time to perform further repair.

One of the disadvantages of scarf repair is that they are difficult and time-consuming to manufacture. Another one is the requirement of the removal of a large amount of undamaged material to form the required taper angle.

3.2.9.2 Stepped-Lap Repair: A stepped-lap joint is also a flush bond between two separate laminates, where the joint is a series of overlap steps. Overlaps usually are 12.5 or 25 mm per ply and each repair ply should be oriented to lap onto a ply of

similar orientation. Since the load-carrying capacity of each step does not increase indefinitely with length, it is necessary to increase the number of steps in a stepped-lap joint to maximize its load-carrying ability.

If correctly designed, a stepped-lap joint repair can have an equal load-carrying capability to the scarf repair. Although they may be more easily manufactured than scarf joints, they are more difficult and time-consuming to manufacture than external patch repairs. They are not too difficult on fiberglass and aramid skins; however, the individual layers are more difficult to see with carbon composites, and extra care is required to avoid cutting through one ply into the next ply.

There are two types of stepped-lap repair: single-lap and double-lap. Both of these techniques have advantages and disadvantages against each other.

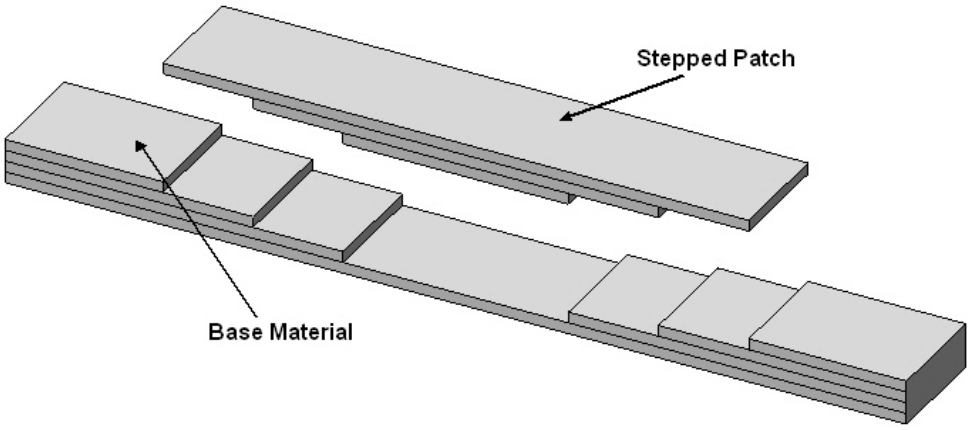

Figure 3.15 Schematic illustration of stepped-lap repair

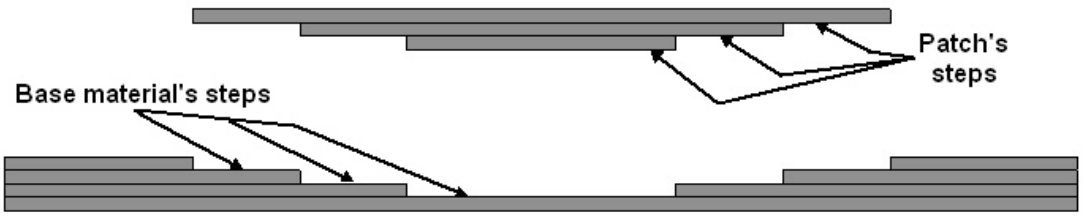

Figure 3.16 The repair steps on both base material and the patch

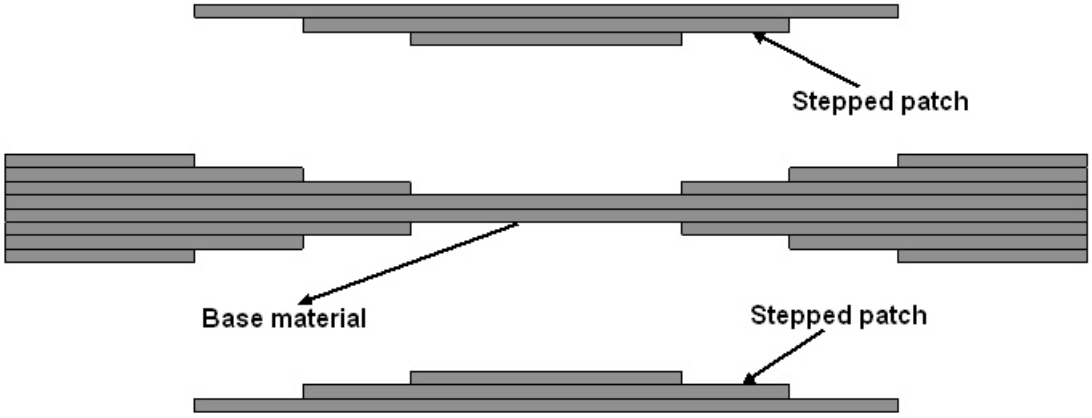

Figure 3.17 Schematic illustration of double-lap repair

CHAPTER FOUR
PREPARATION OF THE SPECIMENS AND EXPERIMENTAL TESTS

There are many composite manufacturing methods such as tow placement, compression molding, autoclave bonding, filament winding, oven curing, lay-up methods which are hand lay-up(wet and pre-preg) and automated lay-up, pultrusion, spray-up, vacuum bagging, resin transfer molding and vacuum assisted resin infusion moulding(VARIM). In this study, the laminated composite specimens are prepared by vacuum assisted resin infusion moulding method, so we will only dwell on this manufacturing method.

4.1 Vacuum Assisted Resin Infusion Moulding Method

Vacuum assisted resin infusion technique has become popular in manufacturing of composites. In the literature, vacuum infusion is known under different acronyms (Ragondet, 2005). The most popular terms to describe vacuum infusion processes are:

- VARTM-Vacuum Assisted Resin Transfer Moulding (Koefoed, 2003),
- VARIM-Vacuum Assisted Resin Infusion Moulding (Khattab, 2005),
- SCRIMP™-Seemann Composites Resin Infusion Moulding Process (Boh et al., 2005),
- VBRTM-Vacuum Bag Resin Transfer Moulding (Kang et al., 2001),
- VARI-Vacuum Assisted Resin Infusion process (Tzetzis et al., 2008) and so on.

All involve basically the same technology, and describe methods based on the impregnation of a dry reinforcement by liquid thermoset resin driven under vacuum (Gören & Ataş, 2008).

Before explaining this method in detail, it will be useful to learn the basic terminology. The following list of terminology is taken from SAE AIR 4844 Composites and Metal Bonding Glossary:

- Bagging : Applying an impermeable layer of film over an uncured part and sealing
- Bagging Film Sealant Tape : This is a soft mastic tape which is slightly tacky and is used to seal bagging film to repair area or to join parts of the bagging film if two sheets are used.
- Bag Side : The side of the part that is cured against the vacuum bag.
- Bleeder : A nonstructural layer of material used in the manufacture of repair of composite parts to allow the escape of excess gas and resin during the cure. They also absorb excess resin present in some composite lay-ups. The bleeder is removed after curing and is not part of the final composite.
- Bridging : 1) A condition in which fibers do not move into or conform to radii and corners during molding, resulting in voids and dimensional control problems. 2) A condition in which one or more plies of a pre-preg span a radius step of the fluted core of a radome without full contact. 3) A condition where part of a vacuum bag does not go down into a radius and thus no pressure can be applied at that point. When making up a vacuum bag, it is important to avoid this.
- Debulking : Compacting of a thick laminate under moderate heat and pressure(i.e., noncuring conditions and/or vacuum to remove most of the air) to ensure seating on the tool and prevent wrinkles. This process ay be carried out by debulking a few layers at a time, in a series of debulking operations, rather than by debulking the whole lay-up in one operation.
- Mold Release Agent : A lubricant, liquid, or powder (often silicone oil and waxes) used to prevent sticking of molded articles in the cavity.
- Parting Agent : A material, liquid or solid film used on the tool surface to ease removal of the assembly. Teflon film is an example.
- Peel Ply : A layer of open-weave material, usually fiberglass or heat-set nylon, applied directly to the surface of the laminate. The peel ply is removed from the cured laminate immediately before bonding operations. It provides a resin-rich, clean, uncontaminated surface for subsequent bonding or painting.
- Release Film : An impermeable layer of film that does not bond to the resin being cured.

- Resin Distribution Medium : A highly permeable layer placed on the top of the perform spreads the resin quickly over the lateral extent of the part.
- Separator : A permeable layer that also acts as a release film. They separate the laminate from the distribution medium. The separators are perforated to ensure that any trapped air or volatiles, which may compromise the quality of the laminate, are removed.
- Vacuum Bag : The plastic or rubber layer used to cover the part to enable a vacuum to be drawn.

Note : All vacuum bagging fabrics, films, and tapes must remain dry to prevent adding moisture to the repair. The storage environment should be noncontaminating and free of dust and oil. Materials should be protected from exhaust fumes, soot, oils, sprayed silicone, mist, rain, or other obvious particulate contaminants.

The basic schema of VARIM and the components of the infusion process utilized in this work are illustrated in Figure 4.1 and 4.2.

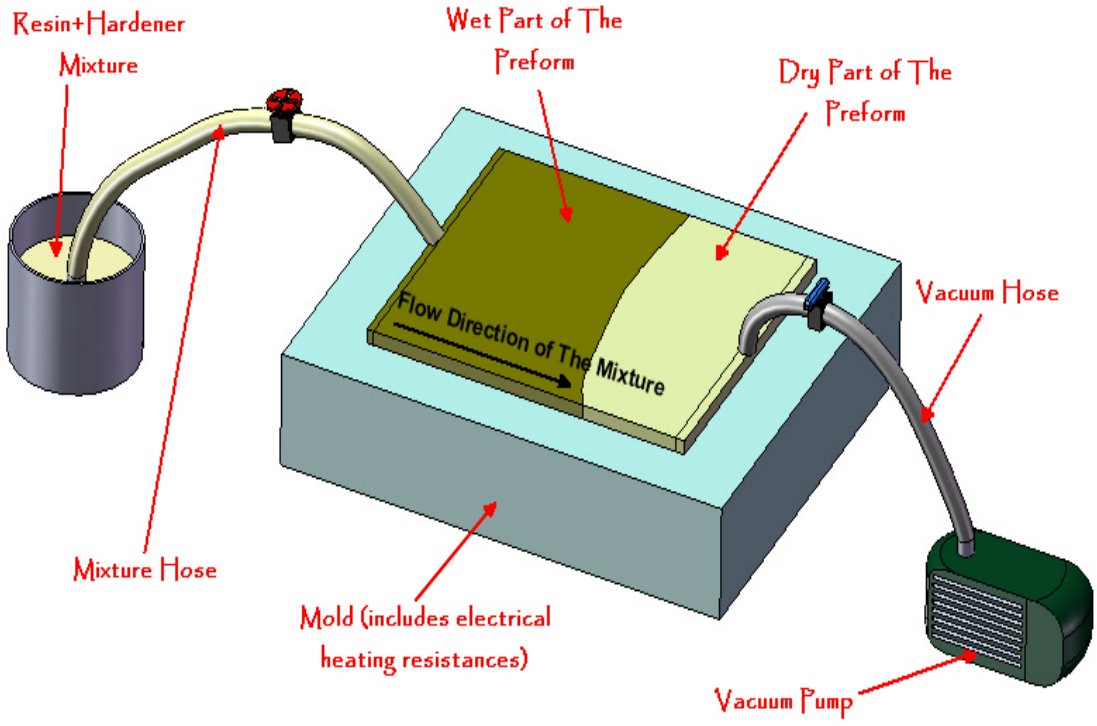

Figure 4.1 Schematic illustration of the vacuum assisted resin infusion moulding

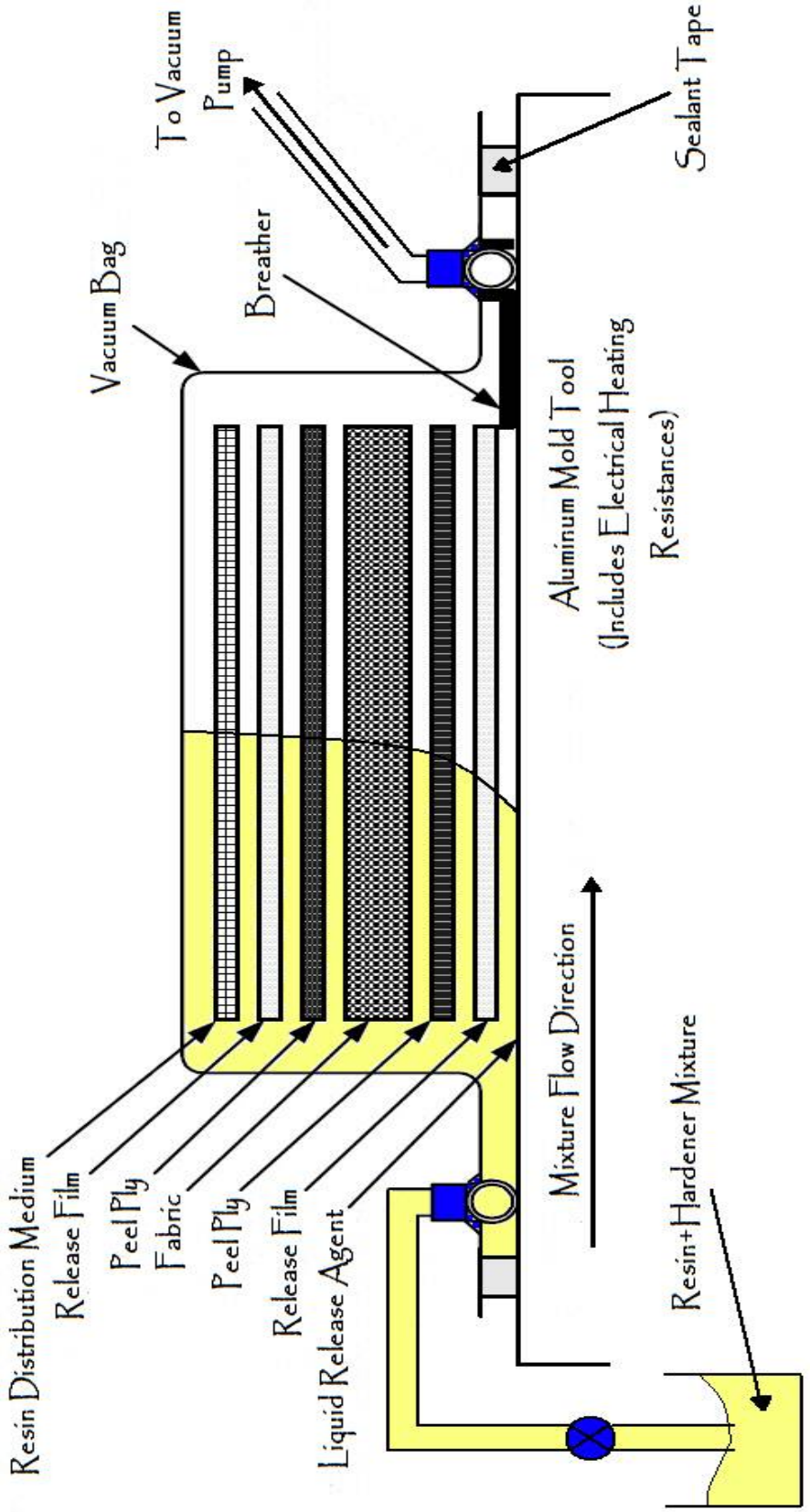

Fig.ure 4.2 Illustration of the components of VARIM process

4.1.1 Automatic Control of the VARIM System

The VARIM production system in this thesis consists of an 1800 mm x 1500 mm table capable of providing control of temperature and vacuum.

Electrical heating resistances are used for heating of table. The temperature control is achieved by means of acquiring temperatures using thermocouples located beneath the table surface. By using a PLC and a touch screen, the system is capable of adjusting the desired temperatures, up to 200°C, and corresponding time intervals for curing cycles. The main advantage of using a PLC as a control unit for this system is to have a flexible control for changing the cure conditions.

During the curing phase of the manufacturing process all regions in a composite part are supposed to be almost at the same curing conditions. By only this way the composite part can gain optimum mechanical properties. So, a uniform temperature distribution through the heating table surface is too important. Because of this the current VARIM table is divided into 8 regions. Each region has an independent closed loop temperature control system, to achieve a constant temperature throughout tool surface. Thus, it becomes possible to control the heating resistances and hence the temperature distribution. Operator can easily program the cure cycle and temperatures using a man machine interface as can be seen in Figure 4.3. This figure gives the block diagram of the control system. However, in this figure, only temperature control system of region 1 is shown to avoid repetition. The controller (PLC) of the VARIM system is programmed to send the realtime temperature values of all regions to the MMI and to a PC for data logging (Gören & Ataş, 2008).

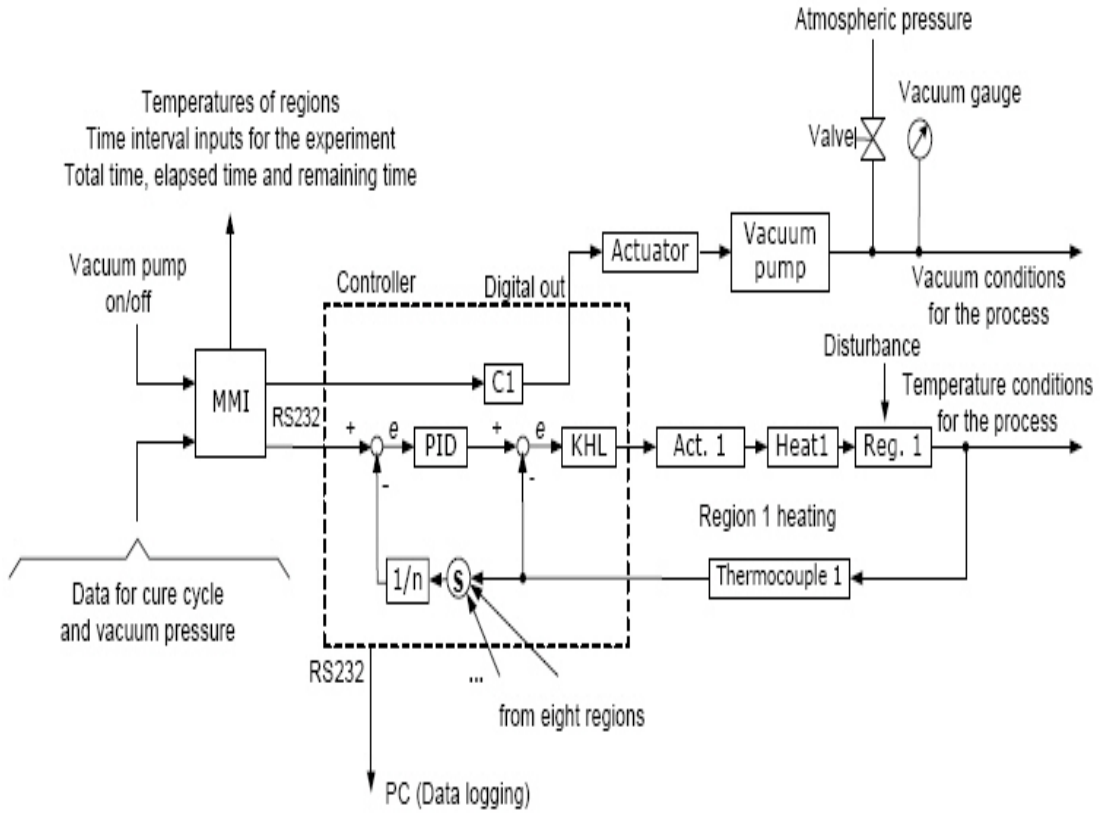

Figure 4.3 Block diagram of the automatic control of the VARIM system (Gören & Ataş, 2008)

The control panel enables to set two or three temperature steps in a cure cycle. Figure 4.4 and 4.5 show schematic illustration of a cure cycle with two temperature steps and variation of vacuum versus time. Cure cycles are formed generally based on the instructions and recommendations of resin suppliers.

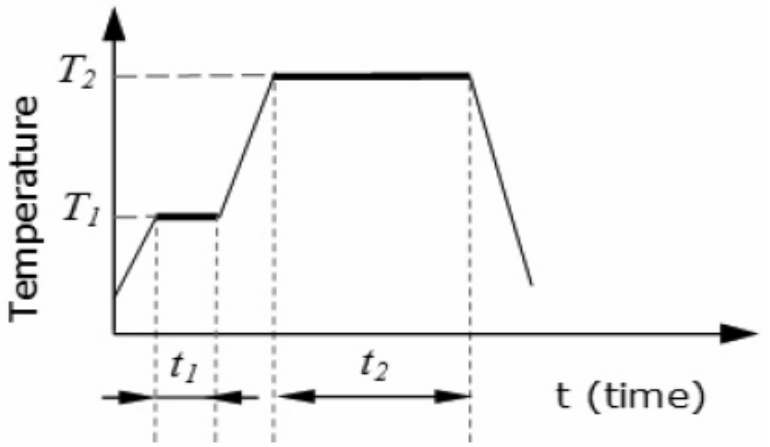

Figure 4.4 The schematic diagram of a cure cycle (Gören & Ataş, 2008)

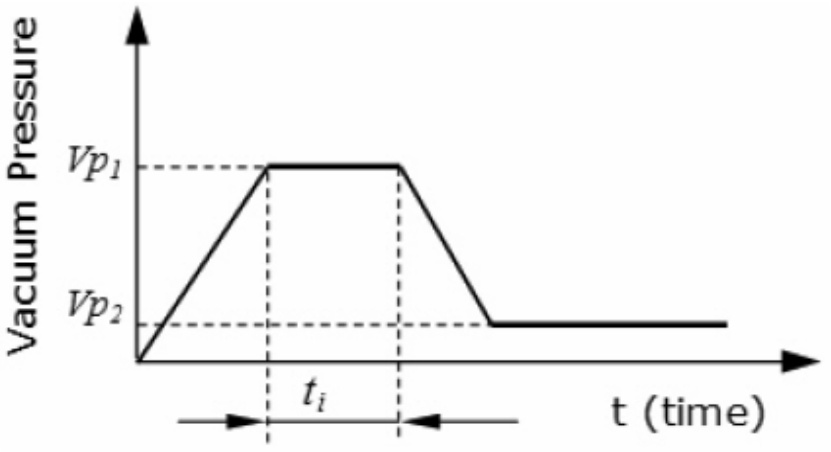

Figure 4.5 The schematic diagram of vacuum variation (Gören & Ataş, 2008)

In Figures 4.4 and 4.5, T_1 and T_2 stand for successive curing temperatures corresponding to t_1 and t_2 time intervals while V_{P1} for the vacuum value during t_i time interval, time of resin infusion, and V_{P2} for the vacuum value applied throughout curing process.

In addition to temperature control system, the VARIM system is also equipped with a vacuum pump and a vacuum regulator with a vacuum gauge. The vacuum pump can be initialized and halted using touch screen. Vacuum value can be adjusted manually by the operator before or during the production. A number of parameters such as the permeability of the reinforcement stack, the resin viscosity and inlet geometry may cause unpredictable cases or problems affects resin flow in the resin infusion moulding process and hence quality of the production. Therefore, the vacuum regulation system is included in PLC program as an open loop control. It enables to control vacuum manually during infusion moulding process (Gören & Ataş, 2008).

4.1.2 Manufacturing a Laminated Composite Plate with Stepped Patch by Using VARIM Method

There are two ways to produce specimen with stepped patch. First one is cutting the desired area of composite plate in a stepped way after the manufacture, filling this part with glass-fiber fabric and impregnating resin. Second one is, cutting fiber fabrics in a stepped way to represent a stepped patch before fabrication. Because there are some difficulties on treating the thin specimens in a stepped way after the manufacture, the second method is improved during this study and it enables to work with thin specimens. Here, manufacturing process of a composite plate with stepped patch (second way) by using VARIM method is explained step by step. Sixteen plies of woven fabric and epoxy resin is used for this production.

Step by step manufacturing of the repaired composite parts can be summarized as:

Step 1, Fiber fabrics are cut in a stepped way layer by layer.

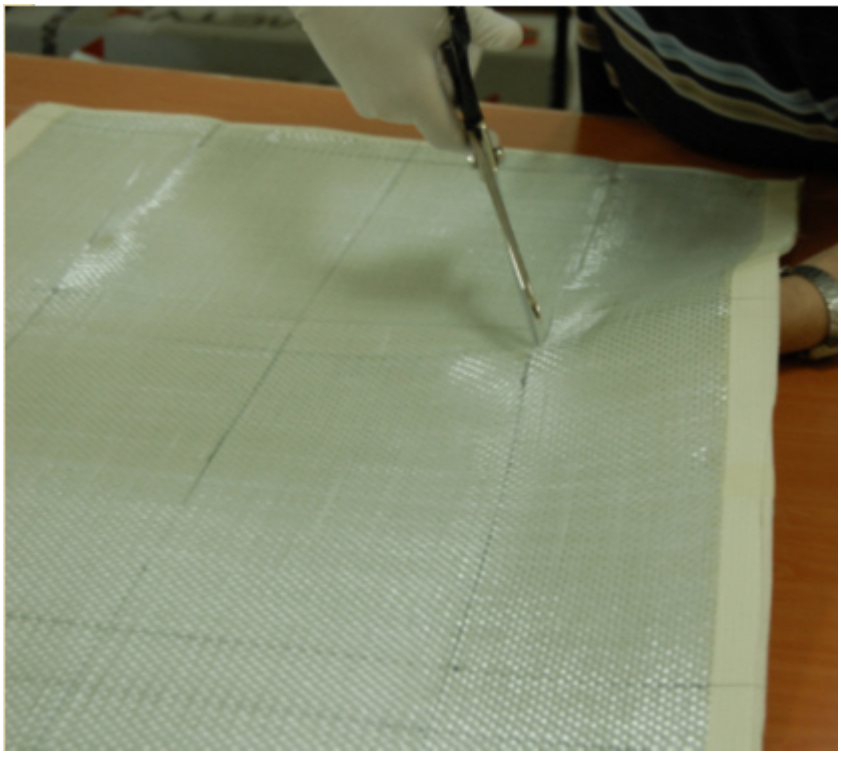

Figure 4.6 Cutting woven fabrics in a stepped way layer by layer.

Step 2, The heating mold (table) is coated with a release agent.

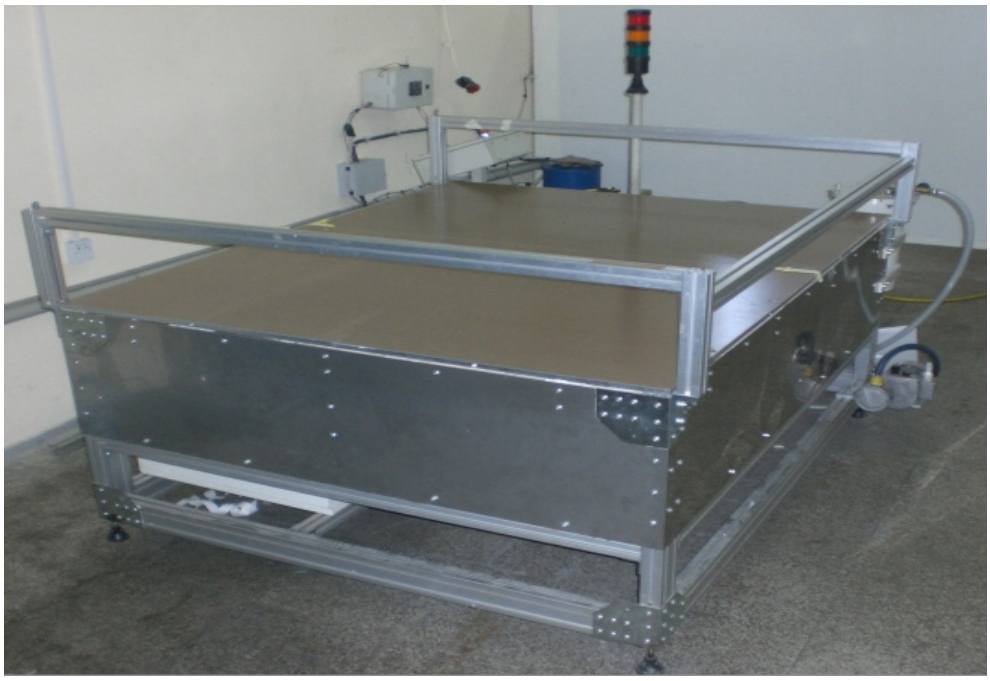

Figure 4.7 Heating table.

Step 3, 6 plies of fibers with 0° orientation are placed onto the table.

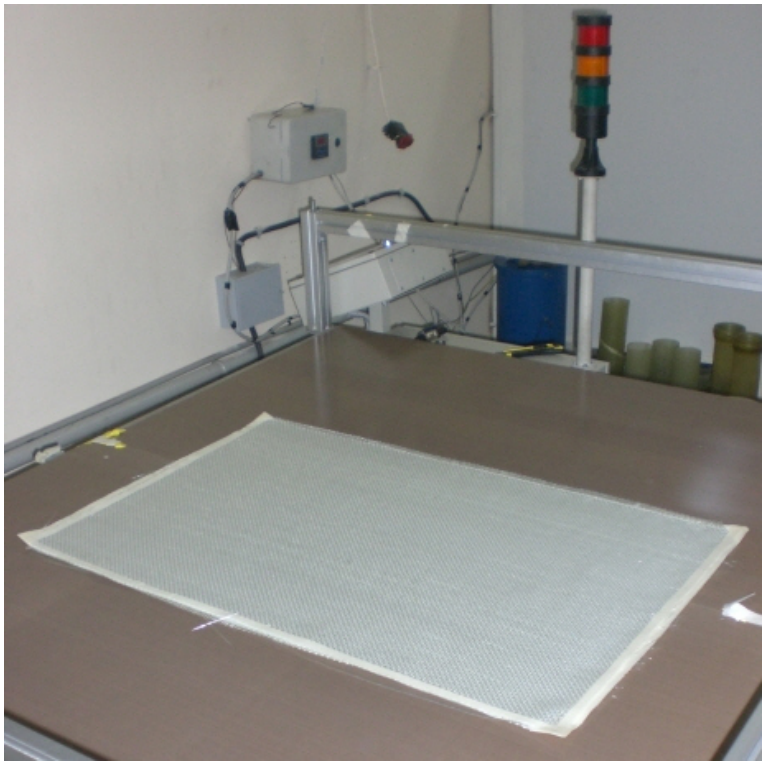

Figure 4.8 Fiber plies placed on the table.

Step 4, Peel ply is placed on the fiber plies.

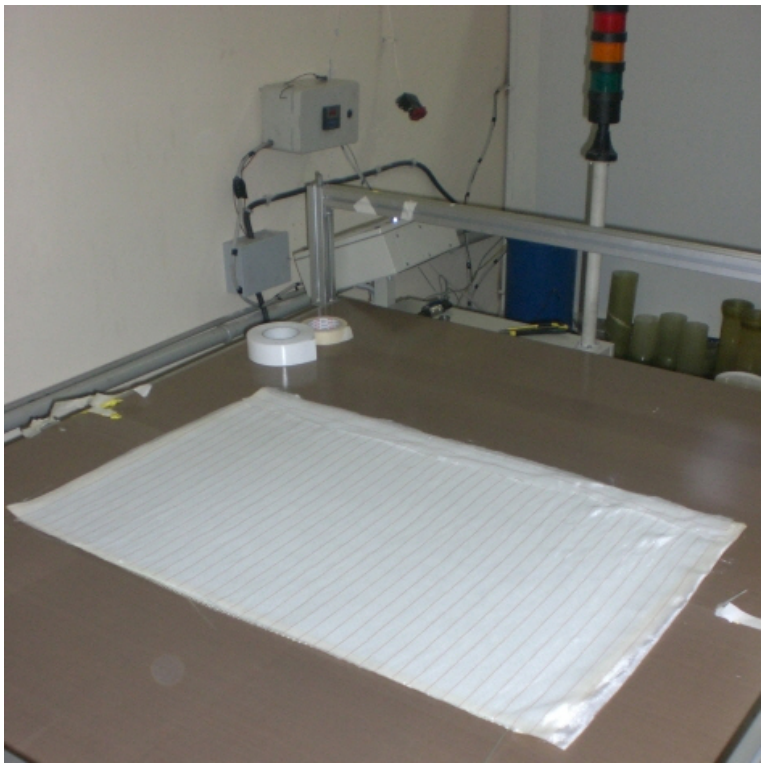

Figure 4.9 Peel ply placed on fiber plies

Step 5, Release film is placed on the peel ply.

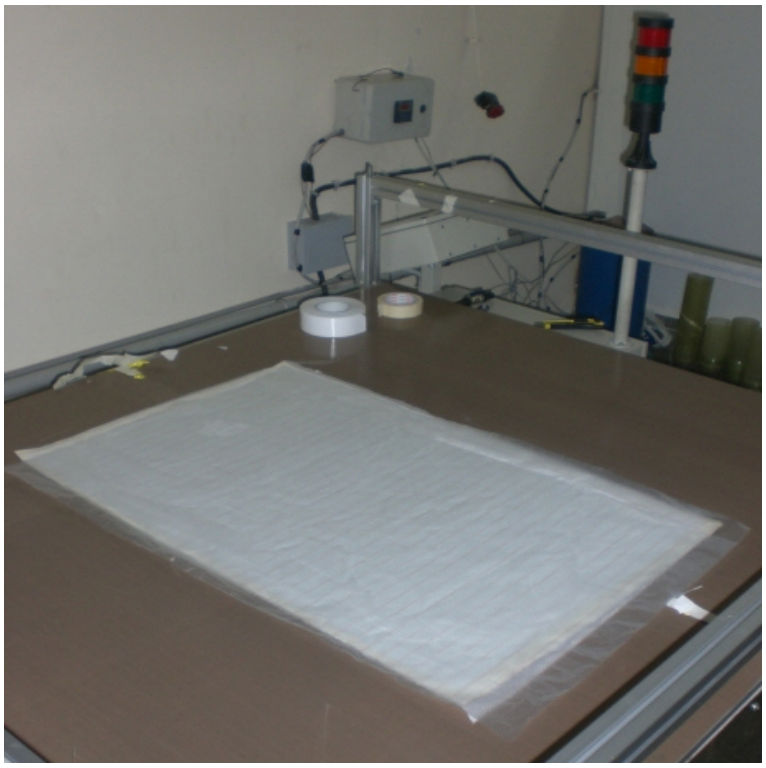

Figure 4.10 Release film placed on peel ply

Step 6, Resin distribution medium is placed on the release film.

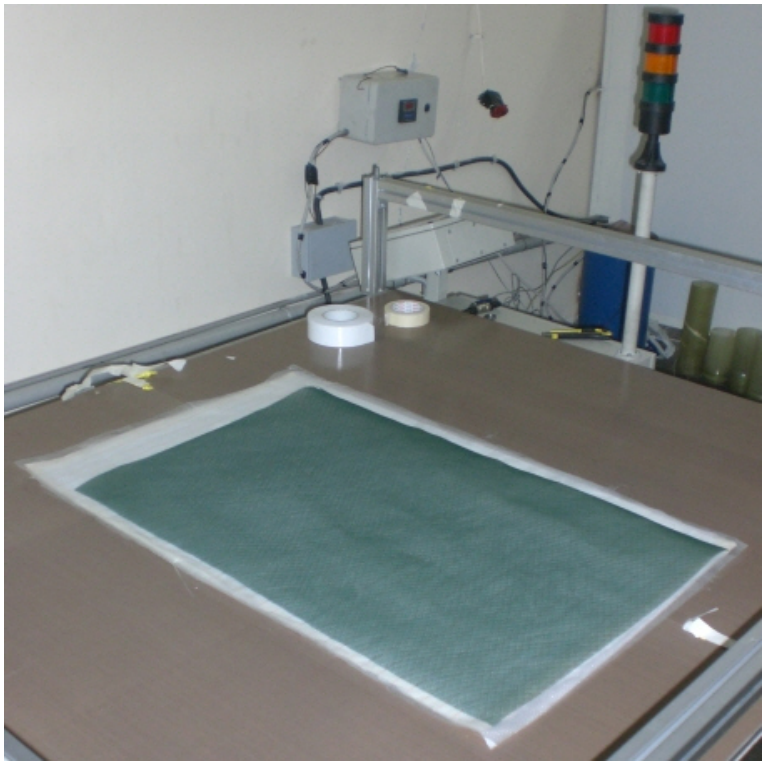

Figure 4.11 Resin distribution medium placed on release film.

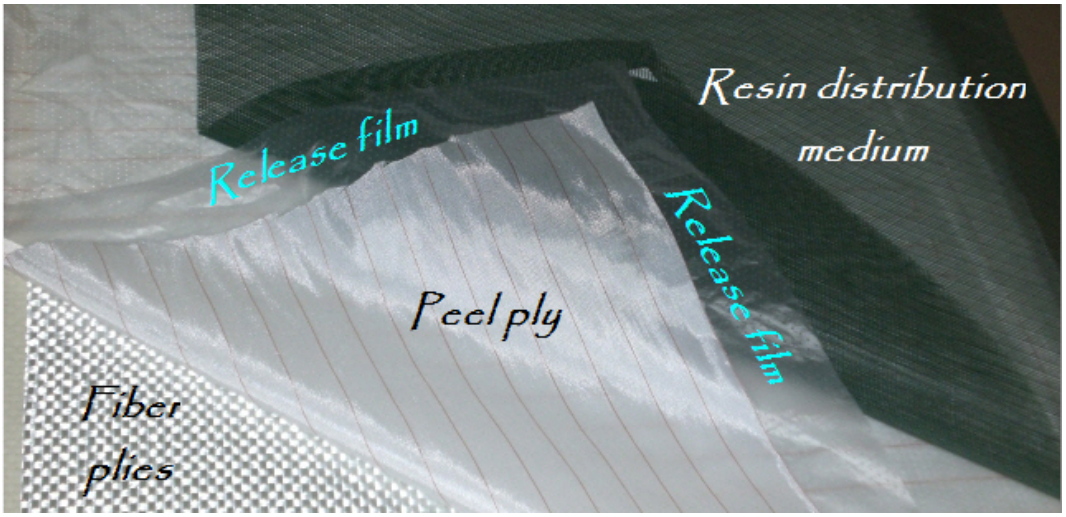

Figure 4.12 Exploded view of the goods used in fabrication.

Step 7, Spiral hoses, which are connected to each other with a T pipe, are placed on the right side of resin distribution medium. Because of the gap between the diameters of spiral hoses and the T pipe, the tips of the spiral hoses are wrapped with tape to fill the gap.

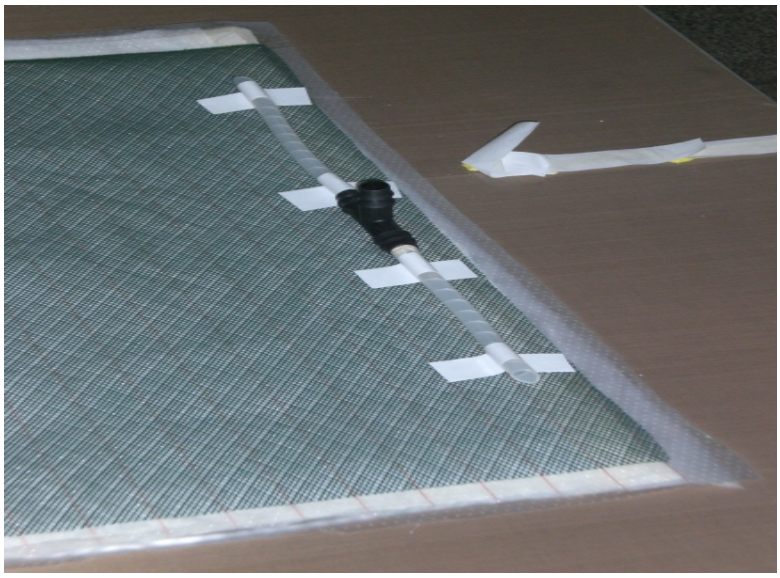

Figure 4.13 The T pipe and spiral hoses placed on the right part of resin distribution medium.

Step 8, Spiral hoses, are placed on teflon film, nearly 5 cm away from left edge of fibers. For continuity of vacuum, breather materials were used. The distance between fibers and hoses is left to prevent excess resin from flowing into the vacuum hose.

Figure 4.14 “T” pipe and spiral hoses placed on the table

Step 9, The stack prepared for resin infusion was surrounded by double sided sealant tapes.

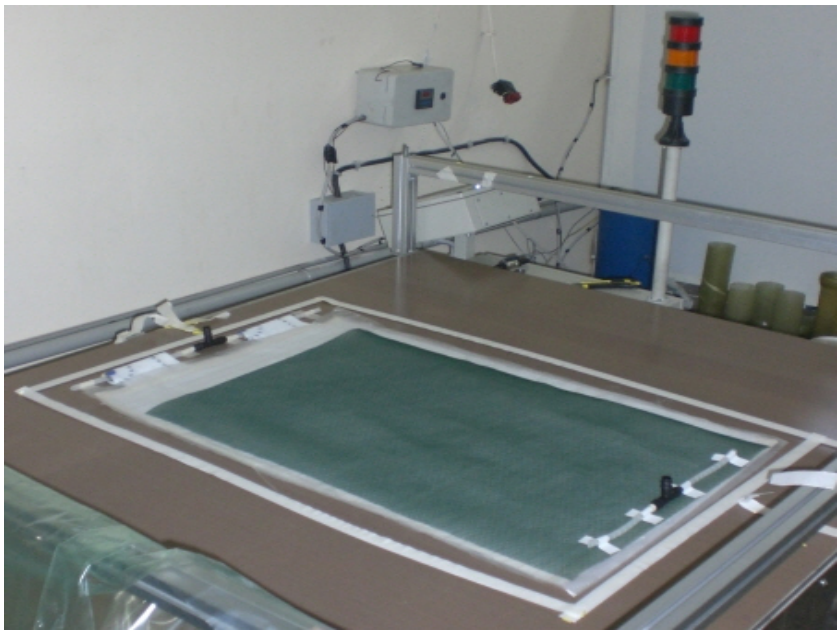

Figure 4.15 Double sided sealant tapes

Step 10, After removing the top part of the sealant tape, vacuum bag is placed and pasted on it carefully. Only two holes were left around T pipes for connection of vacuum line and resin inlet hoses. By this way all materials were covered with vacuum bag.

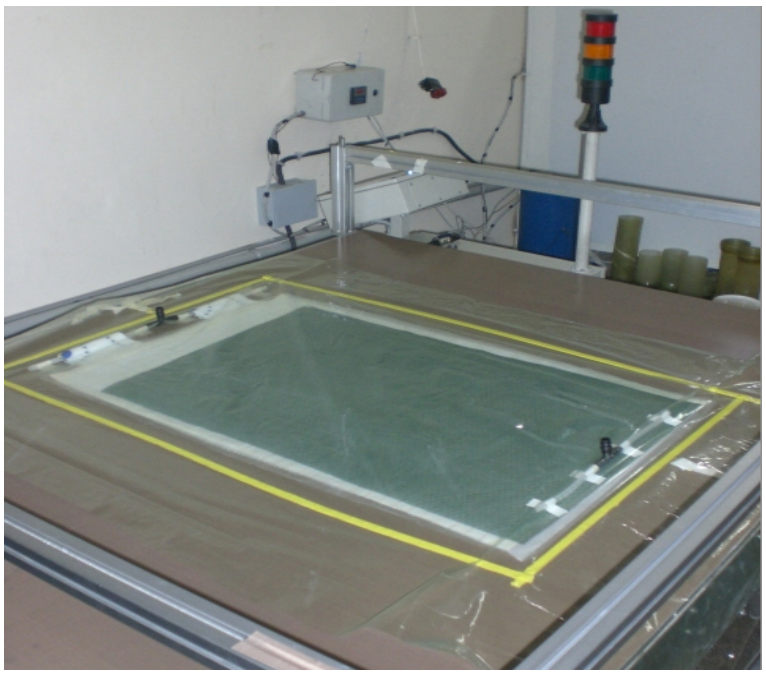

Figure 4.16 Vacuum bagging.

Step 11, Vacuum and resin hoses were connected with the left T pipes by using clamps. Sealant tape is pasted on the connection part of the T pipe and vacuum hose to prevent any vacuum leakage. Also vacuum and resin hoses were fixed to the security bar with sticky tape.

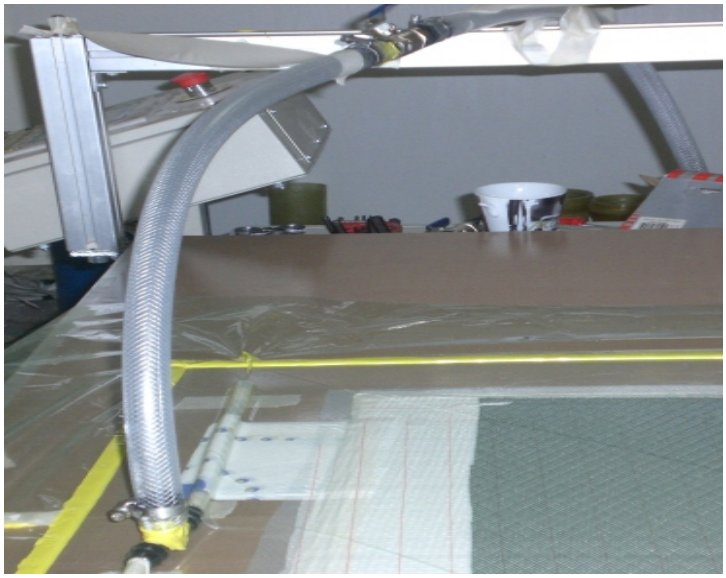

Figure 4.17 Vacuum hose connected with the left T pipe

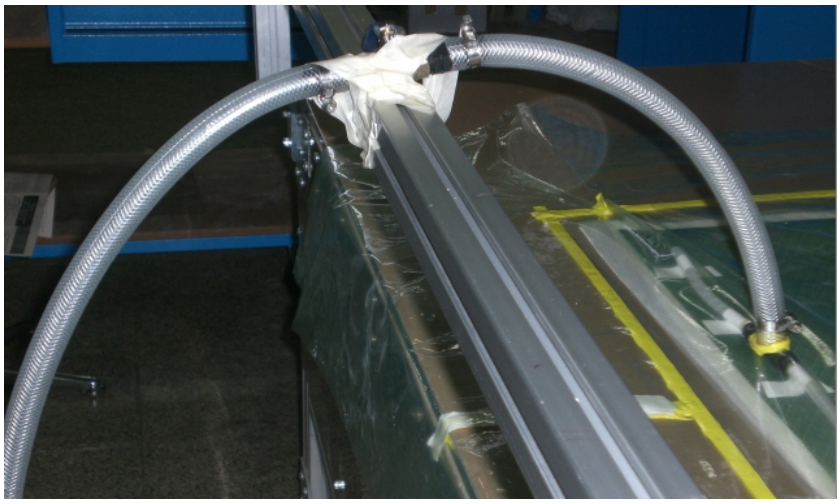

Fig. 4.18 Resin hose connected with the right T pipe

Step 12, Checking vacuum whether there is any leakages or not by using a PLC touch panel. Some detailed pictures of PLC are shown below.

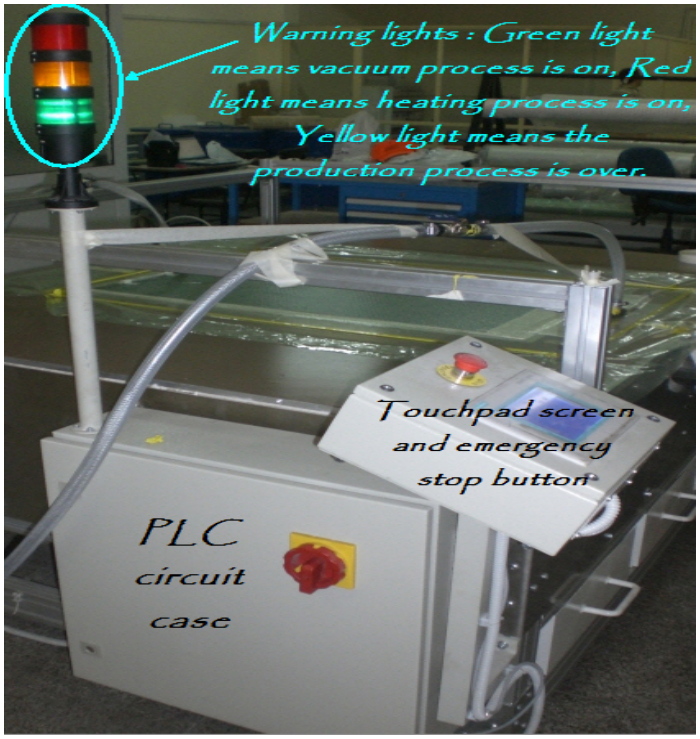

Figure 4.19 Basic figure of PLC with control pad

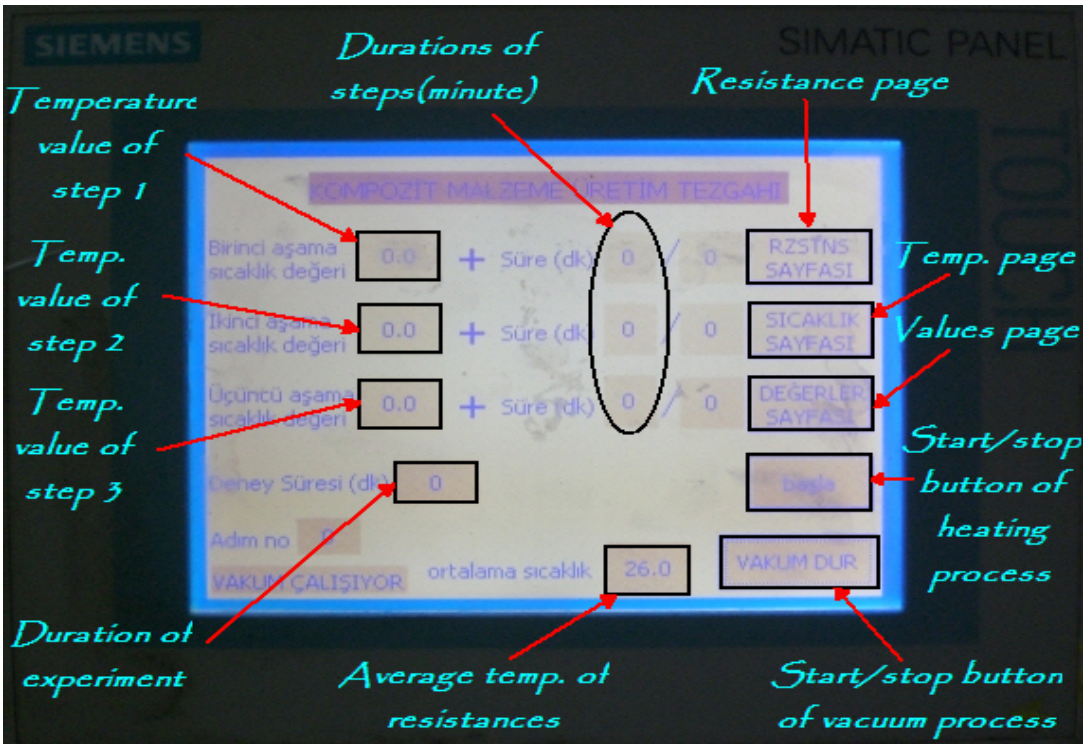

Figure 4.20 Touchpad control screen (before the beginning of the process) and the explanations of the buttons

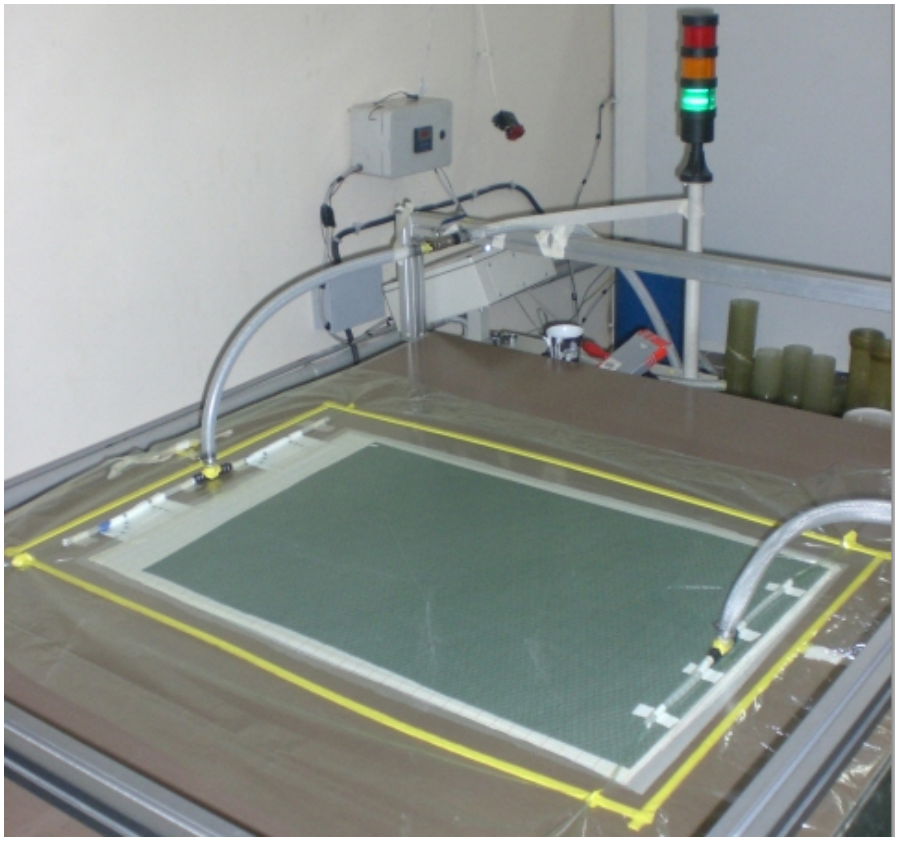

Figure 4.21 Appearance of materials after vacuum process start

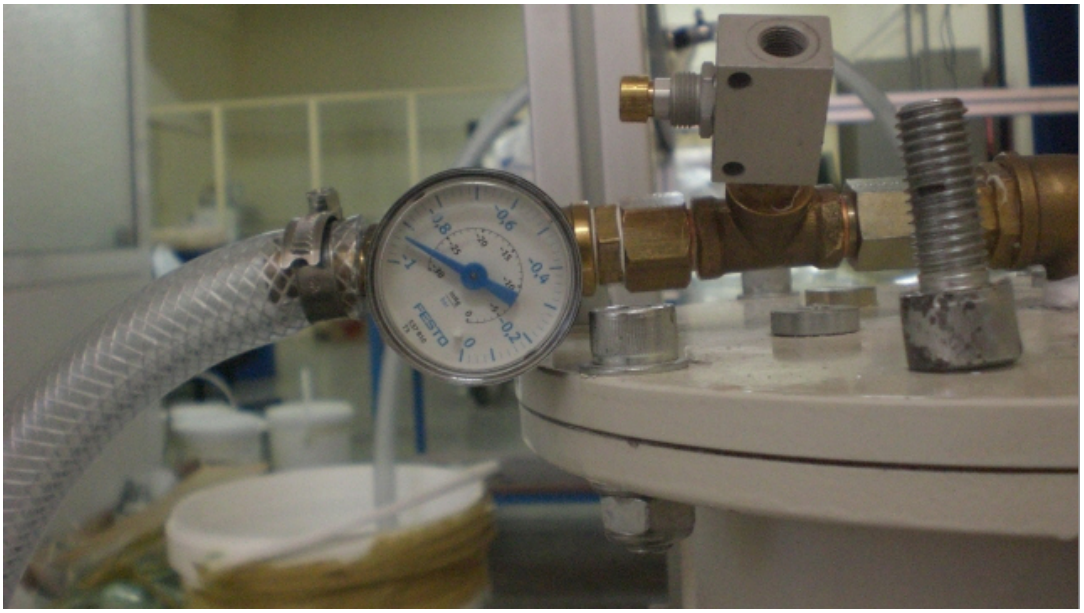

Figure 4.22 Vacuum pressure indicator

Step 13, After reaching the desired vacuum pressure and being sure that there are no leakages in the vacuum bag, the necessary curing process steps are entered in the PLC. There are two curing process steps in this production: The first one is standing 30 minutes at 50°C. The second one is standing by 120 minutes at 90°C.

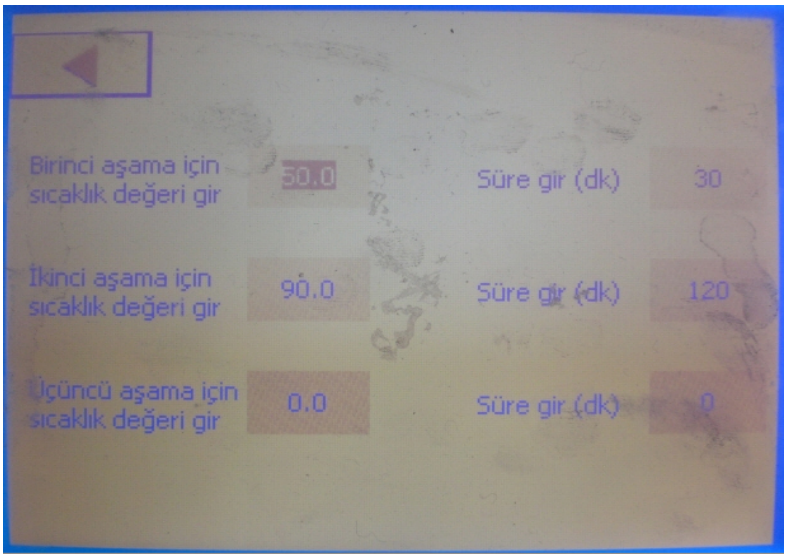

Figure 4. 23 Program screen that two curing steps with durations and temperatures entered

Step 14, While the average temperature of 8 resistances were increasing up to 50°C, resin and hardener are added in a container with a ratio of 3/1 (resin=3x, hardener=x). After that, the mixture is scrambled with a mixer for 5 minutes (till the temperature of resistances is reached at 50°C).

Figure 4.24 Scrambling the resin and hardener with a mixer

Step 15, When the average temperature of resistances is reached at 50°C, the resin infusion process is initiated. The advance of resin and hardener mixture from resin infusion hose to vacuum hose, can be seen in the next four pictures.

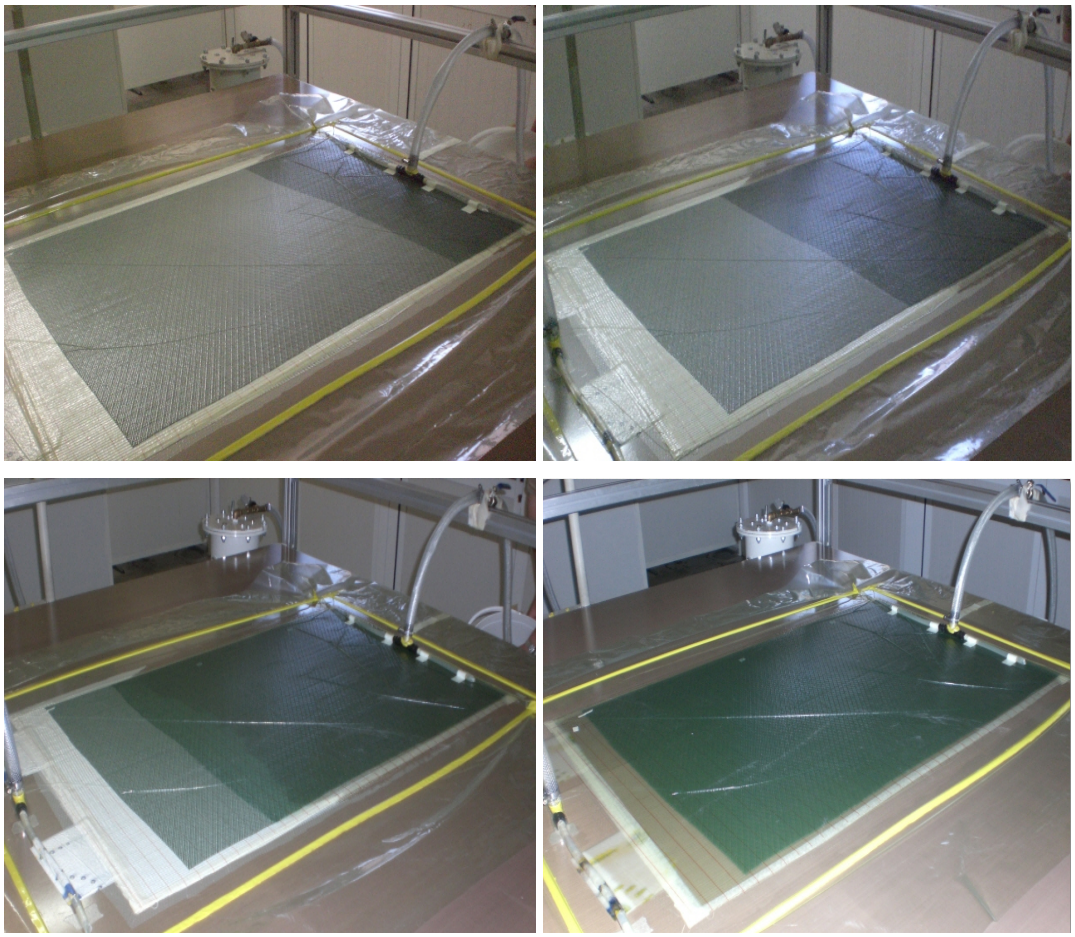

Figure 4.25 Advance of the resin and hardener mixture from resin infusion hose to vacuum hose

Step 16, When the impregnation of resin and hardener mixture is completed, the resin hose valve was closed. Then the curing process was checked in every 10-15 minutes till the end.

Figure 4.26 The general appearance of the production at the curing process

Step 17 (Final Step), When the curing process is over, the PLC was shut down. After gradual cooking of the composite stack, the produced parts were removed from the production table.

Figure 4.27 The final appearance of the composite plate that is manufactured by VARIM method

In this study, three types of specimens, including specimen with no patch, with two stepped patch and with three stepped patch were manufactured with VARIM method for the tensile tests. Specimen with no patch consisted of 16 identical plies. Specimen with two stepped patch was produced by placing 4 continuous plies in the bottom, 6 plies that have 50 mm wide discontinuous area in the middle and 6 plies that have 130 mm discontinuous area on the top. Three stepped patch repair was also performed in a similar way as illustrated in Figure 4. 27.

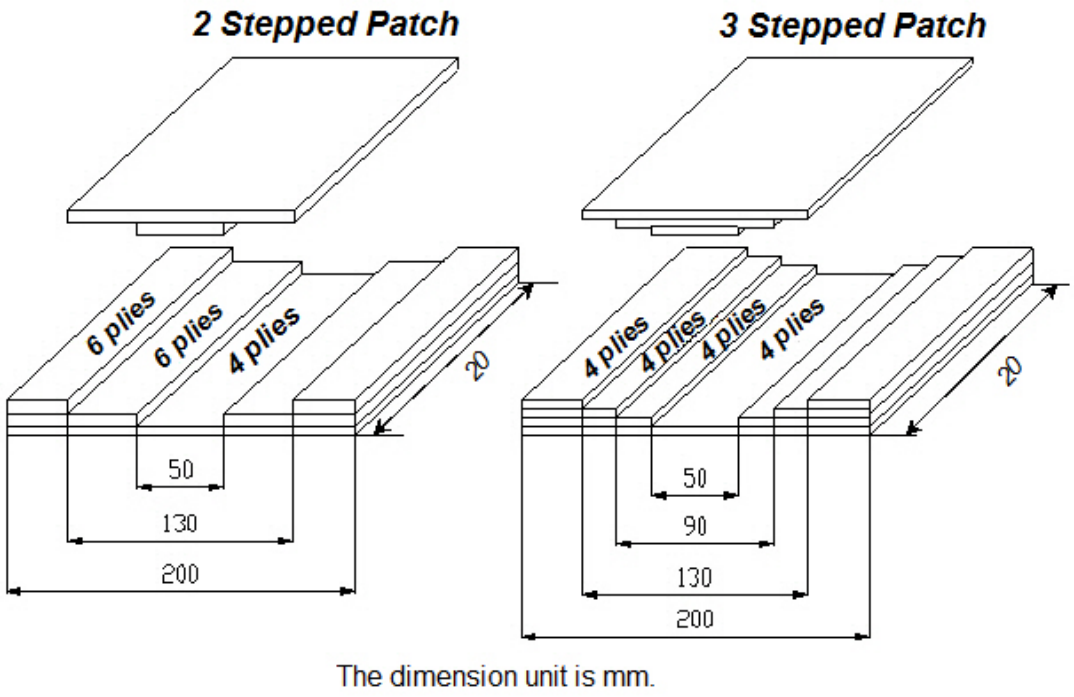

Figure 4.28 Producing the two stepped patch and three stepped patch

Woven glass-fibers were used in fabrication. The determined mechanical properties of the composite plates are listed below.

Table 4.1 Mechanical properties of woven glass-fiber plates

Young's Modulus X (E_1)	*20 GPa*
Young's Modulus Y (E_2)	*19 GPa*
Young's Modulus Z (E_3)	*8 GPa*
Shear Modulus XY (G_{12})	*4,2 GPa*
Shear Modulus YZ (G_{23})	*4,2 GPa*
Shear Modulus XZ (G_{13})	*4,2 GPa*
Poisson's Ratio XY (ν_{12})	*0,13*
Poisson's Ratio YZ (ν_{23})	*0,38*
Poisson's Ratio XZ (ν_{13})	*0,38*
Mass density (ρ)	*1,9 gr/cm³*
Longitudinal Tensile Strength X_T	*302 MPa*
Longitudinal Compressive St. X_C	*299 MPa*
Ply Shear Strength	*69 MPa*
Transverse Tensile Strength Y_T	*64 MPa*
Transverse Compressive St. Y_C	*124 MPa*

4.1.3 Tensile Tests and Results

Tensile tests are performed according to the ASTM D-3039 standards. In the tests a Shimadzu AUTOGRAPH AG-IS Series universal tension test machine with video extensometer and 100kN load cell are used. Trapezium computer software is used for controlling the machine and transmitting data. The tests are performed at room temperature and 2 mm/min of crosshead speed.

From the tension tests, maximum tensile loads of three different specimens are shown in Figure 4.28. Fracture surfaces of specimens are shown in

Figure 4.29. As it can be seen from the figures, fractures have occurred in patch areas. In two stepped patched specimen, fracture has occurred around points of steps. In three stepped patched specimen, fracture has occurred again around points of steps. Comparison of the fracture strengths shows that three stepped patched composites have higher strengths than two stepped patched ones.

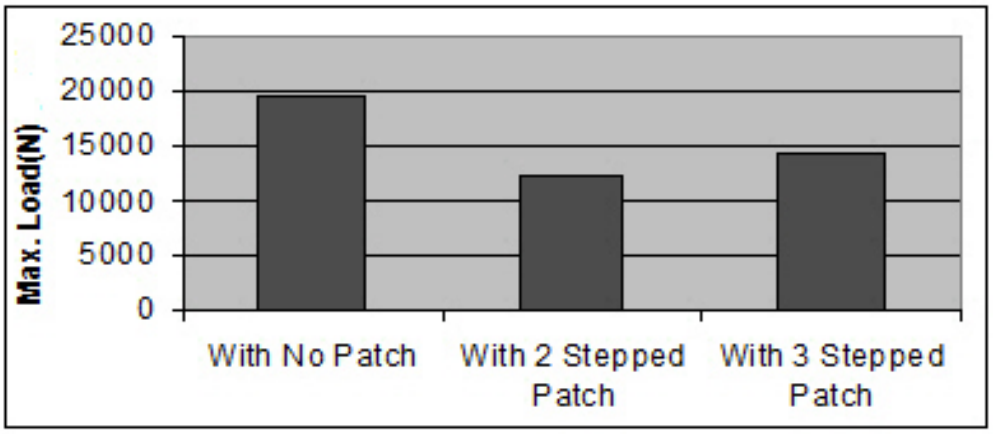

Figure 4.29 Tension load capacity of woven glass/epoxy composites produced by VARIM.

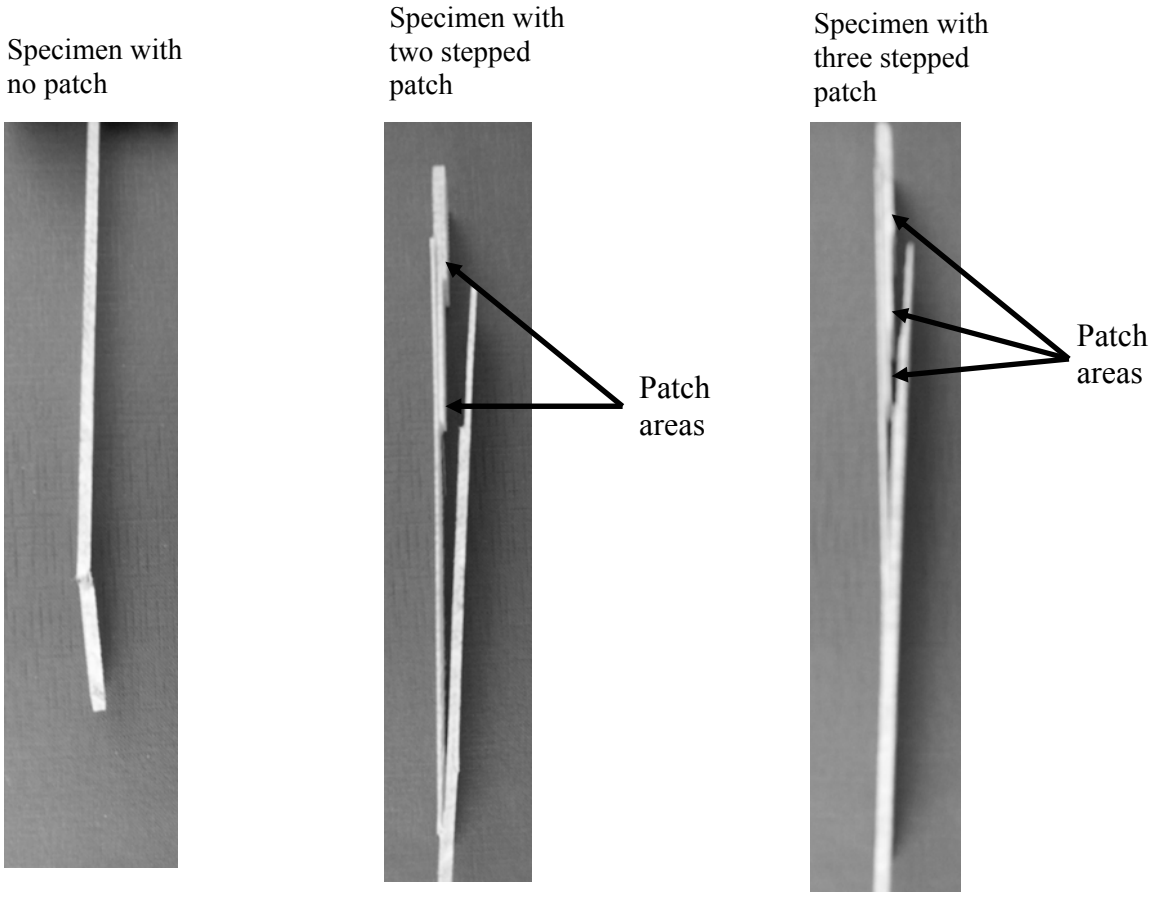

Figure 4.30 Fracture surfaces of woven glass/epoxy composite specimens after the tension

CHAPTER FIVE
NUMERICAL ANALYSIS WITH LUSAS

The objective of this chapter is to analyze the three main repair types (no patched, 2 stepped patched, 3 stepped patched) of composite specimens numerically.

5.1 What is LUSAS?

LUSAS is a software which provides solutions for linear and nonlinear stress, dynamic and thermal/field problems by using finite element method. The finite element method has become a powerful tool for the numerical solution of a wide range of engineering problems. Application range is from deformation and stress analysis of automotive, aircraft, building, and bridge structures to field analysis of heat flux, fluid flow, magnetic flux, seepage, and other flow problems. In this method of analysis, a complex region defining a continuum is discretized into simple geometric shapes called finite elements. The material properties and the governing relationships are considered over these elements and expressed in terms of unknown values at element corners. An assembly process, duly considering the loading and constraints, results in a set of equations. Solution of these equations gives the approximate behavior of the continuum (Chandrupatla, 1991).

The two main components of the LUSAS system are:

-LUSAS Modeller: an interactive graphical user interface for model building and viewing of results from an analysis.

- LUSAS Solver - a finite element analysis engine that carries out the analysis of the problem defined in LUSAS Modeller.

Each of the analysis involve three main stages:

-Modelling : Modelling involves creating a geometric representation of a structure and defining its characteristic behaviour in terms of its physical properties such as material, loading and support.

-Running The Analysis : Once the modelling process is complete, the model is passed to LUSAS Solver for analysis. Then LUSAS Solver creates results that are automatically loaded and can be viewed in the next stage.

-Viewing The Results : Once LUSAS Solver has analysed the problem, the results become available in LUSAS Modeller. Results are available to be viewed in many different ways, and the results can, if desired, be combined with attribute visualisation to make a plot.

5.2 Informations About the Analysis Executed with LUSAS

In the analysis of repaired samples nonlinear solution option of LUSAS was utilized.

5.2.1 What is Nonlinear Analysis?

Linear finite element analysis assumes that all materials are linear elastic in behaviour and that deformations are small enough to not significantly affect the overall behaviour of the structure. Obviously, this description applies to very few situations in the real world, but with a few restrictions and assumptions linear analysis will suffice for the majority of engineering applications.

The following indicate that a nonlinear finite element analysis is required:

- Gross changes in geometry
- Permanent deformations
- Structural cracks
- Buckling
- Stresses greater than the yield stress
- Contact between component parts

Three types of nonlinear analysis may be modelled using LUSAS:

- Geometric Nonlinearity e.g. large deflection or rotation, large strain, non-conservative loading.
- Boundary Nonlinearity e.g. lift-off supports, general contact, compressional load transfer, dynamic impact.
- Material Nonlinearity e.g. plasticity, fracture/cracking, damage, creep, volumetric crushing, rubber material.

5.2.2 Nonlinear Solution Procedures

For nonlinear analysis, since it is no longer possible to directly obtain a stress distribution which equilibrates a given set of external loads, a solution procedure is usually adopted in which the total required load is applied in a number of increments.

Within each increment a linear prediction of the nonlinear response is made, and subsequent iterative corrections are performed in order to restore equilibrium by the elimination of the residual or out of balance forces.

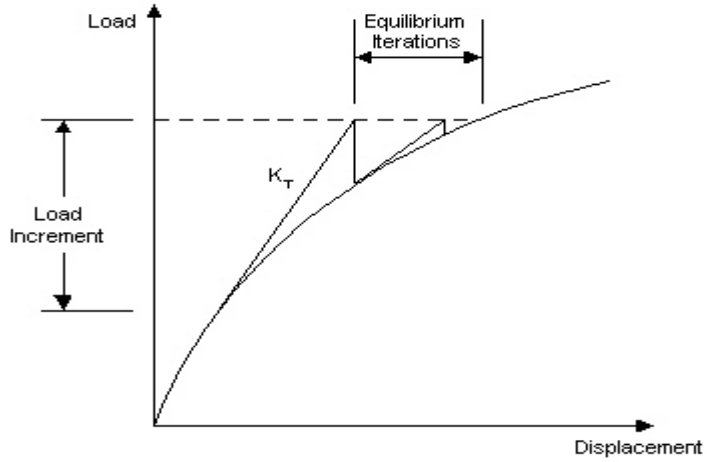

Figure 5.1 Load-displacement graph of a nonlinear analysis
(LUSAS Modeller Online Help)

The iterative corrections are referred to some form of convergence criteria which indicates to what extent an equilibrium state has been achieved. Such a solution procedure is therefore commonly referred to as an incremental - iterative (or

predictor-corrector) method shown in Figure 5.1. In LUSAS, the nonlinear solution is based on the Newton-Raphson procedure. The details of the solution procedure are controlled using the nonlinear control properties assigned to loadcase.

For the analysis of nonlinear problems, the solution procedure adopted may be of significance to the results obtained. In order to reduce this dependence, wherever possible, nonlinear control properties incorporate a series of generally applicable default settings, and automatically activated facilities.

5.2.2.1 Iterative Procedures

In LUSAS the incremental-iterative solution is based on Newton-Raphson iterations. In the Newton-Raphson procedure an initial prediction of the incremental solution is based on the tangent stiffness from which incremental displacements and their iterative corrections may be derived.

5.2.2.2 Delamination Interface Materials

Interface elements may be used at planes of potential delamination to model inter laminar failure, and crack initiation and propagation. If the strength exceeds the strength threshold value in the opening or shearing directions, the material properties of the interface element are reduced linearly as defined by the material parameters. Also complete failure is assumed to have occurred when the fracture energy is exceeded. No initial crack is inserted so the interface elements can be placed in the model at potential delamination areas where they lie dormant until failure occurs.

5.2.2.3 Fracture Modes

Three fracture modes exist: open, shear, and tear (orthogonal shear for 3D models). The number of fracture modes corresponds to the number of dimensions of the model. The diagram below illustrates the three modes. In our models, mode 2 and mode 3 results are equal.

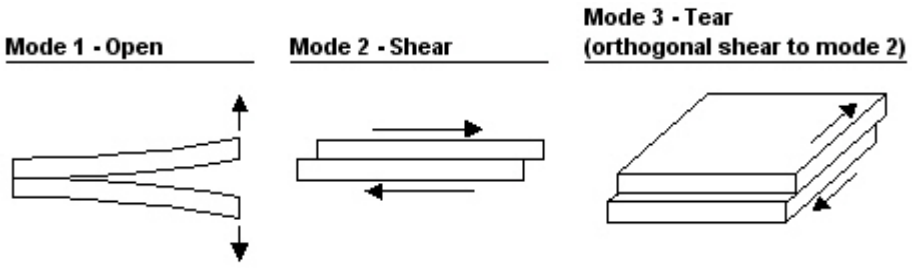

Figure 5.2 Fracture modes (LUSAS Modeller Online Help)

The interface elements are used to model delamination in an incremental nonlinear analysis. These elements have no geometric properties and are assumed to have no thickness. (LUSAS Software Modeller On-line Help)

5.2.2.4 Interface Material Parameters

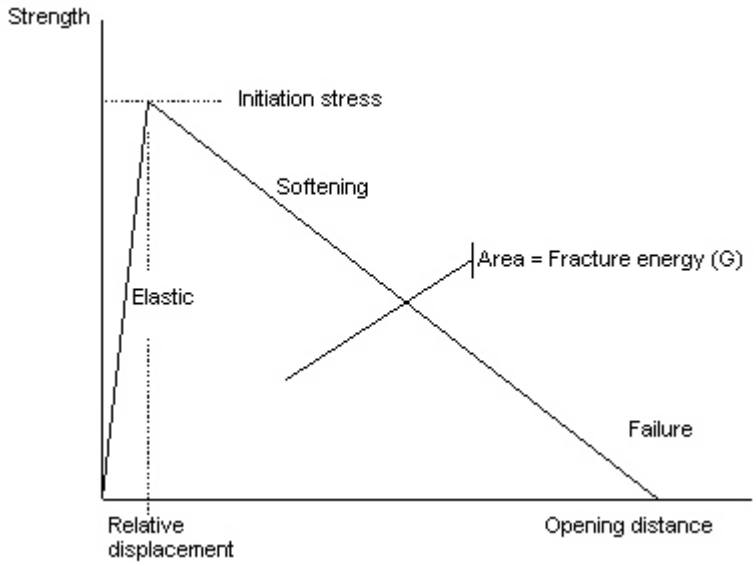

Figure 5.3 Strength - opening distance of interface material
(LUSAS Modeller Online Help)

In this study, the strength-opening distance graph of the specimens show big similarities. So, only the maximum load values are used for comparison to see the differences between the specimens.

- Fracture Energy: Measured values for each fracture mode depending on the material being used, e.g. carbon fibre, glass fibre.

- Initiation Stress: The tension threshold /interface strength is the stress at which delamination is initiated. This should be a good estimate of the actual delamination tensile strength but, for many problems, the precise value has little effect on the computed response. If convergence difficulties arise it may be necessary to reduce the threshold values to obtain a solution.

- Relative Displacement: The maximum relative displacement is used to define the stiffness of the interface before failure. Provided it is sufficiently small to simulate an initially very stiff interface it will have little effect.

5.2.2.5 Solution Termination

Termination may be specified in 3 ways:

- Limiting the maximum applied load factor.
- Limiting the maximum number of applied increments.
- Limiting the maximum value of a named freedom.

In this study to find out the maximum load factor for the specimens, the third way is used.

5.2.2.6 Constrained Solution Methods (Arc-Length)

Constrained methods differ from constant level methods in that the load level is not required to be constant within an increment. In fact the load and displacement levels are constrained to follow some pre-defined path. The use of the arc-length method has the following advantages over constant load level methods:

- Ability to detect and negotiate limit points
- Improved convergence characteristics

In this study Crisfields modified arc-length method is used. This procedure in which the solution is constrained to lie on a spherical surface defined in displacement space. For the one degree of freedom case this becomes a circular arc.

5.3 Main Steps of a Tension Analysis Executed by LUSAS 14.1

In this part, the laminated composite specimen with 2 stepped patch, manufactured by VARIM, is modelled and analyzed by using the commercial software LUSAS 14.1.

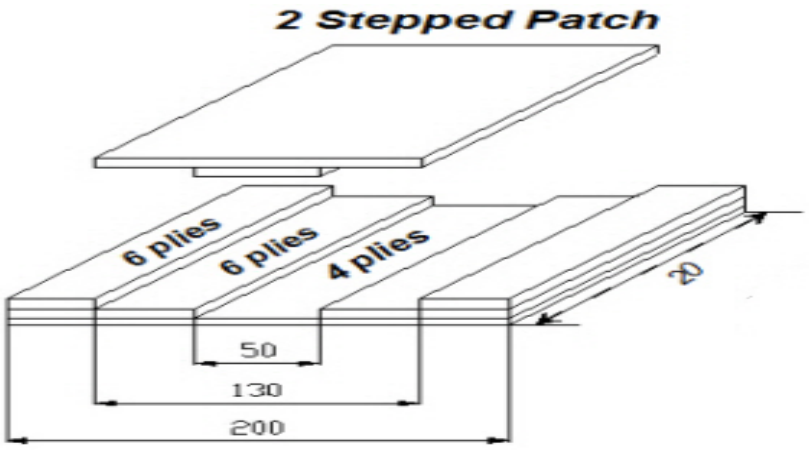

Figure 5.4 The specimen modelled and analyzed with LUSAS

5.3.1 Entering the Point Coordinates

The first step of the modeling is entering the point coordinates. These coordinates are determined according to the patch step length.

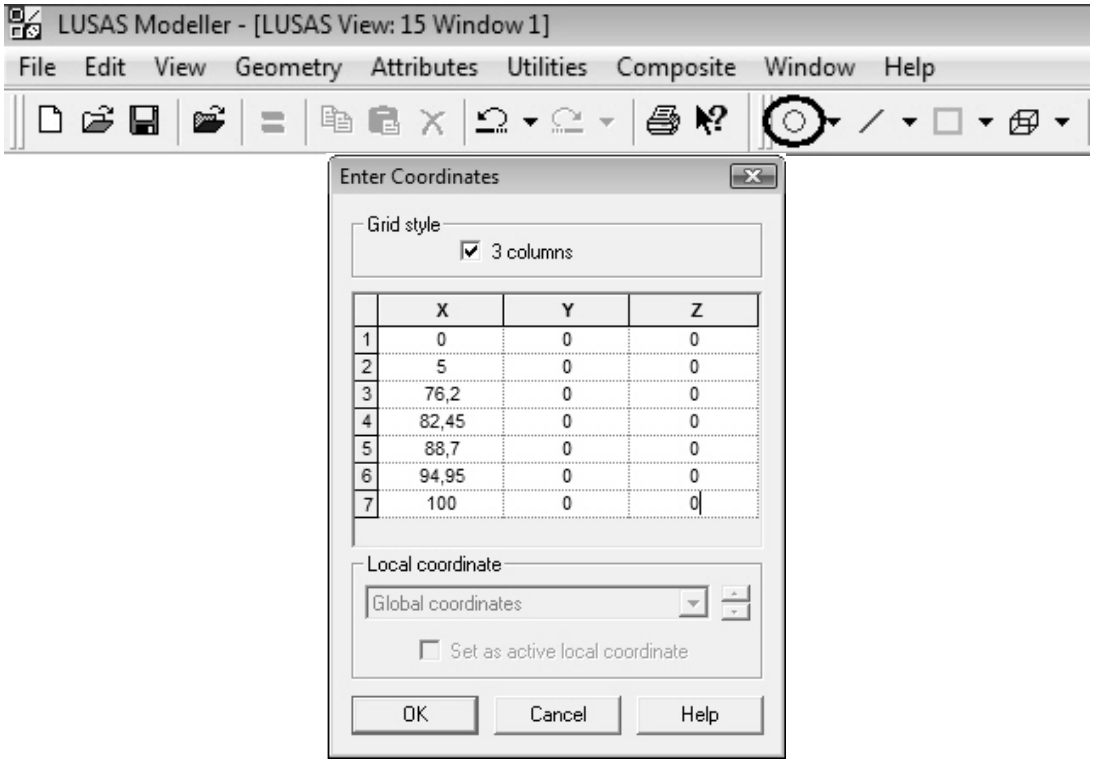

Figure 5.5 The coordinates of the points that are entered

Figure 5.6 The points assigned to the graphic screen

5.3.2 Forming the Surfaces and Assigning Line Meshes

The surfaces are formed by selecting and combining each 4 points separately. Then line meshes are assigned to the edges of these surfaces one by one.

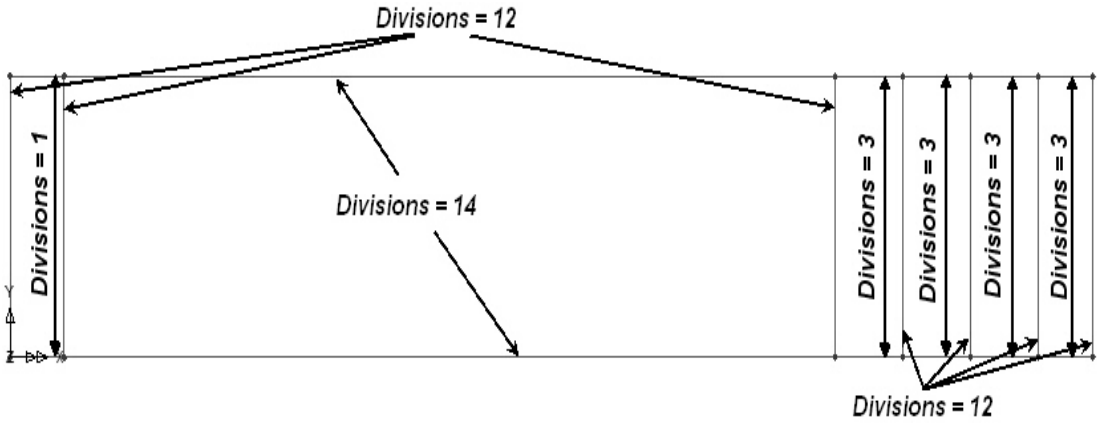

Figure 5.7 The surfaces formed by combining the points and line mesh values of these surfaces' edges

5.3.3 Forming the Volumes and Assigning Thickness Meshes

The volumes are formed by sweeping the surfaces at definite thicknesses. Then line meshes are assigned to these thicknesses. And composite brick (HX16L) mesh is assigned to all volumes.

Figure 5.8 Half volumes of the specimen formed by sweeping the surfaces.

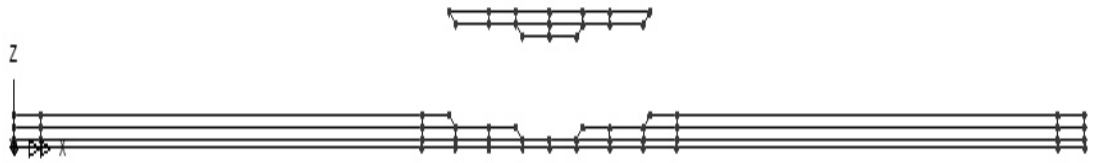

Figure 5.9 The specimen form after the mirror command. Patch is in above while base material is in below.

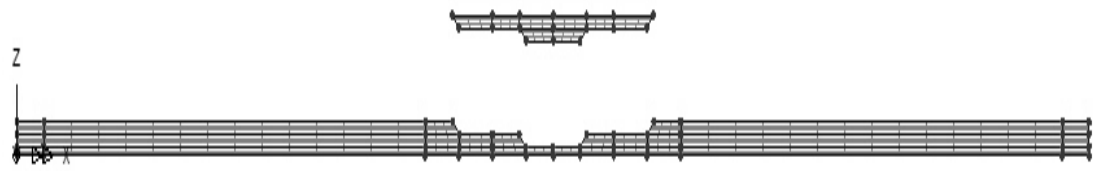

Figure 5.10 Composite Brick (HX16L) mesh assigned to all volumes.

5.3.4 Assigning Interface Mesh and Material Between Patch and Base Material

After forming the volumes, interface mesh and material is assigned between patch and base material. In here, interface material represents the resin and hardener mixture. Its mechanical properties are taken from LUSAS tutorials.

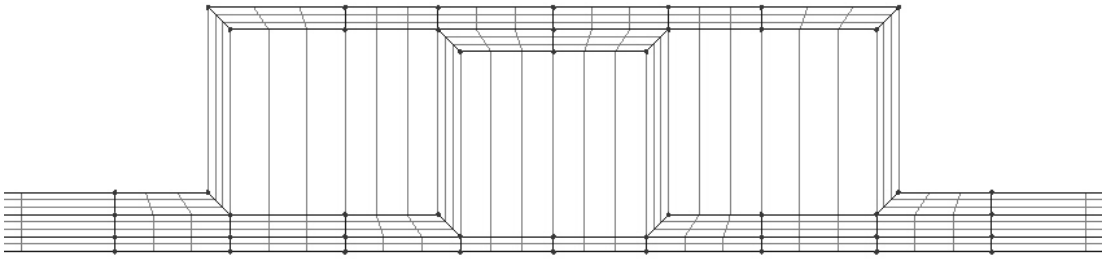

Figure 5.11 Interface mesh assigned between base material and patch

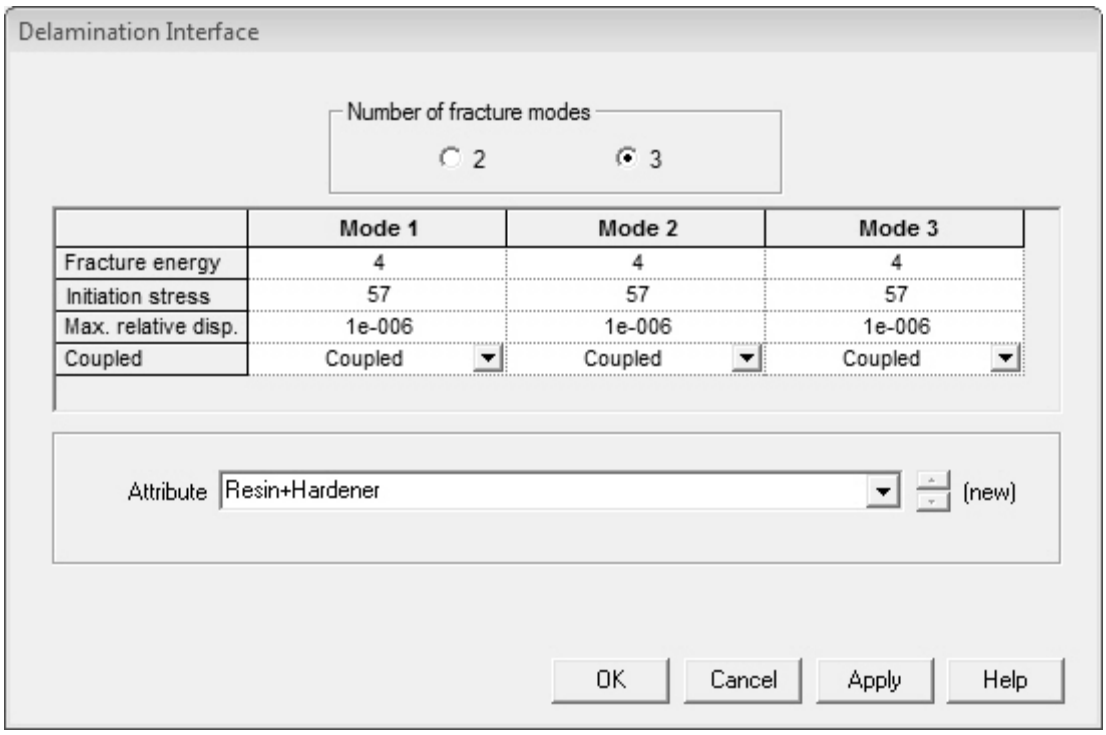

Figure 5.12 Resin + hardener mixture's assigned mechanical properties (taken from LUSAS tutorials)

5.3.5 Assigning Composite Material to the Volumes

The mechanical properties of the woven glass-epoxy composites which were obtained experimentally are used in numerical analysis. In the analysis Hashin failure criterion is selected.

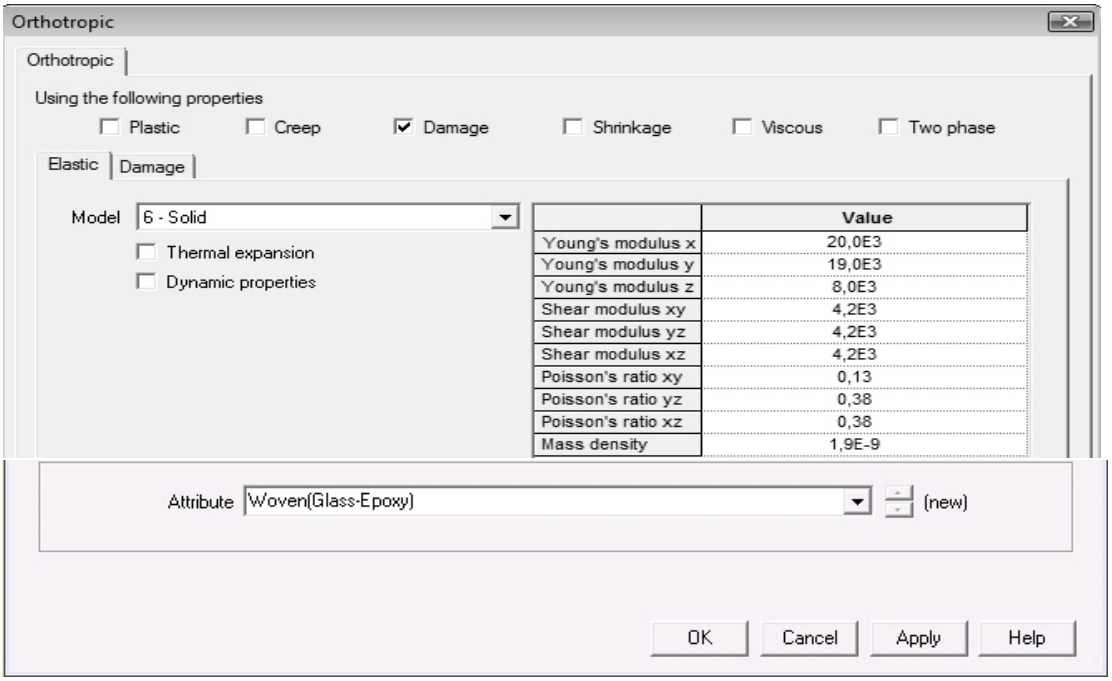

Figure 5.13 Entering mechanic properties of composite

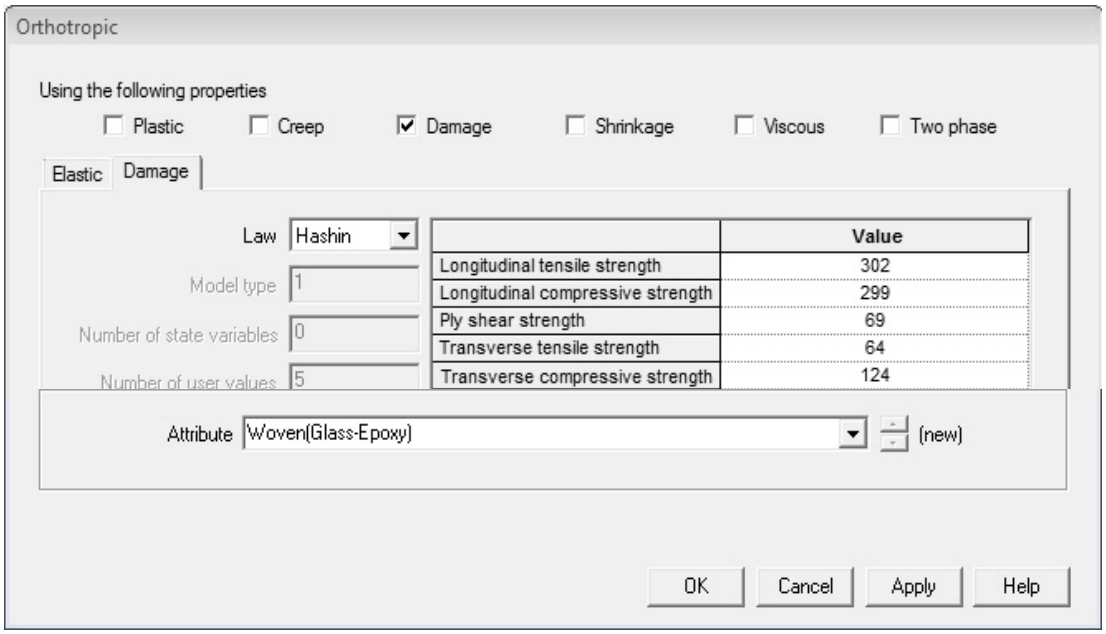

Figure 5.14 Entering Hashin damage properties

Hashin Failure Criterion

Hashin failure criteria is polynomial failure criteria similar to the quadratic failure envelope except that in Hashin formulation there are distinct polynomials corresponding to the different modes. Hashin-type failure criteria is ideal for use in finite element models, especially when adapted to progressive damage models. This failure criterion can be used to product fiber and matrix damaged nodes. When a failure occurs in plane the material properties in that location are degraded.

Tensile fiber mode

$$\left(\frac{\sigma_{11}}{X_T}\right)^2 + \frac{1}{S^2}\left(\sigma_{12}{}^2 + \sigma_{13}{}^2\right) = 1 \quad \text{or} \quad \sigma_{11} = X_T$$

Compressive fiber mode

$$|\sigma_{11}| = X_C$$

Tensile matrix mode

$$\left(\sigma_{22} + \sigma_{33}\right) > 0 \quad ; \quad \frac{1}{Y_T^2}\left(\sigma_{22} + \sigma_{33}\right)^2 + \frac{1}{S_T^2}\left(\sigma_{23}^2 - \sigma_{22}\sigma_{33}\right) + \frac{1}{S^2}\left(\sigma_{12}^2 + \sigma_{13}^2\right) = 1$$

Compressive matrix mode

$$\frac{1}{Y_C}\left[\left(\frac{Y_C}{2S_T}\right)^2 - 1\right]\left(\sigma_{22} + \sigma_{33}\right) + \frac{1}{4S_T^2}\left(\sigma_{22} + \sigma_{33}\right)^2 + \frac{1}{S_T^2}\left(\sigma_{23}^2 - \sigma_{22}\sigma_{33}\right) + \frac{1}{S^2}\left(\sigma_{12}^2 + \sigma_{13}^2\right) = 1$$

where ; σ_{11} is the normal stress in the direction of the fibers of the lamina. σ_{22}, σ_{33} are the normal stresses in the transverse directions to the fibers of the lamina. σ_{12}, σ_{23}, σ_{13} are the shear stresses in the lamina. X_T is the tensile strength of the fibers. X_C is the compressive strength of the fibers. Y_T is the tensile strength in the transverse direction of the fibers. Y_C is the compression strength in the transverse direction of the fibers. S is the shear strength, in the 1-2 plane of the lamina. S_T is the transverse shear strength in the 1-3 and 2-3 planes of the lamina.

5.3.6 Assigning Ply Orientations to the Composite Laminates

In this study, only 0° ply oriented composite laminates are examined. The first ply contains 4 laminates, the other plies contain 6 laminates. Because of the thickness difference the assignments are done separately.

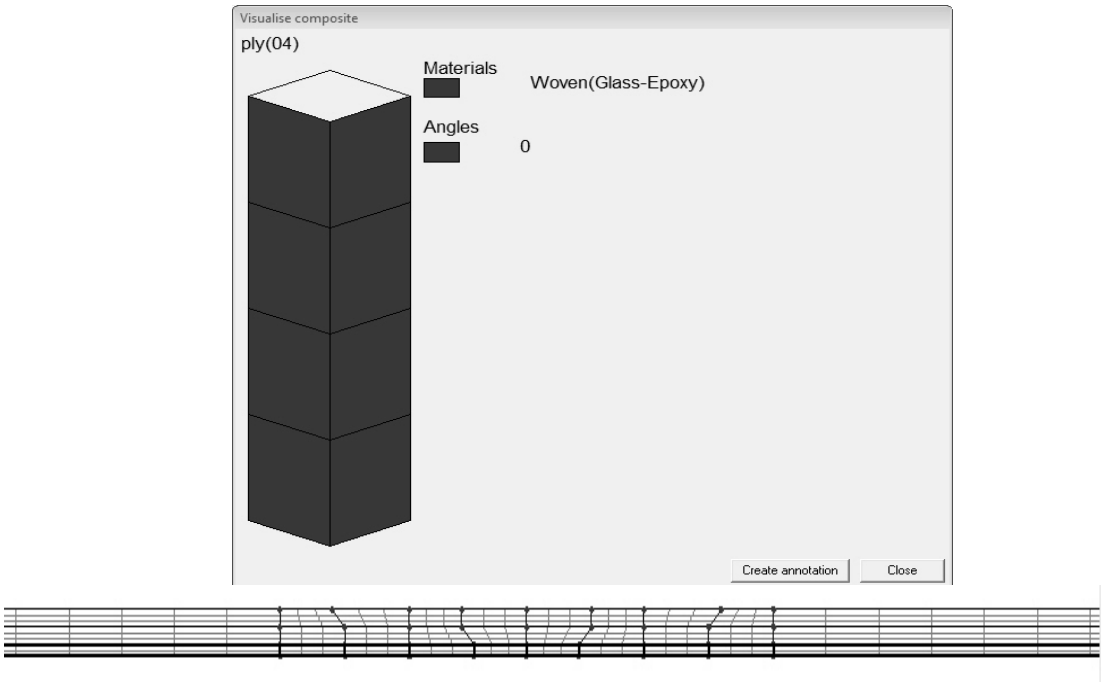

Figure 5.15 0° oriented 4 laminates assigned to the first ply

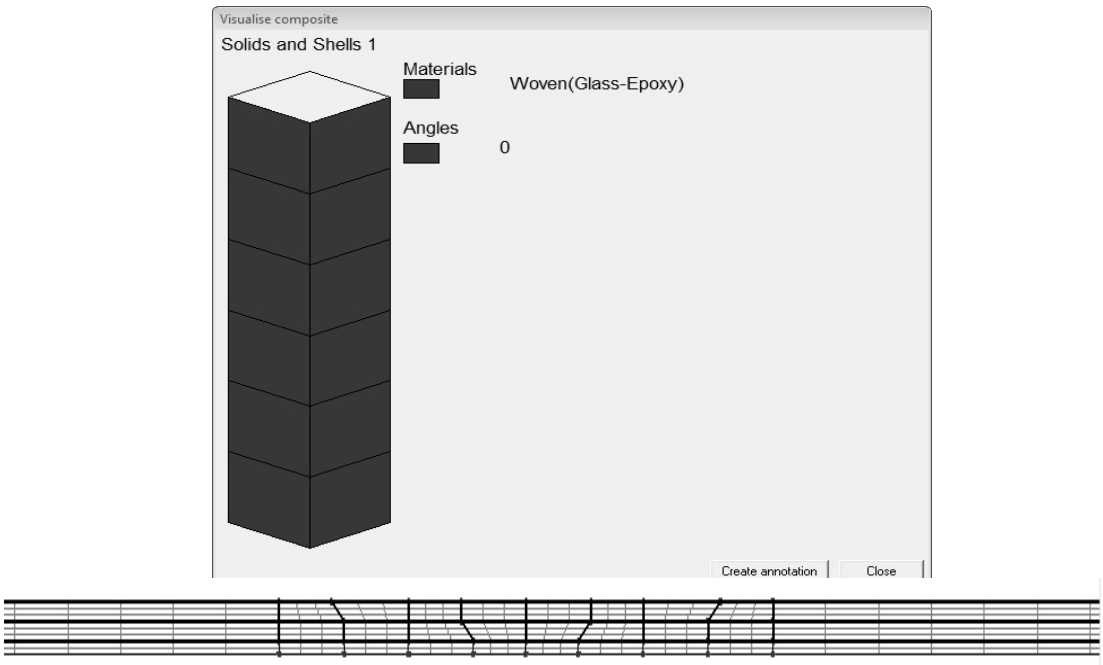

Figure 5.16 0° oriented 6 laminates assigned to the upper two plies

5.3.7 Assigning Boundary Conditions

Because of working on a tension specimen, the supports are determined as in experimental test supports. “Fully Fixed” is assigned to one end of the specimen and “Fixed in Z” is assigned to the other end of the specimen. By this way the specimen will extend only in the +X direction.

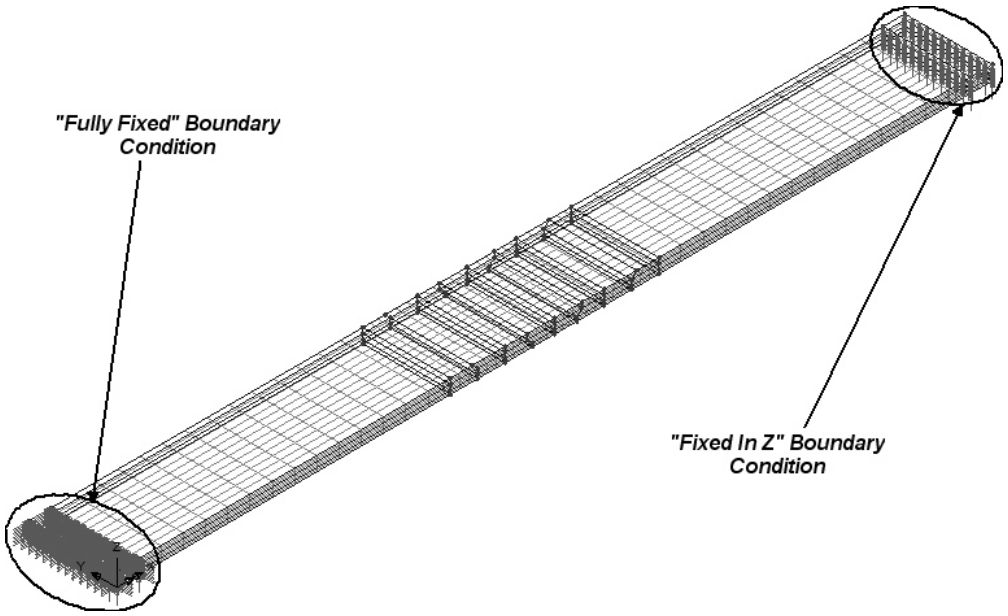

Figure 5.17 Boundary conditions assigned to each end of the specimen

5.3.8 Assigning the Tensile Load

The tensile load is assigned to the “fixed in Z” end of the specimen. The load is a global distributed load and in the +X direction.

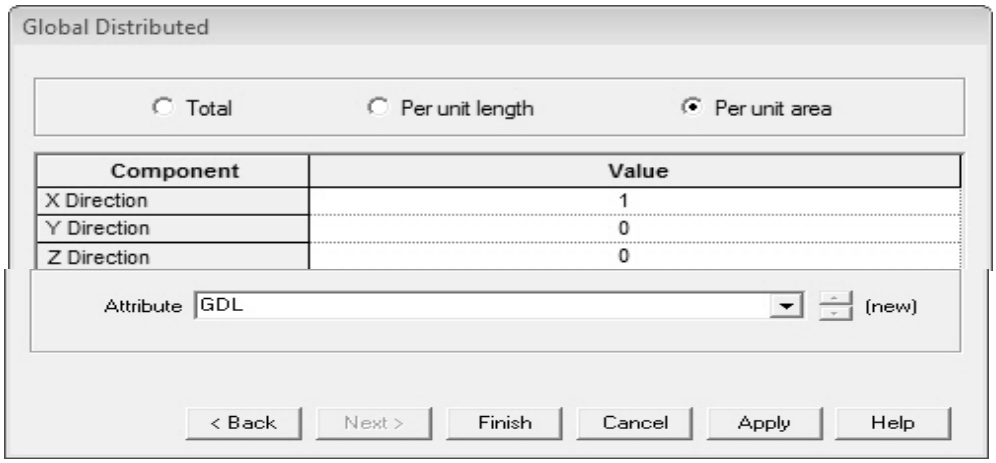

Figure 5.18 Global distributed load properties

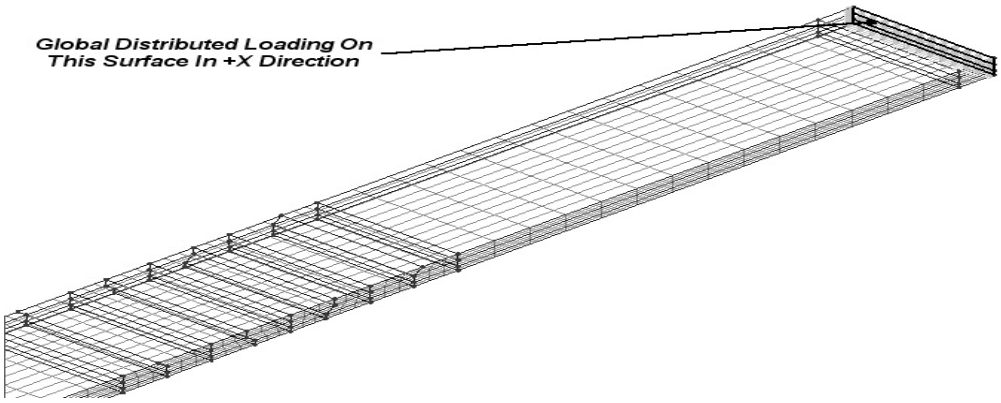

Figure 5.19 Tensile load in the +X direction assigned on the specimen

5.3.9 Entering Nonlinear Solution Properties

Automatic incrementation is selected to enter starting load factor, max. change in load factor, max. total load factor and max. time steps or increments. One of the aim of this study is to find out the strength of the specimens. So, no values are entered in max. total load factor. 50 increments are enough to see the maximum load capacity of the specimen. Also, Crisfield modified arc-length method is selected to allow the change of the load levels in an increment.

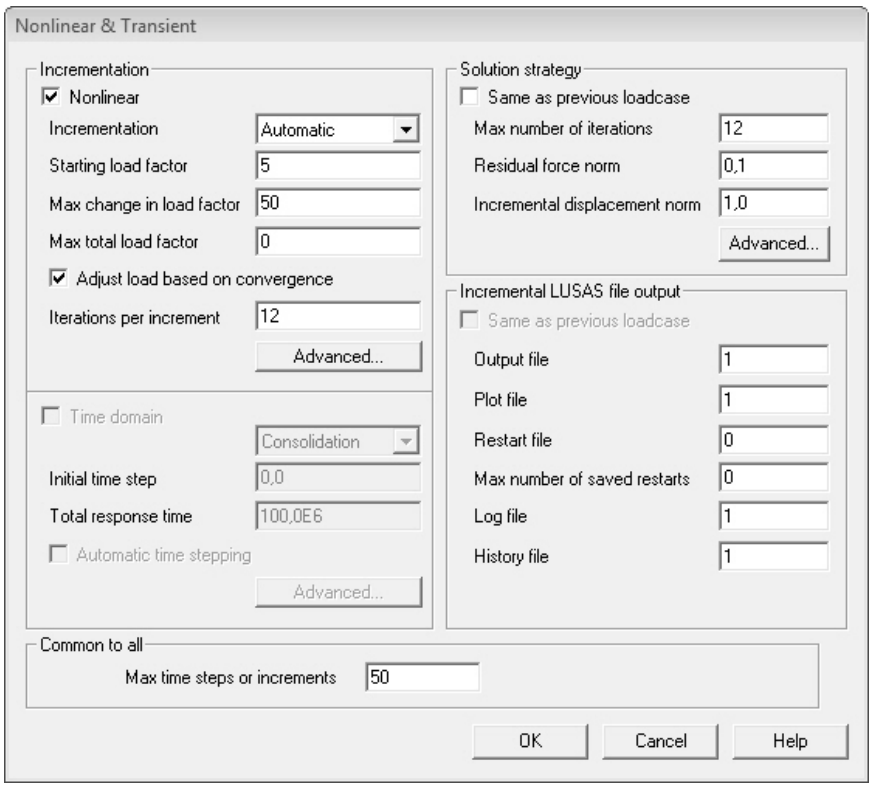

Figure 5.20 Values entered in the nonlinear solution properties screen

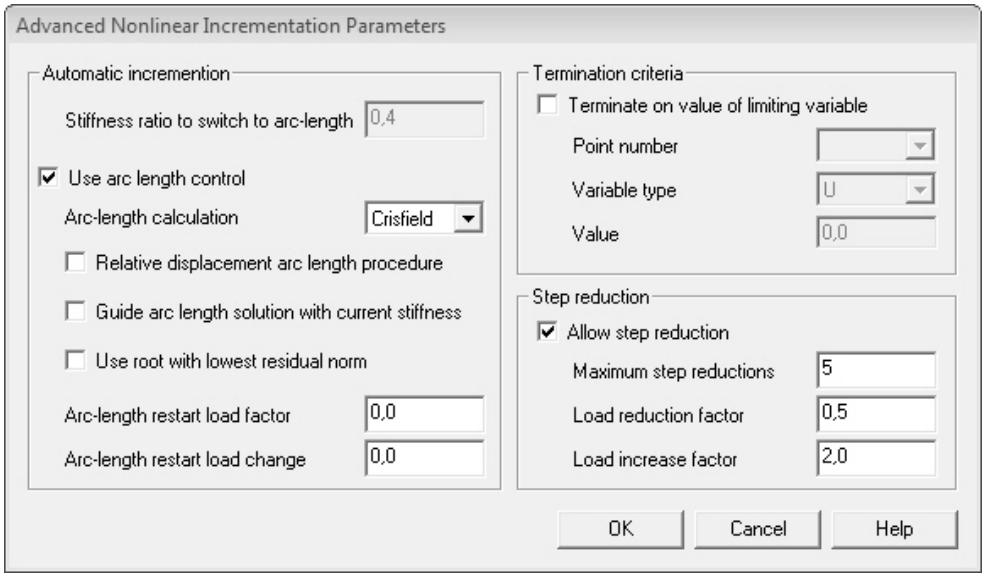

Figure 5.21 Crisfield modified arc-length method selected in the nonlinear properties screen

5.3.10 Starting the Analysis and Evaluating the Results

After all of the adjustments, the nonlinear numerical analysis is started. The convergence of the increments are controlled to see the probable errors.

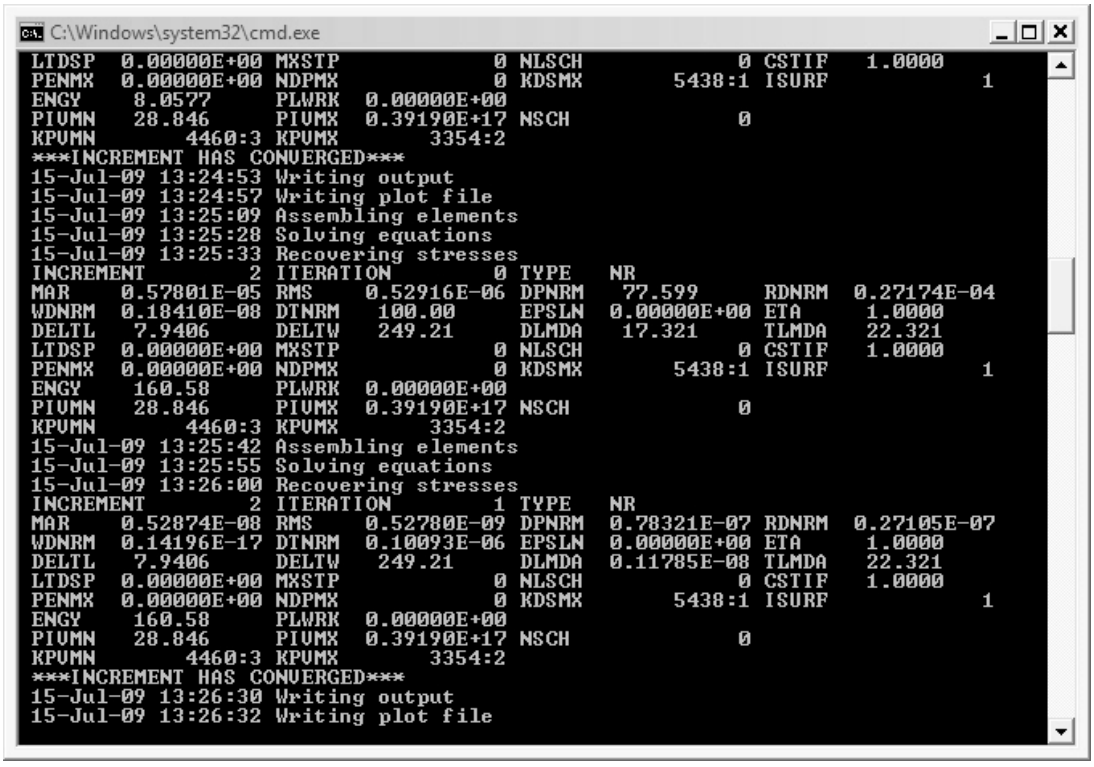

Figure 5.22 Nonlinear solution screen

When the analysis is finished, the increment list is examined to find out the maximum load capacity of the specimen.

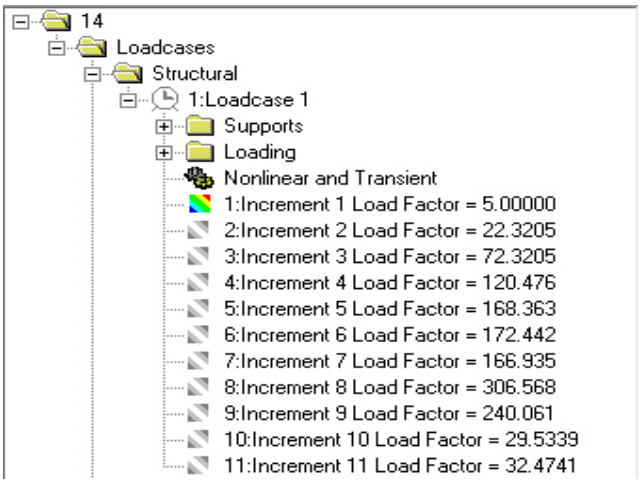

Figure 5.23 Increment list of the specimen that shows the maximum load capacity

The distribution of the stress in the +X direction contours are examined to find out where the max. stress occurred in the specimen. It is seen that the max. stresses occurred at the point of the patches. Also, maximum displacement in the +X direction is checked, and found that the max. displacement is occurred at the side of the specimen that loading was assigned.

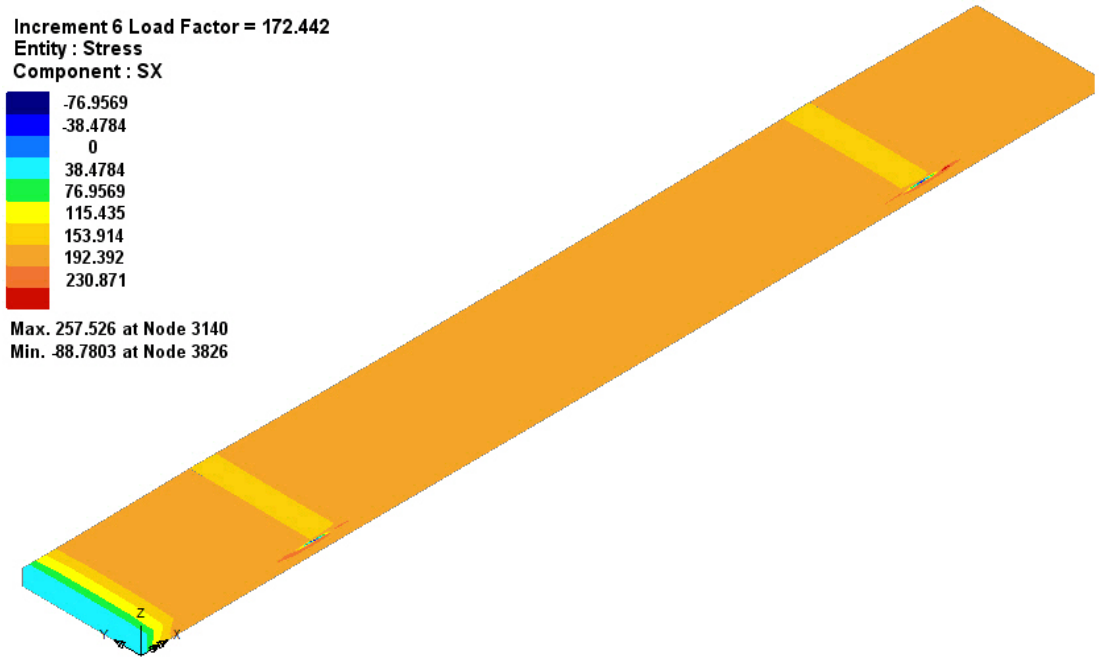

Figure 5.24 Distribution of the stress in the +X direction

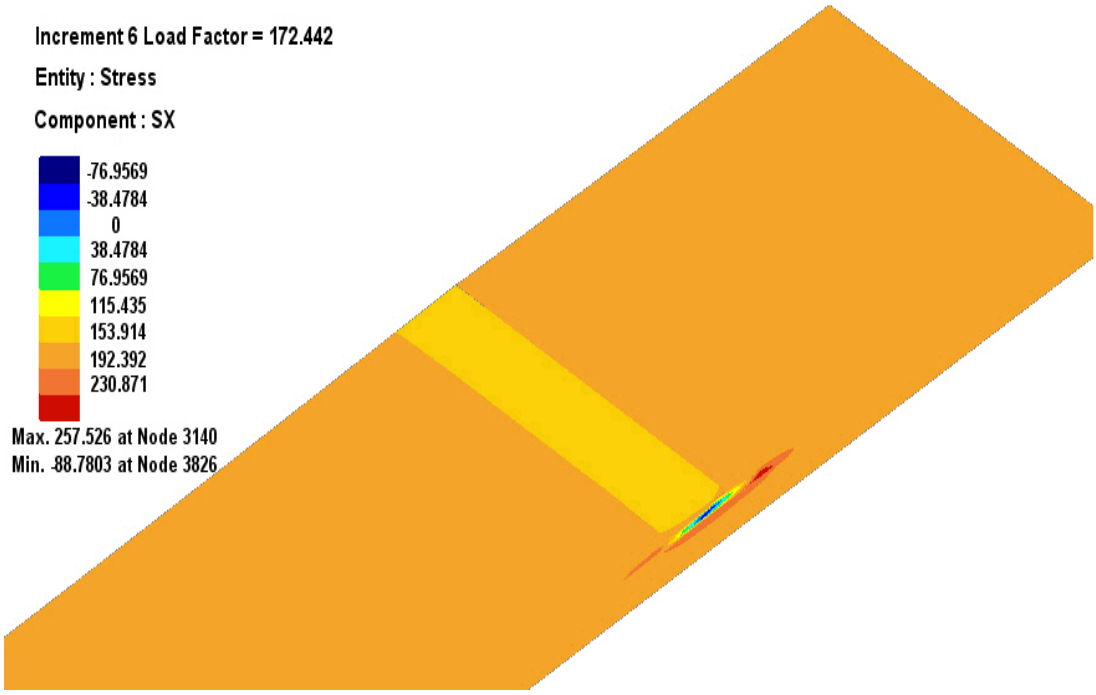

Figure 5.25 Distribution of the stress in the +X direction(zoomed in the patch edge)

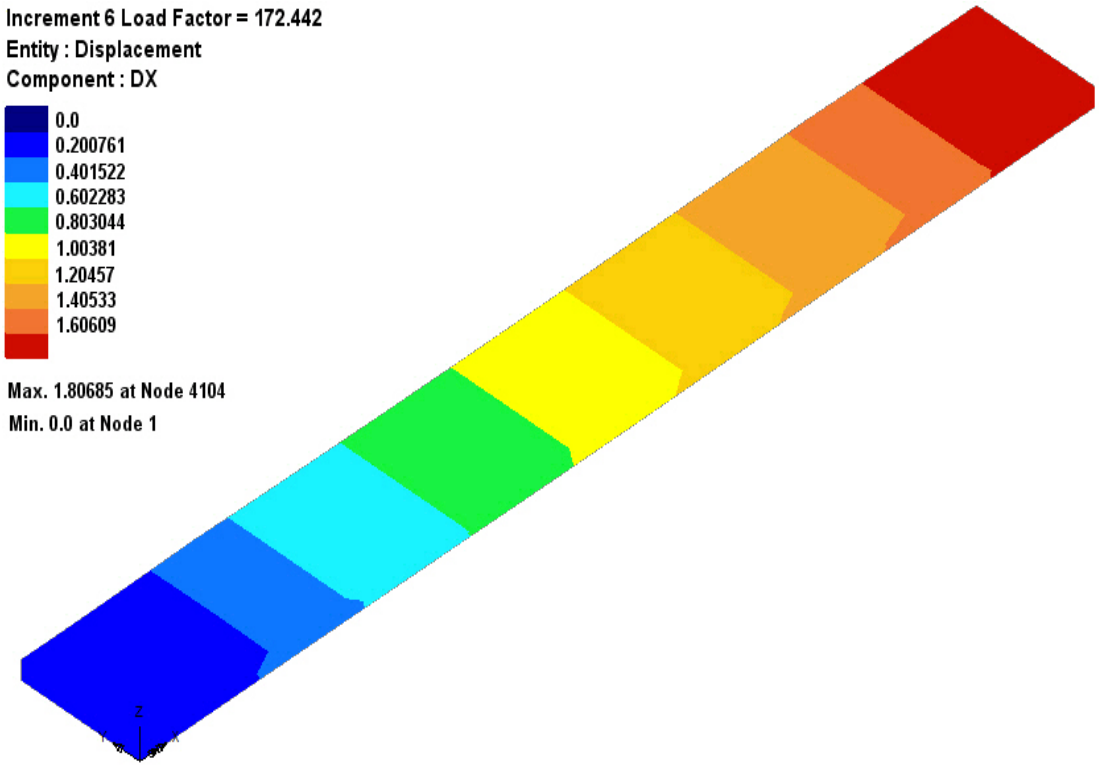

Figure 5.26 Distribution of the displacement in the +X direction

The interface material's (resin+hardener mixture) softening areas are examined and found that the patchs edges are the critical points (locations) for the specimen.

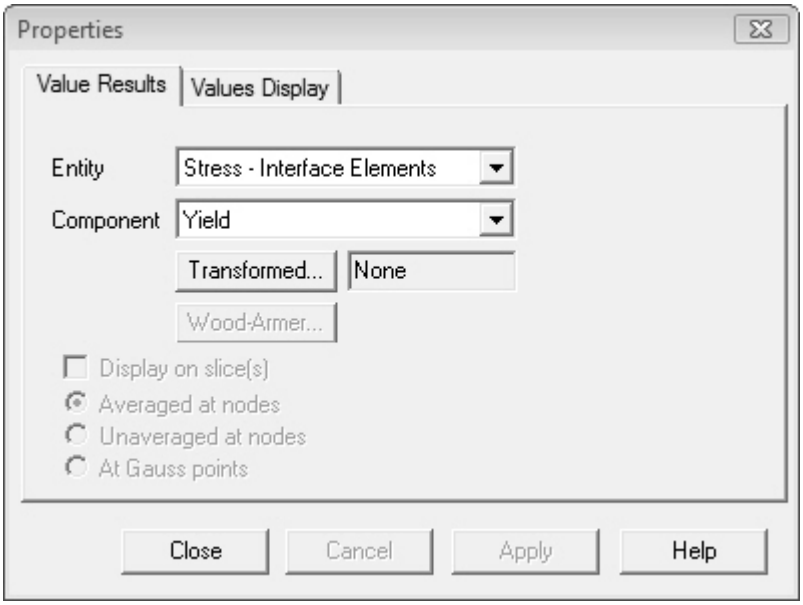

Figure 5.27 Result properties screen of interface material

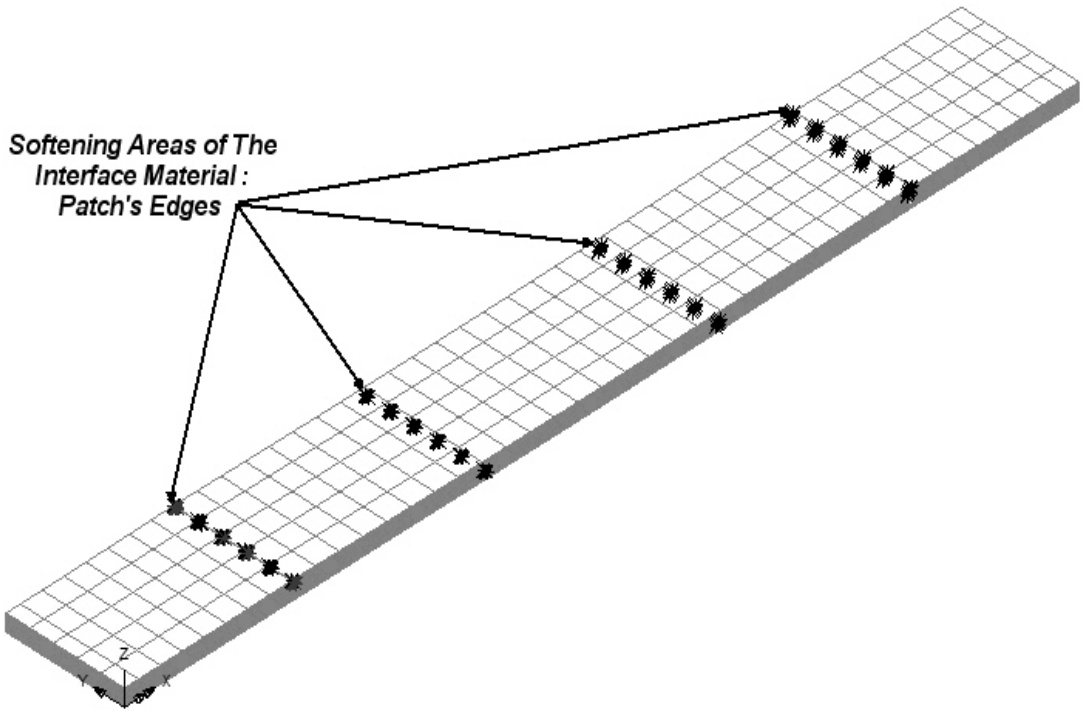

Figure 5.28 Softening areas of the interface material

5.4 Comparison of the Experimental Tests and Numerical Analysis

The three numerical analysis results showed that the patched specimens' strengths are less than the normal specimen. Two stepped patched specimen has less strength than the three stepped patched specimen. Figure 5.29 also shows that the experimental tests and numerical analysis have similar results.

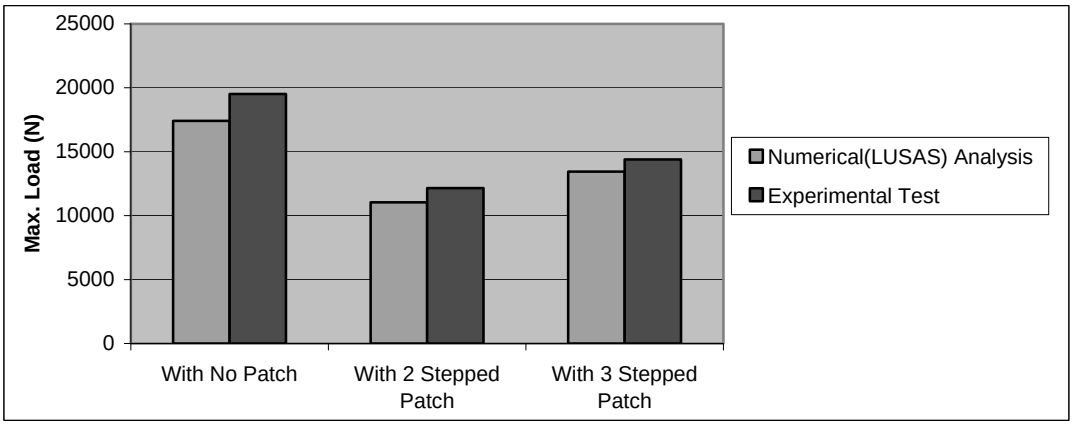

Figure 5.29 Comparison of the experimental and numerical results of tension specimen analysis

5.5 Numerically Analyzed Tensile Specimens with Different Dimensions

Besides the analysis which are done to compare with the experimental tests, different types of tensile specimens are modelled and analyzed with LUSAS according to standards (width = 12.4 mm, length = 228.4 mm). Because of the inconvenience of showing every different dimensions and properties in a graph, code numbers are given to these models. With the submodels, 47 different tensile specimen models are examined. Eleven of these are the main models.

The list of the abbreviations used in the models are:

H = Height , *L* = Length , *OPF* = Outer Patch Feature , *LOOP* = Length of Outer Patch , *LOPS* = Length of Patch Step , *NOP* = Number of Plies , *TNOP* = Total Number of Plies , *W* = Width.

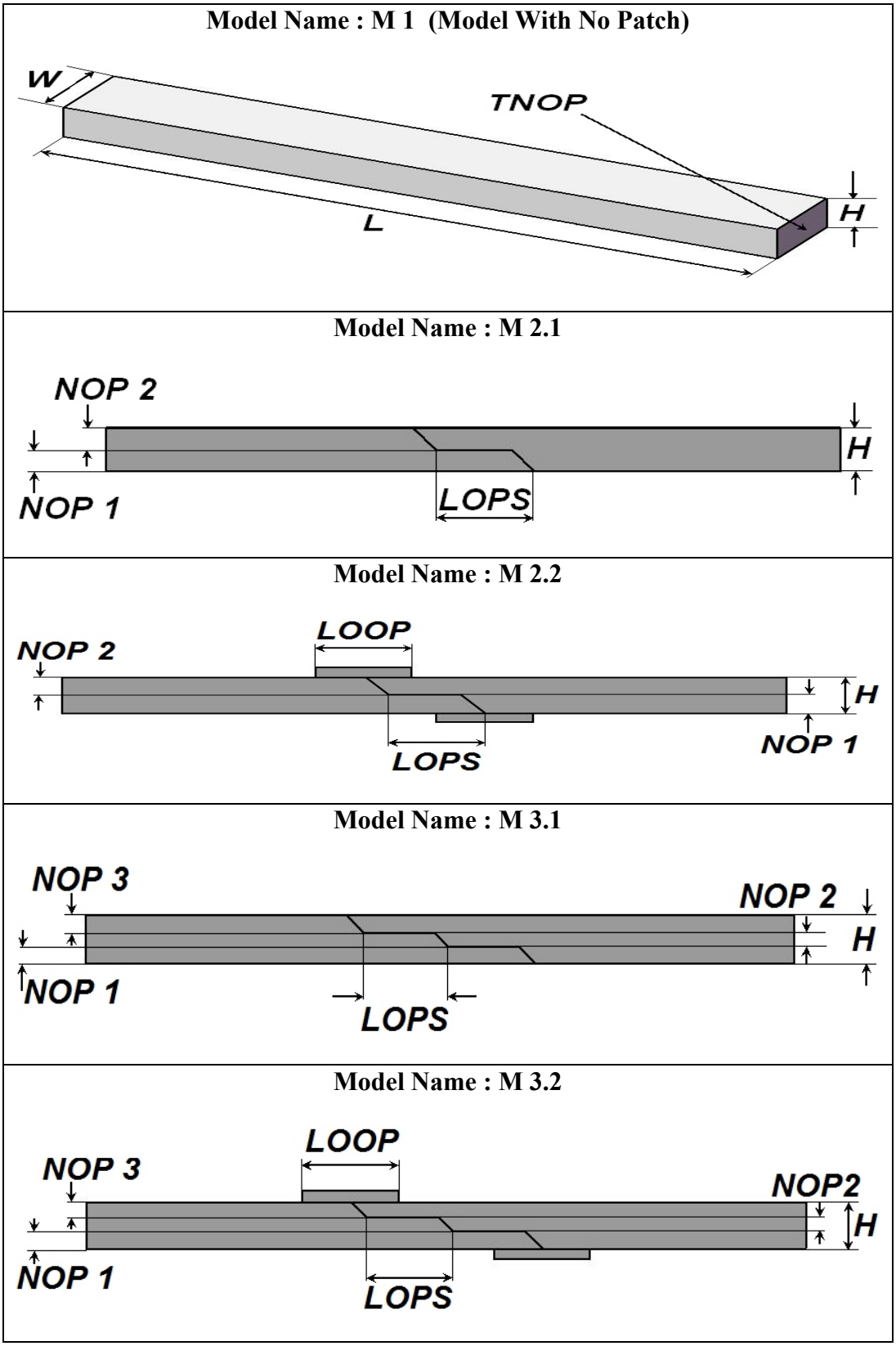

Figure 5.30 Figures of main tensile specimen models designed with LUSAS

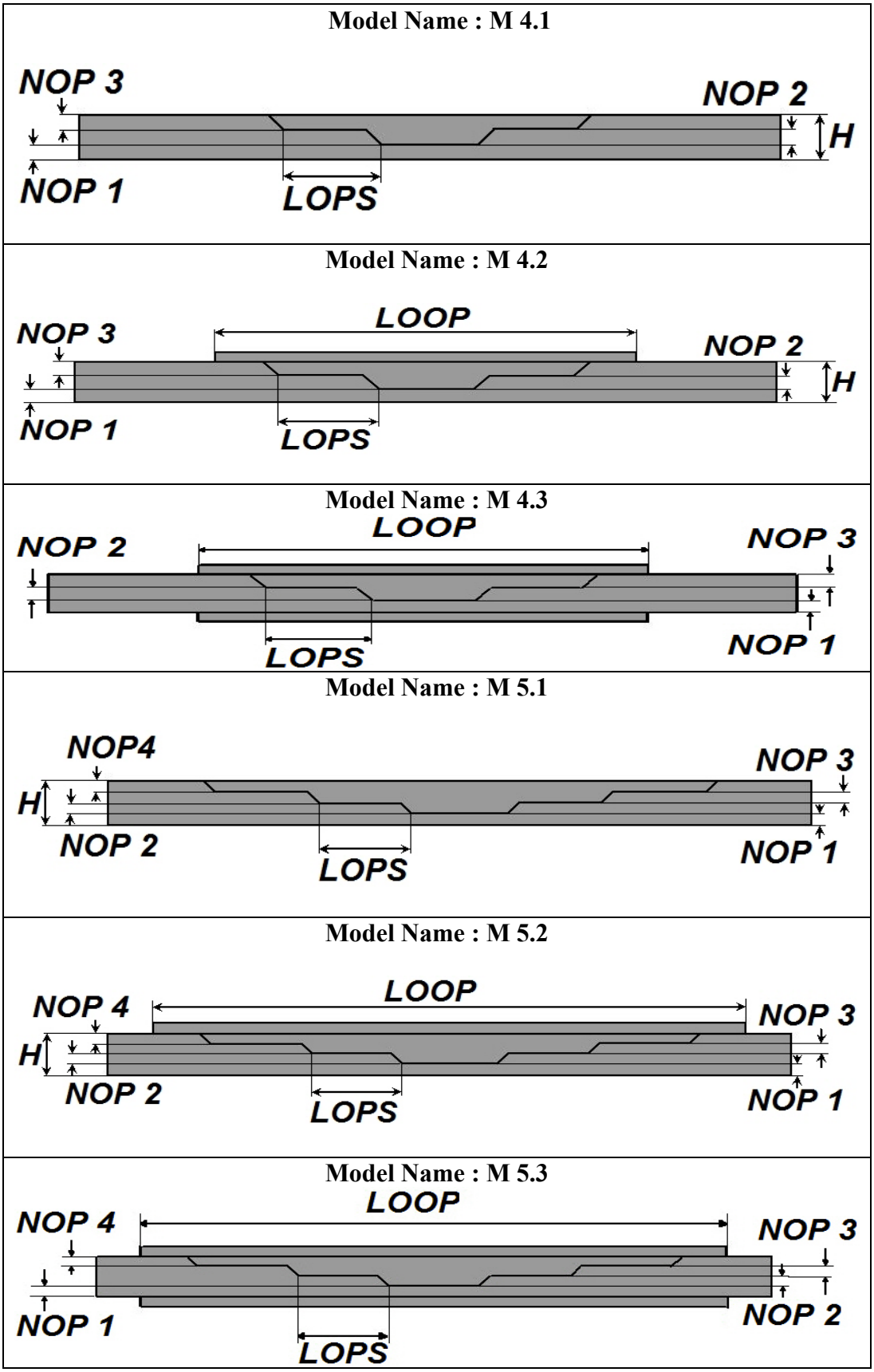

Figure 5.30 (continued) Figures of main tensile specimen models designed with LUSAS

The dimensions and properties of 47 tensile specimen models are listed in the table below. Before checking these values, some important notes about these models are:

- The total length and width of all specimens are equal :
  Length = 228.4 mm, Width = 12.4 mm

- The outer patches' widths, heights and ply numbers are equal for the related specimens.
  Height = 0.4 mm, Width = 12.4 mm, Ply Number = 2

- All of the specimens have 8 total plies. Every single ply has a height of 0.2 mm according to the measured dimensions of specimens that are manufactured with the VARIM. So, every specimen's total height is 1.6 mm.

Table 5.1 The list of the dimensions and features of the tensile specimens modelled with LUSAS

Model Code	LOPS(mm)	OPF	LOOP(mm)	NOP 1	NOP 2	NOP 3	NOP 4
M 1	-	-	-	-	-	-	-
M 2.1	12.5	-	-	4	4	-	-
M 2.2.1	12.5	Double sided	12.5	4	4	-	-
M 2.2.2	12.5	Double sided	25	4	4	-	-
M 3.1	12.5	-	-	2	3	3	-
M 3.2.1	12.5	Double sided	12.5	2	3	3	-
M 3.2.2	12.5	Double sided	25	2	3	3	-
M 4.1.1	10	-	-	2	3	3	-
M 4.1.2	12.5	-	-	2	3	3	-
M 4.1.3	20	-	-	2	3	3	-
M 4.1.4	25	-	-	2	3	3	-
M 4.2.1.1	10	One sided	50	2	3	3	-
M 4.2.1.2	10	One sided	70	2	3	3	-
M 4.2.2.1	12.5	One sided	62.5	2	3	3	-
M 4.2.2.2	12.5	One sided	87.5	2	3	3	-
M 4.2.3.1	20	One sided	100	2	3	3	-
M 4.2.3.2	20	One sided	140	2	3	3	-

M 4.2.4.1	25	One sided	125	2	3	3	-
M 4.2.4.2	25	One sided	175	2	3	3	-
M 4.3.1.1	10	Double sided	50	2	3	3	-
M 4.3.1.2	10	Double sided	70	2	3	3	-
M 4.3.2.1	12.5	Double sided	62.5	2	3	3	-
M 4.3.2.2	12.5	Double sided	87.5	2	3	3	-
M 4.3.3.1	20	Double sided	100	2	3	3	-
M 4.3.3.2	20	Double sided	140	2	3	3	-
M 4.3.4.1	25	Double sided	125	2	3	3	-
M 4.3.4.2	25	Double sided	175	2	3	3	-
M 5.1.1	10	One sided	-	2	2	2	2
M 5.1.2	12.5	One sided	-	2	2	2	2
M 5.1.3	20	One sided	-	2	2	2	2
M 5.1.4	25	One sided	-	2	2	2	2
M 5.2.1.1	10	One sided	70	2	2	2	2
M 5.2.1.2	10	One sided	90	2	2	2	2
M 5.2.2.1	12.5	One sided	82.5	2	2	2	2
M 5.2.2.2	12.5	One sided	112.5	2	2	2	2
M 5.2.3.1	20	One sided	140	2	2	2	2
M 5.2.3.2	20	One sided	180	2	2	2	2
M 5.2.4.1	25	One sided	175	2	2	2	2
M 5.2.4.2	25	One sided	228.4	2	2	2	2
M 5.3.1.1	10	Double sided	70	2	2	2	2
M 5.3.1.2	10	Double sided	90	2	2	2	2
M 5.3.2.1	12.5	Double sided	82.5	2	2	2	2
M 5.3.2.2	12.5	Double sided	112.5	2	2	2	2
M 5.3.3.1	20	Double sided	140	2	2	2	2
M 5.3.3.2	20	Double sided	180	2	2	2	2
M 5.3.4.1	25	Double sided	175	2	2	2	2
M 5.3.4.2	25	Double sided	228.4	2	2	2	2

After the analysis, the results are checked and some graphs are drawn. It is seen that the slopes of stress-displacement graphs of these specimens are nearly equal. In comparison graphs, this situation caused confusion about checking the results. So, it is decided that bar graphs will be more suitable for comparison of the maximum load capacity of the specimens.

Only M1's (specimen with no patch) stress-displacement graph is shown below in Figure 5.31 to give an idea. The other graphs are maximum load capacity comparison graphs.

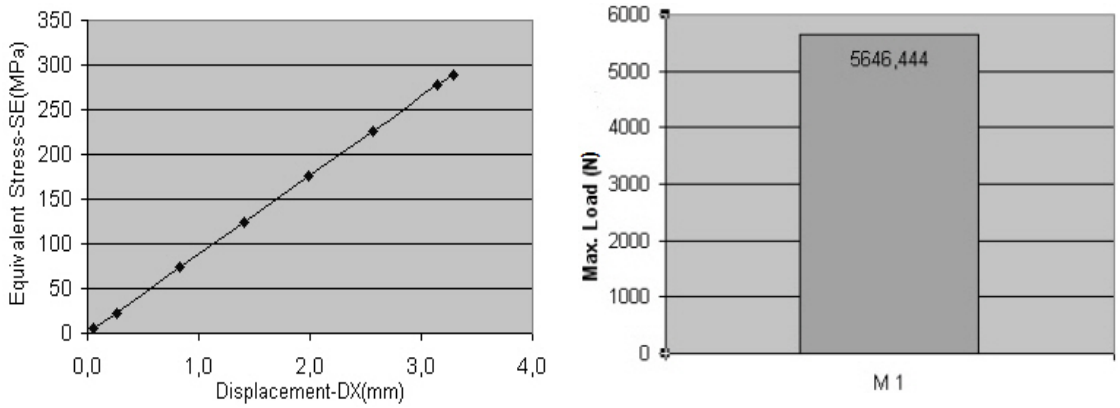

Figure 5.31 M 1's stress - displacement graph (on the left) and max. load capacity graph (on the right)

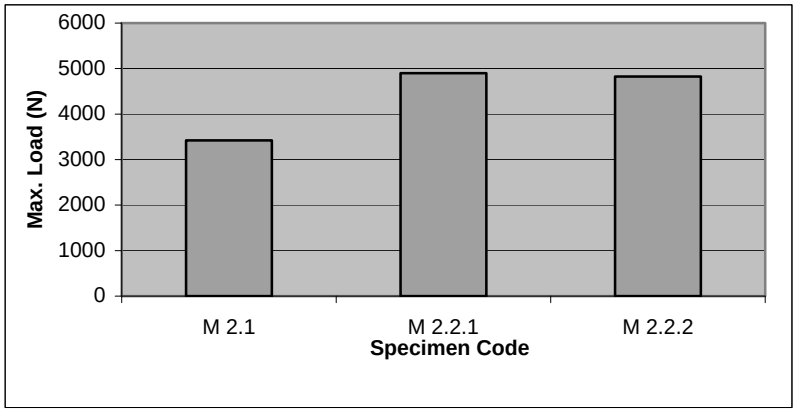

Figure 5.32 Comparison of max. load capacity for specimens M 2.1, M 2.2.1, M 2.2.2

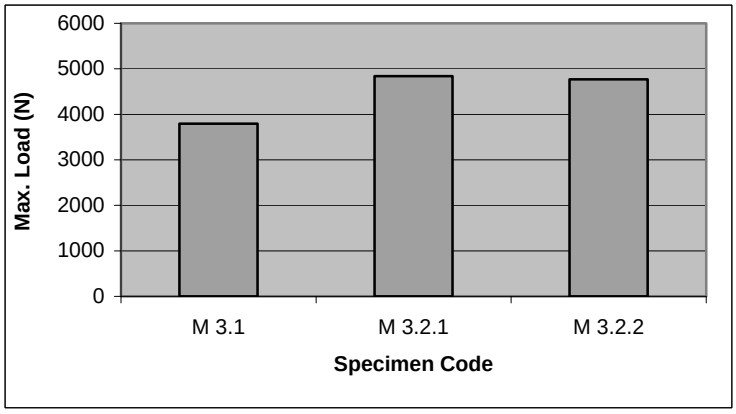

Figure 5.33 Comparison of max. load capacity for specimens M 3.1, M 3.2.1, M 3.2.2

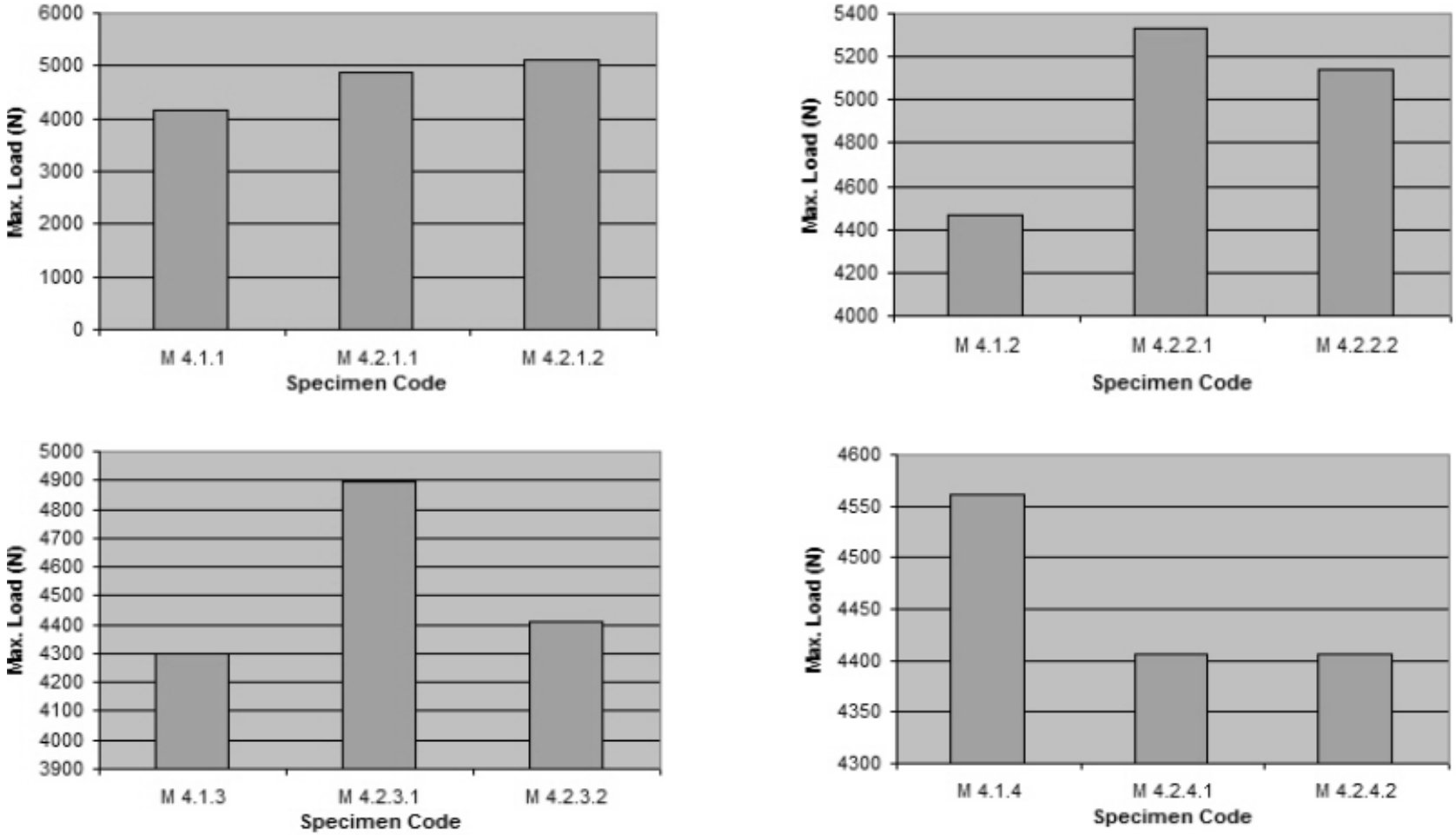

Figure 5.34 Comparisons of max. load capacity for different types of 2 stepped patched specimens (specimens with four digit codes have one sided external patch)

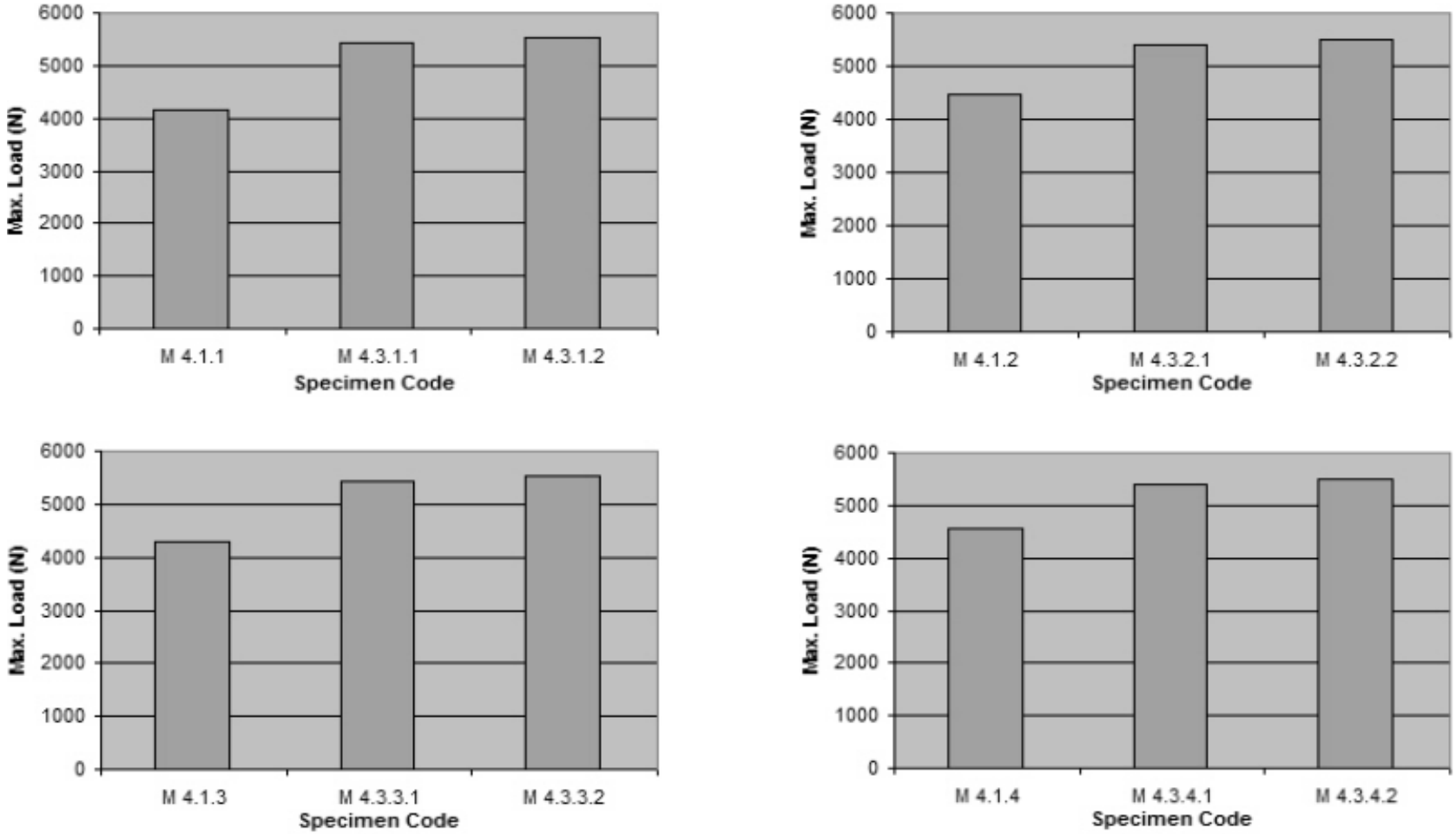

Figure 5.35 Comparisons of max. load capacity for different types of 2 stepped patched specimens (specimens with four digit codes have double sided external patch)

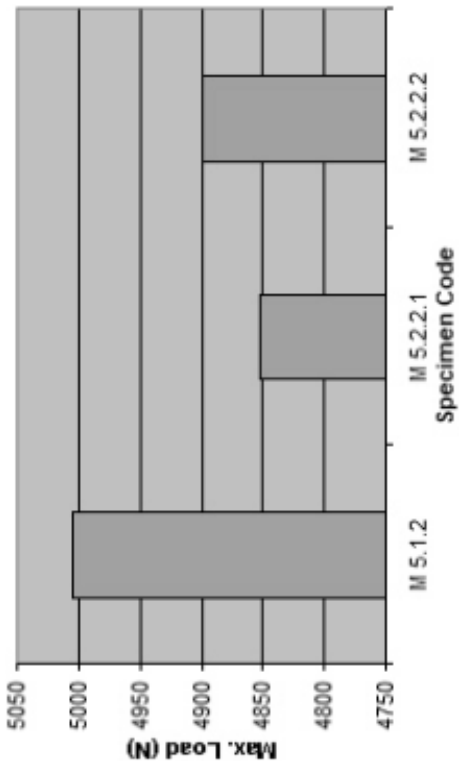

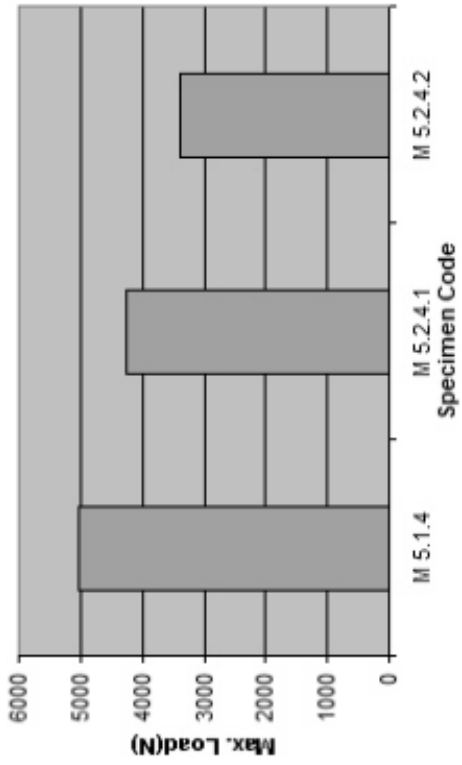

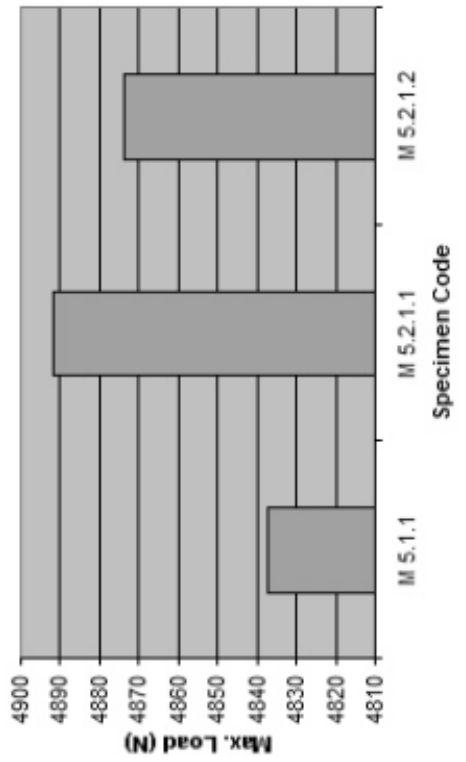

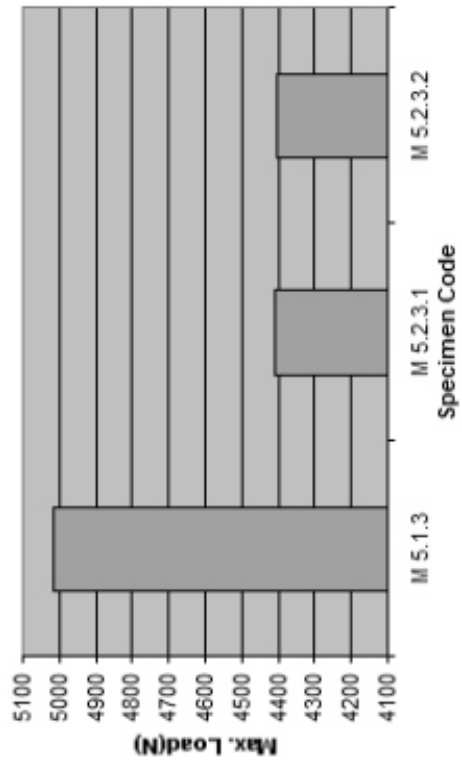

Figure 5.36 Comparisons of max. load capacity for different types of 3 stepped patched specimens (specimens with four digit codes have one sided external patches)

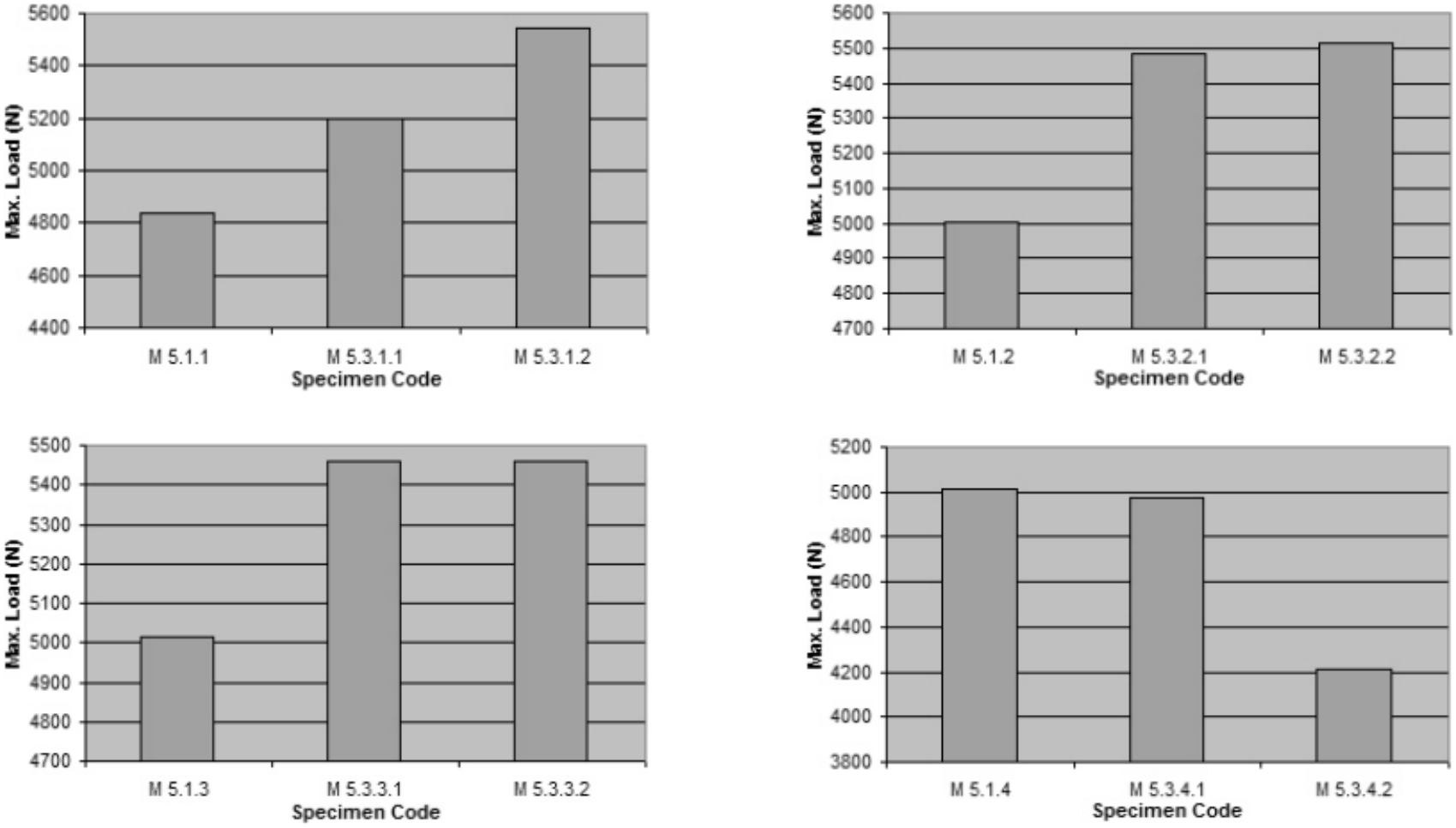

Figure 5.37 Comparisons of max. load capacity for different types of 3 stepped patched specimens (specimens with four digit codes have double sided external patches)

5.6 Numerically Analyzed Bending Specimens with Different Dimensions

Different types of bending specimens; specimen with no patch, specimen with two stepped patch, specimen with three stepped patch, are modelled and analyzed with LUSAS : height = 4 mm, width = 10 mm, length = 80 mm, support span = 64 mm. Patch lengths of the specimens with stepped patchs are 10 mm. External patches weren't used on these specimens.

Two types of bending load (in –Z and +Z direction) are applied to the specimens through a line (Figure 5.38 & 5.40). The max. load capacities of these specimens are compared with each other (Figure 5.39 & 5.41).

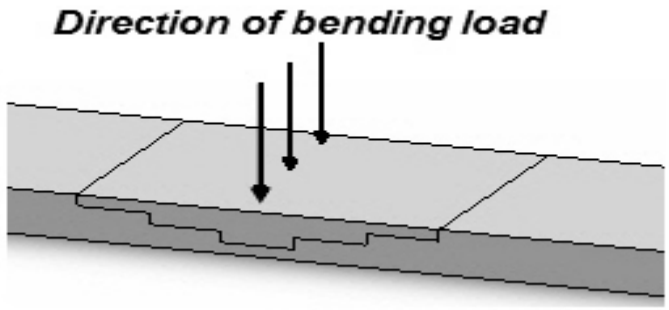

Figure 5.38 Bending load applied on the specimens in –Z direction

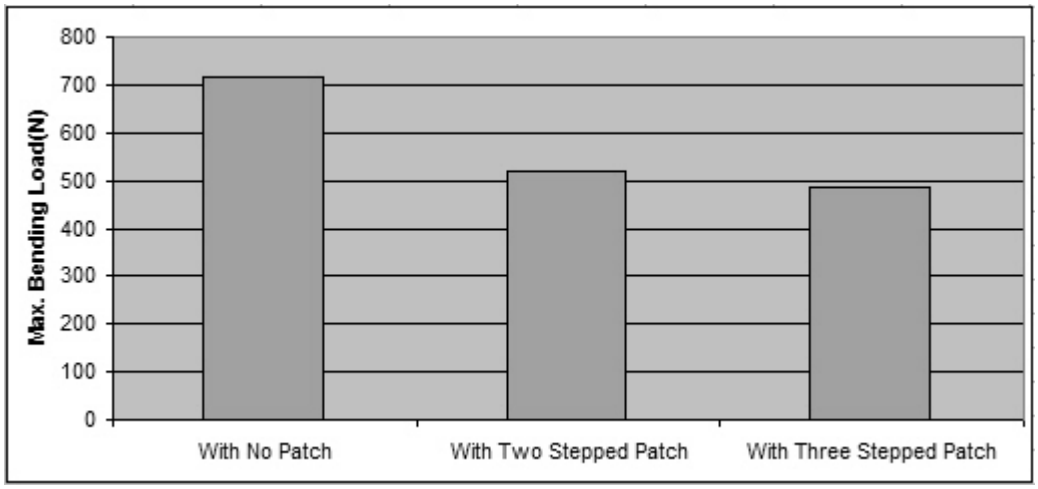

Figure 5.39 Comparison of max. bending loads applied in –Z direction on specimens

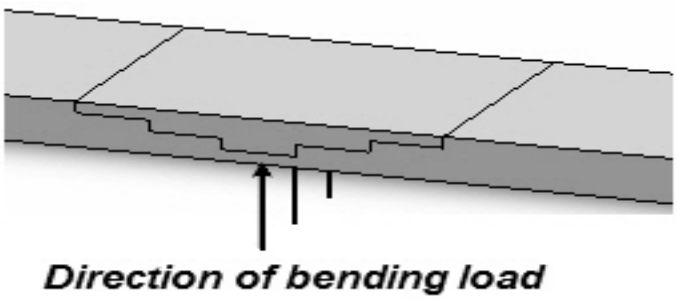

Figure 5.40 Bending load applied on the specimens in +Z direction

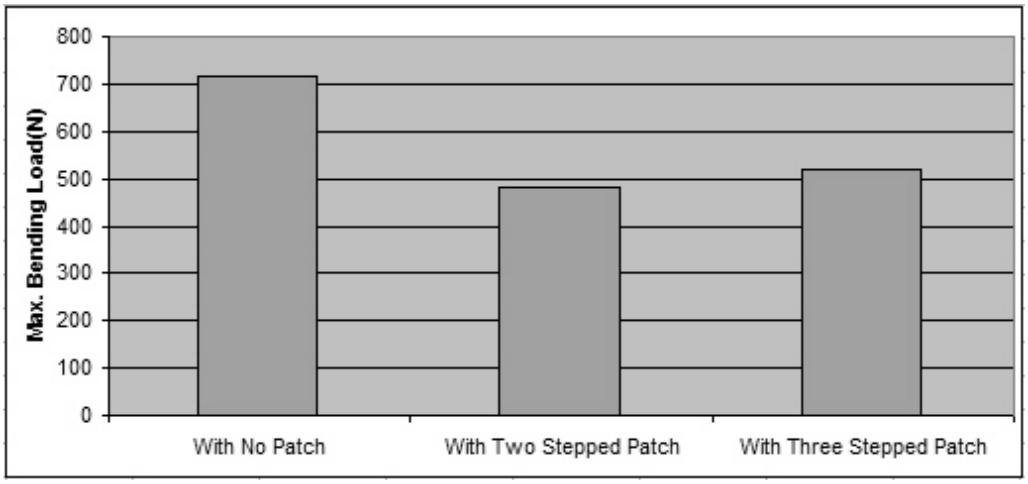

Figure 5.41 Comparison of max. bending loads applied in +Z direction on specimens

CHAPTER SIX
CONCLUSIONS

In this study, the repair of damaged woven glass-epoxy composite laminates is examined experimentally and numerically and the results are compared with each other.

- It is seen from these graphs, as expected that the maximum load capacities of specimens with no patches are higher than the others.

- Experimental and numerical results are found to be in good agreement.

- Regardless of the patch type, it is observed that stress concentrations occur at the patch locations.

- Three stepped patched specimens seem to have better results than two stepped patched ones. This is because of that the area of the interface elements are higher for three stepped patch. That is, three stepped patches have a larger interface area than that of two stepped patches. Therefore, the stress concentrations in the patch area is less in three stepped patched specimens.

- The specimens patched from their edges and have double sided outer patches (M 2.2.1, M 2.2.2, M 3.2.1, M 3.2.2) showed better results than the specimens without any external patches (M 2.1, M 3.1). Because, in the second group, only resin holds the specimen together. And a high stress concentration occurs at the contact area. In the first group, the external patches help the load transfer at the contact area. By this way the stress concentration decreases to a lower level.

- The specimens that have base material in the bottom (M 4.1.1, M 4.1.2, M 4.1.3, M 4.1.4, M 5.1.1, M5.1.2, M 5.1.3, M 5.1.4), showed better results than

the specimens patched from their edges (M 2.2.1, M 2.2.2, M 3.2.1, M 3.2.2). This is because that fixing a totally damaged specimen is more difficult than fixing a half damaged specimen. If the patches have some supporting undamaged plies in the bottom, the stress concentration will be less than the others.

- Some of the patched specimens having base material in the bottom and one-sided external patch on top (M 4.2.4.1, M 4.2.4.2, M 5.2.2.1, M 5.2.2.2, M 5.2.3.1, M 5.2.3.2, M 5.2.4.1, M 5.2.4.2) showed worse results than patched specimens with no external patches (M 4.1.4, M 5.1.2, M 5.1.3, M 5.1.4). This is due to the bending moments resulted from one sided patches. When the tensile load is being transferred from the external patch, it is not balanced with a symmetrical external patch on the other side. So, an extra bending moment occurs at the external patch area.

- Patched specimens having base layers in the bottom and external patches on both sides (double-sided patch) showed the best results in all patched specimens. By the increase of the external patch area, the maximum load capacity of the specimens increased. There are some exceptions like the specimens with 25 mm patch length. This is due to the large removal area of the original material for a standard tensile specimen.

- Consequently, for tensile specimens the best way for forming a patch is to increase the step number with patch length, while avoiding the removal of large areas (that includes undamaged parts) from the original material and adding external patches on both sides.

- From three point bending analysis performed numerically, it is seen that two stepped patched specimens show similar results with three stepped patched specimens. The small difference is owing to the inequality of thickness of patch steps. Three stepped patched specimens have less patch thickness than two stepped patched specimens.

REFERENCES

Armstrong, K. B., Barrett, R. T. (1998). *Care and repair of advanced composites.* Warrendale, PA: SAE(Society of Automative Engineers), Inc.

Baker, A. (1999). Bonded composite repair of fatigue – cracked primary aircraft Structure. *Journal of Composite Structures, 47,* 431-443.

Barut, A., Hanauska, J., Madenci, E., Ambur, D.R. (2002). Analysis method for bonded patch repair of a skin with a cutout. *Journal of Composite Structures, 55,* 277-294.

Belhouari, M., Bouiadjra, B.B., Megueni A., Kaddouri K. (2004). Comparison of double and single bonded repairs to symmetric composite structures: a numerical analysis. *Journal of Composite Structures, 65,* 47-53.

Bleay, S.M., Loader, C.B., Hawyes, V.J., Humberstone, L., Curtis, P.T. (2001). A smart repair system for polymer matrix composites. *Journal of Composites: Part A, 32,* 1767-1776.

Boh, J. W., Louca, L.A., Choo Y.S., Mouring S.E., Damage modeling of SCRIMP woven roving laminated beams subjected to transverse shear, Composites B 36 (2005) 427-438.

Bohlmann, R. E., Renieri, G. D., Libeskind, M. (1981). Bolted field repair of graphite / epoxy wing skin laminates. *ASTM (American Society for Testing and Materials) STP, 749,* 97–116.

Bouiadjra, B.B., Belhouari, M., Serier, B. (2002). Computation of the stress intensity factor for repaired cracks with bonded composite patch in mode I and mixed mode. *Journal of Composite Structures, 56,* 401-406.

Bouiadjra, B.B., Ouinas, D., Serier, D., Benderdouche, N. (2008). Disbond effects on bonded boron/epoxy composite repair to aluminum plates. *Journal of Computational Materials Science, 42,* 220-227.

Caliskan, M. (2006). Evaluation of bonded and bolted repair techniques with finite element method. *Journal of Materials and Design, 27,* 811-820.

Campilho, R.D.S.G., de Moura, M.F.S.F., Domingues, J.J.M.S. (2005). Modelling single and double-lap repairs on composite materials. *Journal of Composites Science and Technology, 65,* 1948-1958.

Carbon Repair To Aluminum (n.d.). Retrieved May 5, 2009, from http://www.azom.com/work

Chan, W., Vedhagiri, S. (2001). Analysis of composite bonded/bolted joints used in repairing. *Journal of Composite Materials, 35,* 1045-1061.

Charalambides, M. N., Hardouin, R., Kinloch, A. J., Matthews, F. L. (1998). Adhesively bonded repairs to fibre-composite materials I: experimental. *Journal of Composites: Part A, 29A,* 1371–1381.

Charalambides, M.N., Kinloch, A.J., Matthews, F.L. (1998). Adhesively bonded repairs to fibre-composite materials II: finite element modelling. *Journal of Composites: Part A, 29A,* 1383–1396.

Chen, D., Cheng, S. (1983). An Analysis of Adhesive - Bonded Single Lap Joints. *ASME Journal of Applied Mechanics, 109-115.*

Chester, R.J., Walker, K.F., Chalkley, P.D. (1999). Adhesively bonded repairs to primary aircraft structure. *International Journal of Adhesion and Adhesives, 19,*1-8.

Chotard, T.J., Pasquiet, J., Benzeggagh, M.L. (2001). Residual performance of scarf patch-repaired pultruded shapes initially impact damaged. *Journal of Composite Structures, 53,* 317-331.

Duong, C.N. (2004). An engineering approach to geometrically nonlinear analysis of a one-sided composite repair under thermo-mechanical loading. *Journal of Composite Structures, 64,* 13-21.

Duong, C. N., Wang, C. H. (2007). *Composite Repair – Theory and Design.* Oxford, Great Britain: Elsevier

Duong, C.N., Verhoeven, S., Guijt, C.B. (2002). Analytical and experimental study of load attractions and fatigue crack growths in two-sided bonded repairs. *International Journal of Solids and Structures, 39,* 1003-1014.

Engels, H., Becker, W. (2002). Closed – form analysis of external patch repairs of laminates. *Journal of Composite Structures, 56,* 259-268.

Fekirini, H., Bouiadjra, B. B., Belhouari, M., Boutabout, B., Serier, B. (2008). Numerical analysis of the performances of bonded composite repair with two adhesive bands in aircraft structures. *Journal of Composite Structures, 82,* 84-89.

Fredrickson, B.M., Schoeppner, G.A., Mollenhauer, D.H., Palazotto, A. N. (2008). Application of three-dimensional spline variational analysis for composite repair. Journal of Composite Structures, 83.

Fujimoto, S., Sekine, H. (2007). Identification of crack and disbond fronts in repaired aircraft structural panels with bonded FRP composite patches. *Journal of Composite Structures, 77,* 533-545.

Glass Repair To Aluminum (n.d.). Retrieved May 5, 2009, from http://civil.queensu.ca/people/faculty/fam/research/images

Goren, A., Atas, C., Manufacturing of polymer matrix composites using vacuum assisted resin infusion molding, Archives of Materials Science and Engineering 34 (2008) 117-120.

Harman, A.B., Wang, C.H. (2006). Improved design methods for scarf repairs to highly strained composite aircraft structure. *Journal of Composite Structures, 75,* 132-144.

Her, S., Shie, D. (1998). The failure analysis of bolted repair on composite laminate. *International Journal of Solids and Structures, 35(15),*1679-1693.

Hexcel Composites (1999). *Composite Repair.* Duxfor.

Hu, F. Z., Soutis, C. (2000). Strength prediction of patch - repaired CFRP laminates loaded in comparison. *Journal of Composite Sciences and Technology ,60,* 1103-1114.

Hosur, M. V., Vaidya, U. K., Myers, D., Jeelani, S. (2003). Studies on the repair of ballistic impact damaged S2 – glass / vinyl ester laminates. *Journal of Composite Structures, 61,* 281-290.

Jones, R., Krishnapillai, K., Pitt, S. (2006). Crack patching: Predicting fatigue crack growth. *Journal of Theoretical and Applied Fracture Mechanics, 45,* 79-91.

Kairuz, K. C., Matthews, F. L. (1993). Strength and failure modes of bonded single lap joints between cross-ply adherends. *Journal of Composites, 24(6),* 475-484.

Kang, M. K., Lee, W. I., Hahn, H. T., Analysis of Vacuum Bag Resin Transfer Molding Process, Composites A 32 (2001) 1553-1560.

Katzenschwanz C. (1996). Spannungen und Verschiebungen in Reparierten Scheiben und Platten unter Berücksiehtigung des Anisotropen Materialverhaltens. *VDI-Fortschrittsberichte, Reihe 18,* Nr. 192.

Kessler, M.R., White, S.R. (2001). Self – activated healing of delamination damage in woven composites. *Journal of Composites: Part A, 32,* 683-699.

Khattab A., Exploratory Development of VARIM Process for Manufacturing High Temperature Polymer Matrix Composites, Ph.D thesis, University of Missouri, 2005.

Koefoed, M. S., Modeling and Simulation of the VARTM Process for Wind Turbine Blades, Industrial Ph.D. Dissertation, Aalborg University, 2003.

Koh, Y.L., Rajic, N., Chiu, W.K., Galea, S. (1999). Smart structure for composite repair. *Journal of Composite Structures, 47,* 745-752.

Kollár, L. P., Springer, G. S. (2003). *Mechanics of Composite Structures.* New York, USA: Cambridge

Leiborich, H., Sason, N., Simon, A., Gren, A. K. (1990). *Repair of cracked aluminum aircraft structure with epoxy/epoxy patches*. Proceedings of the Ninth International Conference on Composite Materials (Madrid, Spain), vol. 4. Cambridge: Woodhead, 461-468.

Li, G., Pourmohamadian, N., Cygan, A., Peck, J., Helms, J.E., Pang, S.S. (2003). Fast repair of laminated beams using UV curing composites. *Journal of Composite Structures, 60,* 73-81.

Liu, X., Wang, G. (2007). Progressive failure analysis of bonded composite repairs. *Journal of Composite Structures, 81,* 331-340.

LUSAS Software Modeller On-line Help (n. d.).

Madani, K., Touzain, S., Feaugas, X., Benguediab, M., Ratwani, M. (2008). Numerical analysis for the determination of the stress intensity factors and crack opening displacements in plates repaired with single and double composite patches. *Journal of Computational Materials Science, 42,* 385-393.

Mahdi, S., Kinloch, A. (2003). The static mechanical performance of repaired composite sandwich beams: part II finite element modelling. *Journal of Sandwich Structural Materials, 5,* 267-303.

Mazumdar, S. K. (2002). *Composite manufacturing - materials, product and engineering.* Florida: CRC Press.

Megueni, A., Lousdad, A. (2008). Comparison of symmetrical double sided and stepped patches for repairing cracked metallic structures. *Journal of Composite Structures, 85,* 91-94.

Mollenhauer, D. H., Fredrickson, B.M., Schoeppner, G.A., Iarve, E.V., Palazotto, A. N. (2008). Moiré interferometry measurements of composite laminate repair behavior: influence of grating thickness on interlaminar response. *Journal of Composites: Part A.*

Naboulsi, S., Mall, S. (1998). Nonlinear analysis of bonded composite patch repair of cracked aluminum panels. *Journal of Composite Structures, 41,* 303-313.

Oztelcan, C., Ochoa, O. (1997). Design and analysis of test coupons for composite blade repairs. *Journal of Composite Structures, 37,* 185-93.

Pang, J.W.C., Bond, I.P. (2005). A hollow fibre reinforced polymer composite encompassing self – healing and enhanced damage visibility. *Journal of Composites Science and Technology, 65,* 1791–1799.

Potted Repair (n.d.). Retrieved May 5, 2009, from http://www.sandwichpanels.org/Images/repair

Ragondet, A., Experimental Characterization of the Vacuum Infusion Process, PhD thesis, University of Nottingham, 2005.

Rao, V.V., Singh, R., Malhotra, S.K. (1999). Residual strength and failure life assessment of composite patch repaired specimens. *Journal of Composites: Part B 30,* 621-627.

Ratwani, M. M. (n.d.). *Analysis of cracked adhesively bonded laminated structures*. AIAA/ASME 19th structures, structural dynamics and materials conference, Bethesda, MD 988-994, Paper No. 78483R.

Resin Sealing (n.d.). Retrieved May 5, 2009, from http://cgi.ebay.es/EPOXY-RESIN-SEALER-REPAIR-WOOD-ROT-WATER-PROOF-1-5-GAL

Schubbe, J. J., Mall, S. (1999). Modelling of cracked thick metallic structure with bonded composite patch repair using three-layer technique. *Journal of Composite Structures, 45,* 185-193.

Seo, D.C., Lee, J.J. (2002). Fatigue crack growth behavior of cracked aluminum plate repaired with composite patch. *Journal of Composite Structures, 57,* 323-330.

Sherwin, G. R. (1999). Non – autoclave processing of advanced composite repairs. *International Journal of Adhesion & Adhesives, 19,* 155-159.

Soutis, C., Duan, D - M., Goutas, P. (1999). Compressive behaviour of CFRP laminates repaired with adhesively bonded external patches. *Journal of Composite Structures, 45,* 289-301.

Speedtape (n.d.). Retrieved May 5, 2009, from http://www.packdaily.com/pk_data%5CManufactures%5C00115000000309%5CAluminum%20Foil%20Tape.jpg

Staab, G. H. (1999). *Laminar Composites.* Woburn, MA: Butterworth-Heinemann

Strong, A. B. (n.d.). *History of composite materials.* Brigham Young University.

Tsai, G.C., Shen, B.S. (2004). Fatigue analysis of cracked thick aluminum plate bonded with composite patches. *Journal of Composite Structures, 64,* 79-90.

Tzetzis, D., Hogg, P.J. (2006). Bondline toughening of vacuum infused composite repairs. *Journal of Composites: Part A, 37,* 1239-1251.

Tzetzis, D., Hogg, P. J. (2008). Experimental and finite element analysis on the performance of vacuum-assisted resin infused single scarf repairs**.** *Journal of Materials and Design, 29,* 436-449.

Vaziri, A., Nayeb - Hashemi, H. (2006). Dynamic response of a repaired composite beam with an adhesively bonded patch under a harmonic peeling load. *International Journal of Adhesion&Adhesives, 26,* 314-324.

Wang, C. H., Gunnion, A. J. (2008). On the design methodology of scarf repairs to composite laminates. *Journal of Composites Science and Technology, 68,* 35-46.

Widagdo, D., Aliabadi, M.H. (2001). Boundary element analysis of cracked panels repaired by mechanically fastened composite patches. *Journal of Engineering Analysis with Boundary Elements, 25,* 339-345.

Wilmarth, D. D. (1982). *BREPAIR Bolted Repair Analysis Program.* Cambridge: Arthur D. Little Inc.

Yala, A.A., Megueni, A. (2008). Optimisation of composite patches repairs with the design of experiments method. *Journal of Materials and Design.*

Yang, C., Huang, H. (2004). Elastic - plastic model of adhesive - bonded single – lap composite joints. *Journal of Composite Materials, 38,* 293-309.

Yunpeng, J., Qingmano, Z., Yi, W., Zhufeng, Y. (2005). Experiment studies and FEM simulation of repaired composite laminates. *Act a Materiac Compositac Sinica, 22,*
190-196.

Zhang, H., Motipalli, J., Lam, Y. C., Baker, A. (1998). Experimental and finite element analyses on the post - buckling behaviour of repaired composite panels. *Journal of Composites: Part A, 29A, 1463-1471 PII: S1359-835X(98)00030-X.*

Zhang, J. M. (2001). Design and analysis of mechanically fastened composite joints and repairs. *Journal of Engineering Analysis with Boundary Elements 25,* 431-441.